Technische Universität München

Fakultät für Medizin

Gene environment interactions in the etiology of metabolic and neuropsychiatric dysfunction

Peter Baumann

Vollständiger Abdruck der von der Fakultät für Medizin der Technischen Universität München zur Erlangung des akademischen Grades eines

Doktors der Naturwissenschaften

genehmigten Dissertation.

Vorsitzender: Prof. Dr. Thomas Korn

Prüfer der Dissertation: 1. Prof. Dr. Paul T. Pfluger

2. Prof. Dr. Wolfgang Wurst

Die Dissertation wurde am 22.08.2019 bei der Technischen Universität München eingereicht und durch die Fakultät der Medizin am 10.03.2020 angenommen.

I Abstract

Dual-specificity phosphatase 8 (Dusp8) is a mitogen activated protein kinase phosphatase (MKP) expressed in the limbic system of the central nervous system (CNS), predominantly in the hippocampus. Although MKPs were extensively studied during the last decades, little is known about the cellular and physiological function of this member of the MKP family. Dusp8 inactivates mitogen-activated protein kinases (MAPKs) by dephosphorylation. MAPKs are crucially involved in physiological and pathophysiological events such as inflammation, cell death, survival, proliferation, and maturation, and are considered as a major nexus for the regulation of cellular stress. Aberrant MAPK signaling has an outreaching impact and causes various alterations in health and disease. In this thesis we investigated the influence of Dusp8 on brain morphology, learning and cognition, and motivational behavior. Furthermore, we were interested in the role of Dusp8 in CNS glucose sensing and in energy metabolism.

We found that female and male global Dusp8 KO mice show a reduced hippocampus size and a hyperactive phenotype that was associated with a mild impairment of spatial memory in female Dusp8 KO mice. Female mice deficient for Dusp8 further revealed a higher consumption of sucrose, but perturbed sucrose seeking behavior when access to sucrose was limited. Western blot analyses of hippocampus lysates revealed unchanged Jnk and p38 phosphorylation, but higher activation of Erk-signaling in Dusp8 KO mice. The investigation of central glucose sensing in the global Dusp8 KO mice by 2-deoxy-glucose (2DG) injections revealed increased Jnk-signaling in the hypothalamus, as well as an increased neuronal activity in the VMH, hippocampus, and parts of the brain stem. *In vitro* studies, however, showed a reduced phosphorylation of Erk and an upregulated expression of Dusp8 in 2DG stimulated cells. The conditional, Grik4-Cre-driven hippocampal ablation of Dusp8 revealed unperturbed metabolic homeostasis, i.e. comparable to food intake, body weight, and blood glucose homeostasis in HFD-fed WT and KO littermates.

Overall, we showed a substrate specificity of Dusp8 towards Erk. Our results suggest that Dusp8 may act as an inducible early gene. Although Dusp8 is not crucially involved in mental health, it is modulating cognitive and anxiety-like behavior. Dusp8 is a component of the glucose sensing circuits in the brain and important for behavioral foraging responses associated with glycolysis-dependent energy depletion. In

summary, Dusp8 plays a modulatory role in the metabolic-cognitive network of the brain.

II Zusammenfassung

Dual-Specificity-Phosphatase 8 (Dusp8) ist eine Mitogen-aktivierte Proteinkinase-Phosphatase (MKP), die im limbischen System des Zentralnervensystems (ZNS), vorwiegend im Hippocampus, exprimiert wird. Obwohl MKPs in den letzten Jahrzehnten ausgiebig untersucht wurden, ist wenig über die zelluläre und physiologische Funktion dieses Mitglieds der MKP-Familie bekannt. Dusp8 inaktiviert Mitogen-aktivierte Proteinkinasen (MAPKs) durch Dephosphorylierung. MAPKs sind maßgeblich an physiologischen und pathophysiologischen Ereignissen wie Entzündungen, Zelltod, Überleben, Zellproliferation und -reifung beteiligt und werden als Hauptregulatoren von Zellstress angesehen. Aberrante MAPK-Signale haben weitreichende Auswirkungen und verursachen verschiedene gesundheitliche und krankheitsbedingte Veränderungen. In dieser Arbeit untersuchten wir den Einfluss von Dusp8 auf die Gehirnmorphologie, das Lernen und die Kognition sowie das Motivationsverhalten. Darüber hinaus interessierten wir uns für die Rolle von Dusp8 bei der zentralnervösen Glukoseerkennung und beim Energiestoffwechsel.

Wir fanden heraus, dass globale weibliche und männliche Dusp8-KO-Mäuse eine verringerte Hippocampusgröße und einen Hyperaktivitäts-Phänotyp aufweisen, der mit einer leichten Beeinträchtigung des räumlichen Gedächtnisses bei weiblichen Dusp8-KO-Mäusen assoziiert war. Weibliche Mäuse, denen Dusp8 fehlt, zeigten weiterhin einen höheren Konsum von Saccharose und ein verändertes Saccharose-Suchverhalten, wenn der Zugang zu Saccharose eingeschränkt war. Western-Blot-Analysen von Hippocampus-Lysaten ergaben eine unveränderte Jnk- und p38-Phosphorylierung, jedoch eine höhere Aktivierung des Erk-Signals bei Dusp8-KO-Mäusen. Die Untersuchung der zentralnervösen Glukoseerkennung in globalen Dusp8-KO-Mäusen durch 2-Desoxy-Glukose (2DG) -Injektionen ergab eine erhöhte Jnk-Signalübertragung im Hypothalamus sowie eine erhöhte neuronale Aktivität im VMH, Hippocampus und Teilen des Hirnstamms. *In-vitro*-Studien zeigten jedoch eine verringerte Phosphorylierung von Erk und eine hochregulierte Expression von Dusp8 in 2DG-stimulierten Zellen. Die spezifische Grik4-Cre-gesteuerte hippocampale Ablation von Dusp8 ergab eine intakte metabolische Homöostase, wie eine vergleichbare Nahrungsaufnahme, Blutzucker-Homöostase und ein vergleichbares Körpergewicht bei HFD-gefütterten WT- und KO-Geschwistertieren.

Insgesamt zeigten wir eine Substratspezifität von Dusp8 gegenüber Erk. Unsere Ergebnisse legen nahe, dass Dusp8 als ein induzierbares frühes Gen wirken kann. Obwohl Dusp8 nicht entscheidend an der psychischen Gesundheit beteiligt ist, moduliert es kognitives und angstähnliches Verhalten. Dusp8 ist eine Komponente in den Glukoseerkennungskreisläufen im Gehirn und wichtig für verhaltensbezogene Futtersuchreaktionen, die mit einem glykolysebedingten Energieverlust verbunden sind. Zusammenfassend spielt Dusp8 eine modulatorische Rolle im metabolisch-kognitiven Netzwerk des Gehirns.

Table of contents

1 Introduction

1.1 Mitogen-activated protein kinases

The role of mitogen-activated proteins kinases (MAPKs) in cellular signaling was extensively studied during the last decades (Avruch 2007, Kyriakis and Avruch 2012). There is a vast amount of literature available covering aspects of MAPK signaling initiation, upstream and downstream signal transduction with mediating mechanisms, and signaling targets in different physiological and pathophysiological conditions. For the focus of the thesis, I will only introduce the general role of MAPKs in cellular signaling without touching the detailed signaling aspects. An overview of the basic principal of MAPK-signaling is given in a simplified diagram in Figure 1.

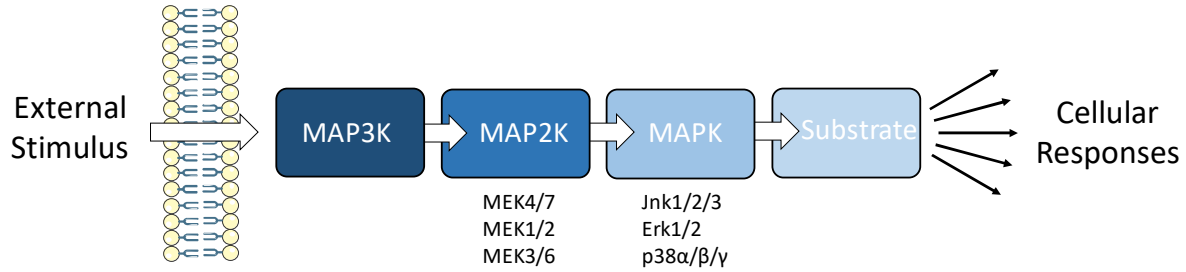

Figure 1. Schematic MAPK-signaling

Mitogen-activated protein kinases are evolutionarily highly conserved Ser/Thr kinases. They transduce external stimuli such as inflammatory stress, endocrine stimuli, or growth factors via internal signaling pathways and contribute in various crucial cellular functions. They are involved in gene expression and mitosis, cell survival and death, as well as proliferation, cell motility, and metabolism (Widmann et al. 1999). MAPKs can be differentiated in two major subgroups. Typical MAPKs include extracellular signaling-regulated kinases 1/2 (Erk1/2), c-Jun N-terminal kinases 1/2/3 (Jnk1/2/3), and p38 with the respective isoforms α, β, γ, δ (Chen et al. 2001, Kyriakis and Avruch 2012). Furthermore, there are the described atypical MAPKs Erk3/4, Erk5, Erk7, and Nemo-like kinase (NLK) (Pearson et al. 2001, Coulombe and Meloche 2007). In this introduction of MAPKs and the entire study we focus our interests on the three typical MAPKs Jnk1/2/3, p38, and Erk1/2. These typical MAPKs are activated by specific MAPK kinases (MAPKK). MAPKK phosphorylate both Thr and Tyr residues in a highly conserved Thr-X-Tyr motif located in the kinase domain of the MAPK protein. Substrates of typical MAPKs are in turn activated by phosphorylation of the respective

MAPK. The substrates include p90 ribosomal S6 kinases (RSK), mitogen- and stress-activated kinases (MSK), MAPK-interacting kinases (MNK), MAPK-activated protein kinase 2/3 (MK2/3), as well as MK5, and are summarized under the expression MAPK-activated protein kinases (MAPKAPK). Besides having a highly selective substrate specificity that is described in detail below, there is an extensive amount of crosstalk between all three typical MAPKs further strengthening the diversity and complexity of the MAPK signaling cascade.

1.1.1 c-jun N-terminal kinase (Jnk)

Jnk kinases are encoded by the genes JNK1-3, that due to different splicing sites, encode twelve different polypeptides. JNK 1 and 2 are expressed ubiquitously throughout tissues, whereas the expression of Jnk3 is restricted exclusively to the brain. All Jnk polypeptides contain the specific Thr183-Pro-Tyr185 Jnk-MAPK motif in the kinase subdomain VIII (Raman et al. 2007, Kyriakis and Avruch 2012). Predominant upstream activators of Jnk are MEK4 and MEK7 that preferentially phosphorylate residue Tyr185 and Thr183, respectively (Lawler et al. 1998). Jnk-MAPK are widely regulated via docking motif (D-motif) of specific inhibitors. Moreover, D-motifs serve as coupling sites for upstream and downstream signaling targets and ensure the specificity of Jnk and its interaction partners (Xu and Cobb 1997, Xia et al. 1998). However, there are Jnk scaffold proteins described that regulate signaling of other Jnk-independent pathways (Raman et al. 2007).

One function of Jnk is the activation of apoptotic pathways in which the activity of Jnk is closely related to its interaction with the tumor suppressor p53. It was shown that the binding interaction of Jnk with p53 leads to ubiquitin-mediated degradation of the transcription factor, which contributes to cell cycle arrest and/or apoptosis (Fuchs et al. 1998, Davis 2000). Other data suggests an involvement of various pathways, e.g. myc, Bcl-2, and caspase 3 for cell death (Krishna and Narang 2008). Looking specifically into the central nervous system, it was shown that combined interaction of Jnk1 and Jnk2 is required for appropriate brain development. Double knockouts are embryonically lethal due to a disruption in reduced apoptotic cell degeneration during brain development. Further, there is evidence that Jnk-signaling is involved in neuronal survival, proliferation, and maturation in the hippocampus. Bendotti and colleagues showed evidence that Jnk-signaling in the brain is substantially involved in

neurodegenerative diseases (Bendotti et al. 2006). The role of Jnk activity and the potential target for treating neurodegenerative diseases such as Alzheimer's and Parkinson`s disease was reviewed by Mehan and colleagues (Mehan et al. 2011). Furthermore the murine knockout models of Jnk1 and inhibitor treatment experiments revealed that reducing Jnk activity promotes proliferation, survival, and maturation at the cellular level and ameliorates anxiety- and depressive-like behavior of animals (Mohammad et al. 2018).

Taken together, Jnk isoforms are crucially involved in brain development, behavior affecting cell proliferation, maturation, survival, and degeneration in the central nervous system.

1.1.2 Extracellular signal-regulating kinase (Erk)

Extracellular signal-regulating kinase (Erk) was the first MAPK identified and the specific Ras-Raf-MEK-signaling pathway was studied extensively (Raman et al. 2007). The two proteins Erk1/2 are encoded by genes ERK1 and ERK2 and are specifically expressed in the brain, heart, thymus, and heart (Boulton et al. 1990). The specific phosphorylation Thr-X-Tyr motif for MAPK for Erk1 and Erk2 are located in the kinase subdomain VIII and consist of Thr203-Glu-Tyr205 and Thr185-Glu-Tyr187, respectively. Initiation of the signaling cascade starts at the cell surface via tyrosine kinases or G protein-coupled receptors and transduces the signal to small G proteins (Krishna and Narang 2008). In the following, activated Raf kinases phosphorylate and thereby activate MEK1/2. MEK1/2 directly phosphorylate Erk1/2 (Cargnello and Roux 2011). Erk1/2-signaling is inhibited and inactivated by dephosphorylation at one or both phosphorylation sites. In general, protein Ser/Thr phosphatases, protein Tyr phosphatases, or Dusps are mediating this inactivation process (Krishna and Narang 2008). The first synthetic inhibitors were developed in 1995, e.g. PD98059 (Alessi et al. 1995, Dudley et al. 1995). They bind the inactive MEK1/2 and prevent their phosphorylation.

The fact that Erk1/2 interacts with more than 150 substrates including cytoskeletal proteins, nuclear, cytosolic, and membrane-bound substrates (Yoon and Seger 2006) underlines the signaling complexity and the diverse cellular functions of Erk-signaling in the cell. However, the RSK family is exclusively activated by Erk in MAPK-signaling (Chen et al. 1992). After activation, a significant amount of Erk accumulates in the

nucleus. Focusing on the central nervous system, there is conflicting evidence that Erk activation not only attenuates neurotoxicity in cells (Zhu et al. 2002), but also has a neurotoxic effect itself resulting from chronic Erk activity. A more complex role of Erk activity is given in Huntington's disease, where an interaction between Erk and huntingtin may have both a neuroprotective and neurotoxic role (Bodai and Marsh 2012). This ambivalent role of Erk activation in neuroprotective and –degenerative effects in different pathophysiological and experimental conditions remain dependent on the co-activation of various other stimuli (Rai et al. 2019).

Mainly, Erk1/2 has a central role in the induction of cell proliferation and induces immediate early genes after stimulation. This also promotes G_1/S transition and allows cell cycle progression (Cargnello and Roux 2011).

1.1.3 p38

There are four isoforms of p38 described (α, β, γ, δ) and homologues are evolutionary conserved in high and low eukaryotes. The expression pattern of p38 is tissue dependent, whereas p38α, β, γ, and δ are expressed ubiquitously in the brain, skeletal muscle, and endocrine glands, respectively (Cuadrado and Nebreda 2010). MAPK-p38 shows many parallels with Jnk, as they are activated by inflammatory stimuli as well as cellular stress, and signaling cascades show a certain amount of cross-talk. Specifically, p38 is involved in osmoregulation, cell cycle events, extracellular stress (Brewster et al. 1993, Shiozaki and Russell 1995), as well as inflammatory cytokines such as interleukin-1 (IL-1) and tumor necrosis factor alpha (TNFα) (Cuadrado and Nebreda 2010). The specific phosphorylation motif of p38 is formed by glycine within the threonine and tyrosine motif and consists of Thr180-Gly-Tyr182 (Wang et al. 1997). It was shown that the main p38 signaling mechanism is similarly transduced as in the Ras/Raf/MEK/Erk pathway via small GTP binding proteins belonging to the Rho family (Zhang et al. 1995). The p38 isoforms are specifically activated by MKK3 and MKK6 (Enslen et al. 1998). Activated p38 translocates to the nucleus and activates various downstream targets, e.g. activating transcription factor 1,2,6 (ATF1/2/6) and MK2/3 through phosphorylation. Activity of p38 mediates apoptosis, acts as a cell cycle and tumor suppressor in cancer development, is critically involved in immune function and inflammatory signaling via post-transcriptional and post-translational control, and is necessary for embryogenic development (Krishna and Narang 2008, Cargnello and

Roux 2011). Trying to establish p38 knockout mouse models revealed that mice deficient for p38 are embryonically lethal (Mudgett et al. 2000).

It is known that p38-signaling is involved in long-term depression of synapses in the hippocampus. This underlines the importance of p38-signaling in the CNS for synaptic signaling. Additionally, inhibitor studies revealed that neuroinflammation from activated microglia and astrocytes is mediated via activation of p38. The involvement of p38-signaling in Alzheimer's disease, as well as the beneficial effects of p38 inhibition on memory, neuronal cell death, and long-term depression in spines were conclusively reviewed by Lee and Kim (Lee and Kim 2017).

Taken together, p38 is crucially involved in embryonic development and cell proliferation, as well as synapse maturation, and neuroinflammatory signaling.

1.2 Dual-specificity phosphatases (Dusp)

Dual-specificity phosphatases belong to the superfamily of protein tyrosine phosphatases (PTP) and are capable of dephosphorylating both phosphotyrosine and phosphoserine/threonine residues within one substrate. Dusps include over 61 distinct members and can be distinguished in six subgroups: atypical Dusps, slingshot phosphatases, phosphatase of regenerating liver (PLR), cdc14 phosphatase, phosphatase and tensin homologue deleted on chromosome 10 (PTEN)-like and myotubularin phosphatases, mitogen-activated protein kinase phosphatases (MKPs), whereas PTEN-like and myotubularin phosphatases are united in one group. The family of MKPs are likely one of the best characterized Dusps (Patterson et al. 2009). As the given name already indicates, MKPs show high specificity towards one or more of the three MAPKs, Erk, Jnk, and p38. They bind to MAPK, dephosphorylate, thus inactivate the kinase, and inhibit the subsequent signaling cascade (Theodosiou and Ashworth 2002b, Kyriakis and Avruch 2012).

1.2.1 Dual-specificity mitogen-activated protein kinase phosphatase (MKP)

The MKP family consists of at least ten Dusps (see Table 1) which show a diverse pattern of tissue expression and target specificity. The inducible nuclear MKPs such as Dusp1 show high promiscuity, i.e. they dephosphorylate Erk, p38, and Jnk. Others show a relative stringent target-selectivity; Dusp6 for instance dephosphorylates only

Erk (Bermudez et al., 2010, Caunt and Keyse, 2013). Both Dusp1 and Dusp6 are presumably the most examined Dusp members.

Table 1. Dual-specificity MAPK phosphatases (MKP)

Dusp	Chrom. Location	Specificity	Cellular Location	Structure
Dusp1	5q34	Jnk, p38, Erk	nuclear	
Dusp2	2q11	p38, Erk	nuclear	
Dusp4	8q11-12	Jnk, p38, Erk	nuclear	
Dusp5	10q25	Erk	nuclear	
Dusp6	12q22-23	Erk	cytoplasmic	
Dusp7	3q21	Erk	cytoplasmic	
Dusp8	11p15.5	Jnk, p38	cytoplasmic, nuclear	
Dusp9	Xq28	Erk > p38	cytoplasmic	
Dusp10	1q41	Jnk, p38	cytoplasmic, nuclear	
Dusp16	12q13	Jnk, p38	cytoplasmic, nuclear	

PEST domain: proline (P), glutamine (E), serine (S), threonine (T) rich domain

Activity of Dusps is regulated on multiple levels, including not only by constitutive or inducible expression, but also by post-transcriptional and post-translational modifications, which include Dusp phosphorylation, acetylation, and cysteine-oxidation, as well as caspase induced cleavage and protein degradation. However, these post-translational modifications can act in both an activating or inhibiting manner (Perez-Sen et al. 2019).

Ubiquitously expressed MKPs such as Dusp1 have been linked to a number of systemic diseases. For instance, global, as well as nuclear, Dusp1 ablation was linked to increased energy expenditure, and thus resistance to diet-induced obesity (Wu et al., 2006). Furthermore, there is evidence for a prominent role of Dusp1 in the central nervous system. Brain-derived neurotrophic factor (BDNF)-induced Dusp1 stabilization plays a central role in axonal branching and dendritic growth during neuronal differentiation (Jeanneteau et al. 2010). Moreover, elevated Dusp1 levels caused a depressive phenotype in rats. This finding was also observed in humans where Dusp1 levels were increased in the hippocampus of depressive patients (Duric et al. 2010).

A recent study showed that mice deficient for Dusp6 had reduced body weight and lean mass, and impaired systemic glucose tolerance (Pfuhlmann et al., 2017). A neurotoxic effect of Dusp6 is present in Alzheimer's disease. It was shown that dysregulation of Dusp6 is involved in tau-mediated cytotoxicity (Banzhaf-Strathmann et al. 2014). The impact of Dusp6 is not only limited to the cellular level, but also shows involvement in behavioral disorders such as bipolar disorder (BD), in which Dusp6 polymorphisms were shown to be associated (Kim et al. 2012).

These few examples illustrating the various functions of MKPs is indicative of the widespread impact in physiological and pathophysiological processes within the organism.

1.2.2 The dual-specificity phosphatase 8 – a poorly studied MKP

One of the least studied MKPs is Dusp8. As reviewed by Seternes and colleagues, little to nothing is known about the function of Dusp8 (Seternes et al. 2019). It was initially described as a homologue of vaccinia virus H1 phosphatase gene clone 5 (vHV-5). Comparisons of the protein sequence revealed the structure of a dual-specificity PTP. They showed an expression predominantly in human heart, skeletal muscle, and the brain. In more detail, vHV-5 is highly abundant in the amygdala, caudate nucleus, hippocampus, and hypothalamus. Furthermore, vHV-5 was inducible by NGF and insulin *in vitro* (Martell et al. 1995). Transfection experiments in COS-7 cells showed a specificity of Dusp8 (referred to as M3/6) for dephosphorylating SAPKβ/Jnk and p38, but not for Erk1 (Muda et al. 1996). However, recently a knockout mouse model showed a specificity of Dusp8 towards Erk and an involvement in cardiac

muscle remodeling (Liu et al. 2016). Moreover, genome wide association studies identified human DUSP8 gene associated polymorphism as a risk gene for type 2 diabetes in men (Kong et al. 2009, Morris et al. 2012) with a parentally inherited imprinting. The gene locus for Dusp8 was also potentially linked to bipolar disorder (Serretti and Mandelli 2008). To date, none of the latter mentioned results of Dusp8 SNP and locus associated studies were further investigated.

1.3 Central connections of cognition and metabolism

Obesity has been a growing problem throughout the last decades: Since 1975 the number of worldwide obese people tripled, more than 650 million adults suffered from obesity in 2016, and obesity is associated with an overall increased mortality compared to the non-obese population (WHO 2018). Along with obesity, there are associated comorbidities such as cancer, cardiovascular diseases, and diabetes (Timper and Bruning 2017). Furthermore, obesity and metabolic dysfunction contribute to cognitive impairment. Obesity leads to a systemic and local inflammation in the brain, likely causing synaptic remodeling, and thus perturbation in cognitive function, as well as increased risk for dementia (Miller and Spencer 2014). The main comorbidity of obesity, diabetes, is independently associated with cognitive dysfunction (Biessels and Despa 2018) and cognitive risk due to neuroinflammation and synaptic remodeling (Stranahan 2015). One of the first regions of the brain to suffer damage in neurodegenerative diseases is the hippocampus, which plays important roles in the consolidation of information from short-term to long-term memory, and in spatial memory that enables navigation (Morris et al. 1982, Lavenex and Amaral 2000).

Energy homeostasis and cognitive behavior are regulated in various centers of the brain, which are closely interconnected and show a fragile system of a counter-regulatory mechanism. Furthermore, there is also a complex interconnection with hedonic sensation and reward system. Moreover, centers for cognition influence food intake and appetitive control (Andermann and Lowell 2017). The regulation of energy metabolism is a crucial physiological aspect of health and welfare in the context of cognitive diseases.

1.3.1 Learning and memory

1.3.1.1 Hippocampal structure and organization

The hippocampus is part of the limbic system, located in the medial temporal lobe of the brain. The hippocampal formation includes the dentate gyrus (DG), and the cornu ammonis (CA). The cornu ammonis is defined in CA1-3, which receives input from different brain structures. The main afferent center is the entorhinal cortex (EC). The classical system of the hippocampal relay is the tri-synaptic loop, which includes the entorhinal cortex, the DG, as well as the CA3 and CA1 region. Main afferent input from the entorhinal cortex is wired through the perforant pathway. Projections originating from the layer II of the entorhinal cortex arrive at the DG (medial and lateral performant pathway). From there, mossy fibers are projecting to the CA3 region, where the afferent information is relayed. Additionally, direct input is given from the EC to the CA3 region. Via the Schaffer collaterals, neurons from the CA3 region are projecting to the CA1 region of the hippocampal formation. The tri-synaptic loop is closed by efferent projections from the CA1 region to deep layers of the entorhinal cortex.

The second, direct input to the hippocampal CA1 region from the EC is the temporoammonic pathway. Those fibers originate from the layer III of the EC and project directly to the CA1 pyramidal neurons. Reviewed and adapted from Deng and colleagues (Deng et al. 2010) in Figure 2.

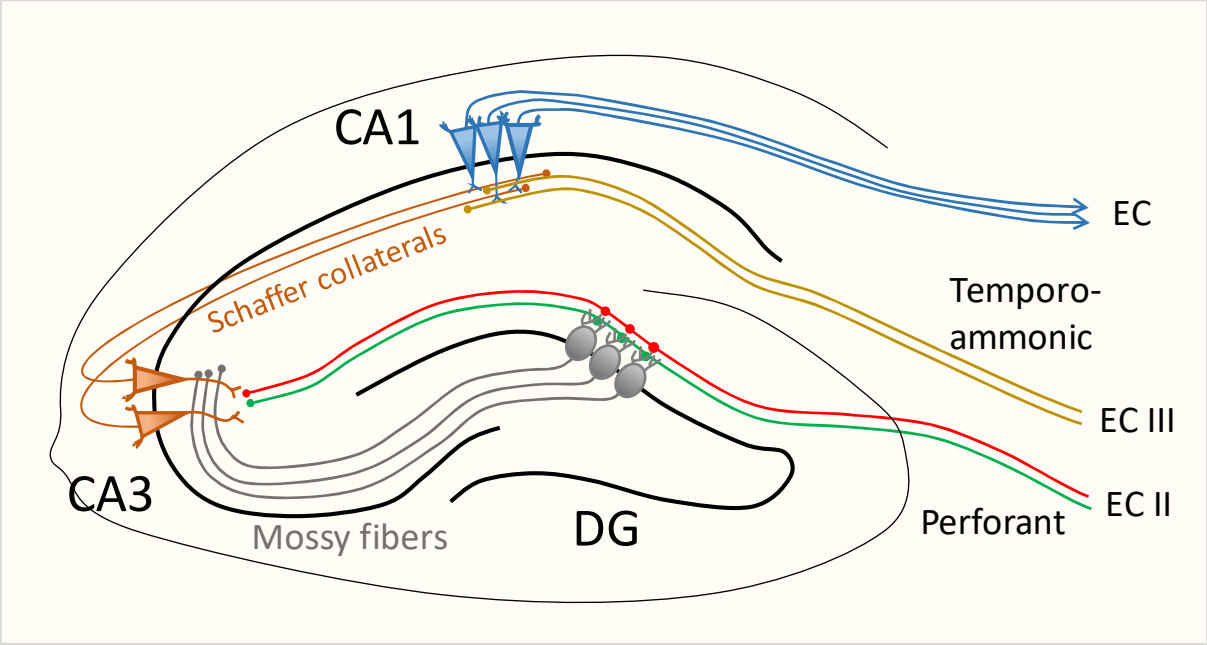

Figure 2. Afferent hippocampal pathways.

The performant pathway originates from the second layer of the entorhinal cortex and provides input to the tri-synaptic loop. Information is relayed at the dentate gyrus (DG) and projects through the mossy fibers to the CA3 region. From there, the information is transmitted through the Schaffer collaterals to the CA1 region and back to the EC. Second, afferences are reaching the CA1 area directly from the third layer of the EC (temporoammonic pathway). Adapted from Deng and colleagues (2010).

In addition to the external input to the hippocampus, several synaptic loops within the single subregions can be found. Granular neurons of the dentate gyrus project to interneurons and mossy cells in the hilus, and receive inhibiting and activating stimuli, respectively. CA3 neurons not only send projections through the Schaffer collaterals to the CA1 regions, but also project back on CA3 pyramidal neurons, forming an activation loop. This classical model of afferent hippocampal projection is by far not sufficient to describe the complexity of hippocampal function. As we will see later in this chapter, there is a much more complex system showing that the hippocampus receives input from various brain centers as well as information from the periphery.

There is not only a specific organization within the coronal section of the hippocampus, but also a distinct differentiation along the longitudinal axis from septal (dorsal) and temporal (ventral). Lesion studies showed that the dorsal part of the hippocampus is more responsible for spatial learning, and the ventral part has more impact on emotions, motivation, and executive function. This is corroborated by the fact that dorsal areas receive more input from visuospatial areas, and ventral parts receive information from prefrontal cortex and other subcortical structures (Moser and Moser

1998, Bannerman et al. 2004). The differentiation of the dorso-ventral axis of the hippocampus is a commonly accepted model, whereas there is also evidence that this distinct separation is not rigorous (Martin and Clark 2007). The incoming information is not only transmitted onto other neurons, but encoded in a coordinated firing ensemble of cells. Zemla and Basu reviewed how different hippocampal cells ensembles work together in microcircuits to sufficiently encode distinct features of internal and external context. Small numbers of cells firing in ensembles are also able to generate, recall, and modulate adaptively learned behavior (Zemla and Basu 2017).

1.3.1.2 Hippocampus and spatial learning

The contribution of the hippocampus to spatial orientation and place learning was extensively studied during the last decades, mostly by rodent hippocampal lesion models tested in a water maze (Morris et al. 1982). Intensive research lead to the discovery of a neuronal cell population within the hippocampus called “place cells” that fire in a specific location dependent manner, thereby forming a representative spatial map important for spatial orientation and navigation (O'Keefe and Dostrovsky 1971). Furthermore, closely hippocampal associated regions such as the entorhinal cortex harvest neurons associated with spatial orientation, e.g. grid cells and cells recognizing head-direction, as well as speed cells (Taube et al. 1990, Moser et al. 2008, Kropff et al. 2015). This network allows the formation of a mental map of the environment, encoded by firing rhythms of distinct neurons. Not only the different cell types identified are responsible for the coding of spatial orientation, but spatial memory is also dependent on plasticity in different subregions of the hippocampus. It was shown that working memory in a familiar environment was disrupted during an ITI of several minutes, not of several seconds, when altering the dentate gyrus or the CA1 region. Furthermore, alterations of the neuronal CA3 network resulted in a transient impairment of spatial orientation (Lee and Kesner 2002). Pharmacological inhibitor studies of NMDA-mediated synaptic plasticity indicate a requirement for rapid memory acquisition in the CA3 region of the hippocampus (Steele and Morris 1999, Lee and Kesner 2002). In a review, Martin and colleagues (Martin and Clark 2007) discussed the role of synaptic plasticity, regardless of which direction (long-term potentiation or long-term depression). Synaptic strengthening and weakening is very likely involved in encoding single and rapid spatial information. Repeated spatial challenging can be learned in a plasticity-independent manner. More recent findings suggest that a

reconsolidation of strong memories in area CA3 is not plasticity-dependent. However, reconsolidation with embedding new information to the memory trace requires protein synthesis (De Jaeger et al. 2014).

1.3.1.3 Hippocampal role in cognition and memory

The hippocampus is involved in explicit memory formation, which can be summarized as where and when a specific event happened, as well as the consolidation of acquisitioned memories and long-term storage (Komorowski et al. 2009).

Next to the hippocampal formation, associated input and output regions are required for memory acquisition and modulation, as well as cognitive performance (Lavenex and Amaral 2000). It is well established that the hippocampus plays a responsible role in spatial and non-spatial working and recognition memory (Olton and Papas 1979, Steckler et al. 1998). Regarding the critical involvement in cognition, Sweatt reviewed the crucial hippocampal function in perception of time and sequencing, as well as multimodal sensory integration (Sweatt 2004). It was shown early that hippocampal damage leads to an impairment in memory for objects, as well as for novel object recognition (Zola-Morgan et al. 1994, Murray and Mishkin 1998). More recent studies suggest a requirement of the hippocampus solely when remembering includes a spatial, temporal, or novelty aspect (Barker and Warburton 2011). The previously mentioned “place cells” are responsible not only for spatial navigation, but also encode for relevant objects or events in particular places (Komorowski et al. 2009). Together with so called “time cells,” they may form a mechanism for memory formation of everyday life experience (Eichenbaum 2013). This coding system of spatio-temporal relations allows a replay of rapidly acquisitioned memory. A mental replay system like this is an essential part of recollection and memory consolidation, which takes place during sleep and quiet resting periods (Ji and Wilson 2007, Karlsson and Frank 2009).

The hippocampus’ role in learning may also cover the representation of links between newly experienced associations. In memory consolidation, it matches overlapping associations from neocortical areas to invariant representations. However, this is not only restricted to the hippocampal formation (or the medial temporal lobe), but includes other neocortical afferences (Preston and Eichenbaum 2013).

1.3.2 Metabolic control and glucose sensing

1.3.2.1 Hypothalamic regulation of metabolism

Where the hippocampus is the center regulating memory and navigation, the hypothalamus is one of the crucial centers for metabolic control. Different hypothalamic nuclei regulate numerous aspects of counter-regulatory actions to imbalanced energy status. The arcuate nucleus (Arc) is the critical regulator within the hypothalamus. Its neuronal population are inter-wired and send projections to extra-hypothalamic nuclei, relaying feedback responses to the periphery (Waterson and Horvath 2015, Timper and Bruning 2017).

The hypothalamus was shown to maintain normal glucose levels in blood (Borg et al. 1997). Glucose metabolism, in particular within the hypothalamus, is regulated by heterogenic neuronal populations, which react to increasing or decreasing levels of blood glucose. They can be divided into glucose excited (GE) neurons and glucose inhibited (GI) neurons, which react with excitation to increasing or reducing levels of extracellular glucose, respectively (Routh et al. 2014, Kohno 2017).

GE neurons can be mostly found in the Arc, the ventromedial (VMH), periventricular nucleus (PVN) of the hypothalamus, as well as the lateral (LH) and anterior hypothalamus. The neurotransmitter identity of the different GE populations in the respective nuclei is not clearly identified. However, the sensing mechanism of the neurons is based on ATP/ADP ratio-dependent closure of ATP sensitive potassium channels, which leads to depolarization (Song et al. 2001). Furthermore, glucose concentrations can be pictured with neuronal activity rate, as the (pancreatic β-cell) glucokinase-dependent phosphorylation of glucose in neurons is not subject to end-product inhibition (Magnuson 1990). However, other glucose sensing mechanisms for respective GE subpopulations have been described: an involvement of GLUT2 and GLUT4, sodium glucose co-transporter (SGLT), and AMP activated protein kinase (AMPK), as well as non-selective or unidentified potassium channels (Routh et al. 2014, Kohno 2017).

Similar to GE neurons, GI neurons can be found in the Arc, VMH, PVN, and LH, but also in the dorso-medial hypothalamus (DMH). Unlike GE neurons, GI neurons can be further categorized into metabolism-dependent and metabolism-independent GI neurons (Routh et al. 2014). Metabolism-dependent GI neurons react to the metabolic

state and are located in the Arc and VMH, and likely use similar sensing mechanisms as GE neurons, as they similarly express GLUT2, GLUT4, SGLT, AMPK, as well as glucokinase (Kang et al. 2004, Kang et al. 2006). In contrast, metabolism-independent GI neurons, which react to the presence of glucose molecules, are preferentially located in the PVN and in the LH (Routh et al. 2014), and are sensitive to both glucose and glucose analogues (González et al. 2008). Interestingly, adapting and non-adapting GI neurons have been described. The latter are continuously inhibited by high glucose levels, whereas adapting GI neurons are only transiently inhibited during the change of glucose levels, returning to basal firing level after several minutes (Williams et al. 2008).

Although, the examples given here focus on the role of distinct hypothalamic nuclei in glucose sensing, there are more centers in the CNS, as well as peripheral glucose sensing sites that are required to initiate a complete and sufficient counter-regulatory response to changing glucose levels.

1.3.2.2 Mesolimbic reward system

Upstream of glucose sensing, there are pathways that regulate motivation, the desire for rewarding stimuli, and reward-related motor function learning. The main center for reward and seeking behavior in the brain is the mesolimibic pathway, a dopaminergic pathway that connects the ventral tegmental area in the midbrain, to the ventral striatum of the basal ganglia in the forebrain. Cortical projections send glutamatergic input to the dopaminergic basal ganglia of the striatum. Together with the ventral tegmental area (VTA), the mesoaccumbal dopamine pathway is essential for integrating motivated behavior. The mesolimbic reward system is able to modulate feeding behavior without any previous relay in the hypothalamus, e.g. via connections from the VTA to the nucleus accumbens (NAcc) that can suppress food intake (Mietlicki-Baase et al. 2014). However, the impact of the reward system is not only reliable on food intake action itself, but also on the quality of the diet. Palatable food induces different reactions than control chow food, i.e. upregulation of hunger and downregulating of satiety signals, resulting in a prolonged and increased food intake (Erlanson-Albertsson 2005). The hedonic information about palatable food, high in fat and sugar, is recognized by the NAcc by input from the brainstem via the NTS and transmitted via three neurotransmitter systems: opioids, dopamine, and serotonin to

the lateral hypothalamus, which then mediates the outcome of food ingestion (Waterson and Horvath 2015). A scheme for this simplified regulation mechanism involving the reward system and the hypothalamus regarding palatable food is given in Figure 3 (reviewed by and adapted from Erlanson-Albertsson, 2005).

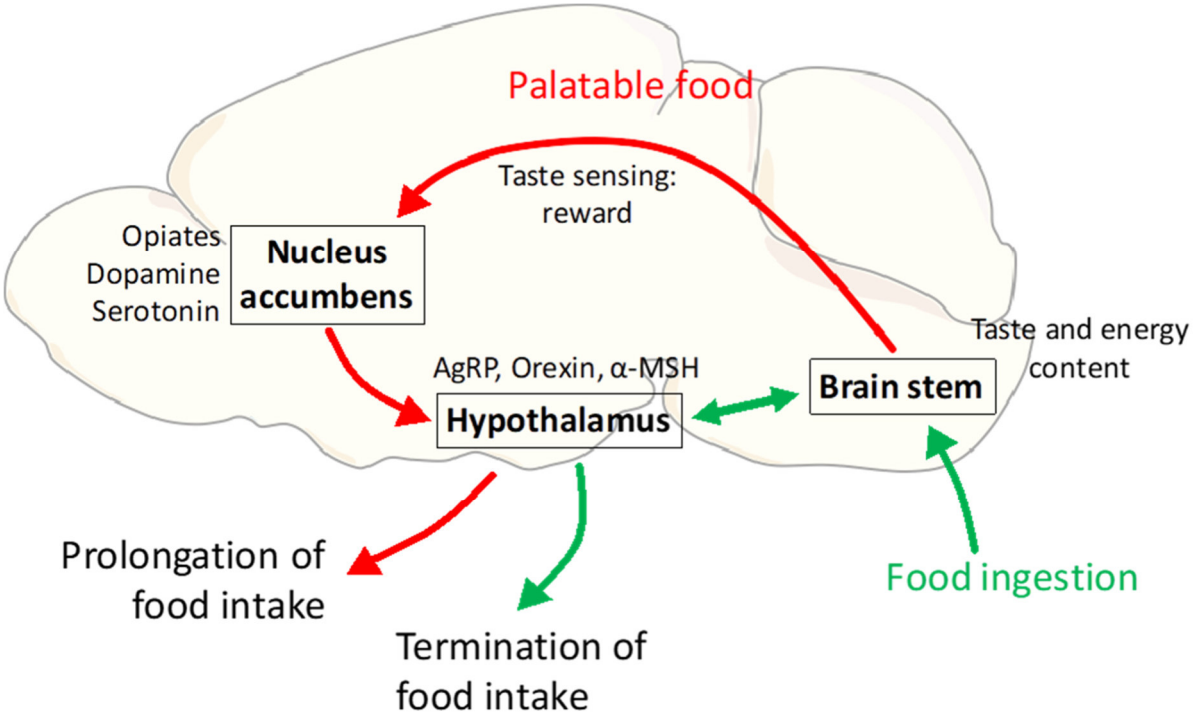

Figure 3. Hypothalamus and reward system control of food intake.

Upon food intake, information about energy content and taste are transmitted to the brain stem. Without hedonic stimulus, the hypothalamus is integrating the nutrient information e.g. via agouti-related protein (AgRP), orexin, or α-MSH and is terminating food intake (green arrows). Palatable food is integrated and relayed in the NAcc, and activates the reward system via opioid-, dopamine-, and serotonin-signaling. Hedonic information is projected to the hypothalamus, and the prolongation of food intake is initiated (red arrows). Adapted from Erlanson-Albertsson (2005).

However, not only the glucose sensing centers in the hypothalamus and the neuronal circuitry network of the mesolimbic reward system are involved in the decision making that contributes to feeding behavior; centers for memory and cognition within the hippocampus also play a role (Timper and Bruning 2017).

1.3.2.3 Hippocampal contribution to food intake and glucose sensing

Kanoski and Grill established a model of food intake control, which goes beyond the arcuate nucleus as the hypothalamic control center and hedonic aspects for regulating food intake, but also includes memory association and cognitive aspects (Kanoski and

Grill 2017). They established that the control of food intake is also integrating information of learned experience, external sensory cues, and internal context.

Learned experience includes hippocampus-dependent episodic memory. Memories of meal ingestion, as well as the recall of already consumed food, are considered when further food consumption onset is cogitated (Higgs 2008, Brunstrom et al. 2012). Rather more implicit, the hippocampus is directly inhibiting meal onset (Henderson et al. 2013). External cues can be differentiated in three aspects: spatial availability of food, nonfood factors influencing behavior, and quality of orally ingested food (Kanoski and Grill 2017). As previously outlined above, visuospatial information is mainly integrated into the dorsal part of the hippocampus. Olfactory, as well as taste information, is reaching the ventral part of the hippocampus from the primary olfactory cortex and the agranular insular gustatory cortex, respectively (Fanselow and Dong 2010, Mathiasen et al. 2015). Furthermore, the internal context of the metabolic state is transmitted to the hippocampal formation, a neuronal network from the hypothalamus, brainstem and cortical areas, and the endocrine system including hunger or satiety hormones like leptin, glucagon-like peptide 1 (GLP1), and ghrelin from the periphery (Kanoski and Grill 2017). A relay of this incoming information is performed in the hippocampus and influences the output of food intake and food seeking behavior. An adapted overview from Kanoski and Grill (2017) is given in Figure 4.

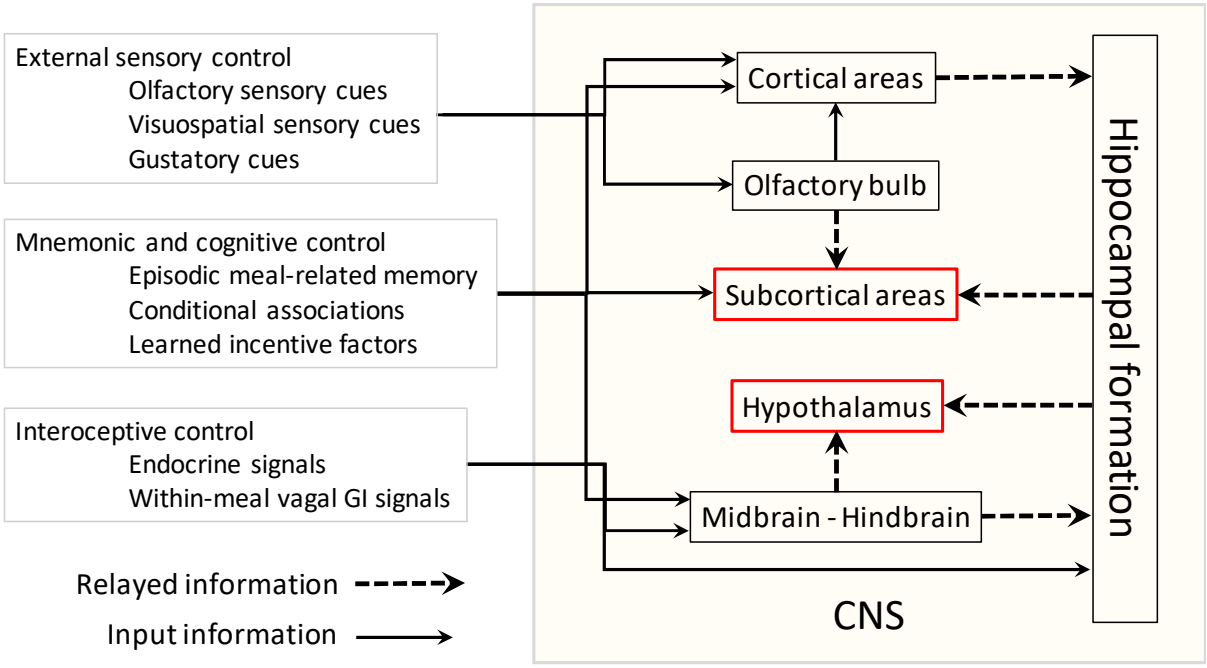

Figure 4. Central network contribution to food intake and appetite.

Information is integrated into the CNS and relayed in various brain centers. The hippocampus is one main relay station and sends back information into the executive metabolic and behavior initiating centers (red boxes). Black lined arrows show direct input information; black dotted arrows show relayed information. Adaption from Kanoski and Grill (2017).

As the hippocampal formation is one unit that interacts with various neuronal centers in the brain, dysfunction in any area might precipitate or exacerbate dysfunction in the others and thus alter food intake behavior.

2 Aims of this thesis

In this study we aimed to shed new light on a poorly studied member of the MKPs, Dusp8, in the context of memory, learning, and glucose sensing using a global and conditional hippocampal knockout mouse model for Dusp8. The predominant expression of Dusp8 in the brain, as well as the genetic associations to diabetes and potentially to bipolar disorder, raises the probability of a central and translational role for Dusp8 in the regulation of glucose homeostasis, cognition, and mood behavior.

Specifically, we aimed to uncover the relevance of Dusp8 in regulating brain morphology and limbic system-related behaviors. Due to its association with diabetes in humans, we hypothesized a role in central glucose sensing and investigated the complex network of glucose sensing brain nuclei in global Dusp8 WT and KO mice. A putative, Dusp8-related link between glucose sensing and cognition was of particular interest. Overall, we wanted to gain further information on the functional role of Dusp8 in health and disease and uncover its contribution to diabetes and cognition.

In the first part of the thesis, we assessed cognition in our global Dusp8 knockout mouse model and investigated brain morphology, learning and memory, spatial memory, as well as motivational behavior. In the second part, we had a closer look at the impact of Dusp8 on sucrose reward behaviors and glucose sensing mechanisms. We used an *in vitro* system to study the cellular impact of Dusp8 on MAPK phosphorylation during glycolysis blockade. We furthermore investigated the influence of Dusp8 on glucose metabolism after 2-deoxy-glucose injections in various brain centers, ranging from homeostatic to limbic and reward systems. As the influence of Dusp8 on hypothalamic control of metabolic homeostasis is already covered by another project in our group, we focused in my third part of the thesis on the metabolic characterization of a hippocampus-specific Dusp8 knockout model in the context of energy and glucose metabolism.

3 Materials

Table 2. List of Chemicals, Enzymes, and Reagents

Chemicals, Reagents, Enzymes	Provider
2-deoxyglucose, 2DG	Sigma-Aldrich Co., St. Louis, MO, USA
4x NuPage buffer	Thermo Fisher Scientific Inc., Waltham, MA, USA
5x Green buffer (Go Taq flexi),	Promega Corporation, Madison, WI, USA
Albumin Bovine Serum Protease Free, BSA (ref. 422361V)	(VWR International LLC., Randor, PA, USA)
Betaine (ref. B0300)	Sigma-Aldrich Co., St. Louis, MO, USA
Chromotrope I2R (ref. A17519)	Alfa Aesar, Haverhill, MA, USA
DABCO (ref. 0718)	Carl Roth GmbH + Co. KG, Karlsruhe, Germany
Deoxynucleotides, dNTPs (ref. 10297018)	Life Technologies/Thermo Fisher Scientific Inc., Waltham, MA, USA
Dithiothreitol, DTT (ref. R0861)	Thermo Fisher Scientific Inc., Waltham, MA, USA
Ethanol, EtOH	Merck Millipore, Burlington, MA, USA
Ethylglycol	Merck Millipore, Burlington, MA, USA
Fetal bovine serum, FBS (ref. 10270-106)	Gibco/Thermo Fisher Scientific Inc., Waltham, MA, USA
Gelatin	Carl Roth GmbH + Co. KG, Karlsruhe, Germany
Gigh glucose DMEM (cat. 41965-039, GibcoTM)	Gibco/Thermo Fisher Scientific Inc., Waltham, MA, USA
Glucose	Carl Roth GmbH + Co. KG, Karlsruhe, Germany
Glycerol	Sigma-Aldrich Co., St. Louis, MO, USA
Halt Phosphatase & Protease Inhibitor Cocktail (ref. 78446)	Thermo Fisher Scientific Inc., Waltham, MA, USA
Hemalum solution acid acc. to Mayer (ref. T685)	Carl Roth GmbH + Co. KG, Karlsruhe, Germany
Lipofectamine 2000 (ref. 11668-019)	Thermo Fisher Scientific Inc., Waltham, MA, USA
Magnesium chloride ($MgCl_{2;}$ 25 mM)	Promega Corporation, Madison, WI, USA
Mannitol	Carl Roth GmbH + Co. KG, Karlsruhe, Germany
Mowiol 4-88 (ref. 0713)	Carl Roth GmbH + Co. KG, Karlsruhe, Germany
Normal goat serum, ref. S26	Merck Millipore, Burlington, MA, USA
Nonfat dried milk powder (ref. #A0830)	AppliChem GmbH, Darmstadt, Germany

O.C.T. Compound (ref. 4583)	Tissue-Tek, Alphen aan den Rijn, The Netherlands
Paraformaldehyde, PFA	Sigma-Aldrich Co., St. Louis, MO, USA
Penicillin-streptomycin, PenStrep (ref. 15140-122)	Gibco/Thermo Fisher Scientific Inc., Waltham, MA, USA
Phenyl-methane-sulfonylfluorid, PMSF	Carl Roth GmbH + Co. KG, Karlsruhe, Germany
Phosphate buffered saline, PBS (ref. cat. 10010015)	Gibco/Thermo Fisher Scientific Inc., Waltham, MA, USA
Polymerase (GoTaq flexi, 5U/µl) (Promega Corporation, Madison USA)	Promega Corporation, Madison, WI, USA
Pursept A Xpress (ref. 230131)	Schülke & Mayr GmbH, Norderstedt, Germany
Radioimmunoprecipitation assay buffer, RIPA (ref. R0278)	Sigma-Aldrich Co., St. Louis, MO, USA
Restore PLUS Western Blot Stripping Buffer (ref. 28358)	Thermo Fisher Scientific Inc., Waltham, MA, USA
Sodium chloride (ref. 92651)	Carl Roth GmbH + Co. KG, Karlsruhe, Germany
Sucrose	Carl Roth GmbH + Co. KG, Karlsruhe, Germany
Tris-sodium-citrat	Carl Roth GmbH + Co. KG, Karlsruhe, Germany
Triton X-100 (ref. T8532)	Sigma-Aldrich Co., St. Louis, MO, USA
Trypsin-EDTA (ref. 25300-054)	Gibco/Thermo Fisher Scientific Inc., Waltham, MA, USA
Tween20 (ref. P1379)	Sigma-Aldrich Co., St. Louis, MO, USA
Xylol	Carl Roth GmbH + Co. KG, Karlsruhe, Germany

Table 3. List of Buffers

Buffer	**Component**
Tris-buffered saline (TBS)	50 mM Tris, 100 mM NaCl, pH7.4
Tris-buffered saline Tween20 (TBS-T)	50 mM Tris, 100 mM NaCl, 0.1 % Tween20, pH7.4
Cryoprotectant buffer	30% glycerol, 30% ethylglycol, 30% sucrose in TBS
Heat induced epitope retrieval (HIER) buffer (Citrat)	0.01 M Tri-sodium-citrat, pH 6.8
Heat induced epitope retrieval (HIER) buffer (Tris)	10 mM Tris, 1 mM EDTA, 0.05% Tween20, pH 9.0
PBS-Triton	01 M PBS, 0.1 % Triton X-100
SUMI buffer	2,5 % gelantin, 0.5 % Triton X-100 in TBS
Elvanol	150 mM Tris, 12 % Mowiol, 2 % DABCO

Table 4. List of Devices and Software

Devices and Software	Company, Provider
ActiMot Box System, TSE ActiMot Version 08.00	TSE Systems, Bad Homburg, Germany
AxioScan.Z1 digital slide scanner	Zeiss, Oberkochen, Germany
Definiens Developer XD 2	Definiens AG, Munich, Germany
GraphPad Prism 8.0.1c, JMP 13	SAS Institute, Cary, NC
EchoMRI, Version 130718, System ID E26-217M	EchoMRI, Houston, TX, USA
Freestyle freedom lite	Abbott Diabetes Care, Alameda, CA, USA
ImageJ (2.0.0-rc-68/1.52f)	Open source Java processing program
iS Version 5.2	LI-COR GmbH, Bad Homburg, Germany
IntelliCage system, IntelliCagePlus Version 3.3.2.0	TSE Systems, Bad Homburg, Germany
Leica CM3050 S Cryostat	Leica Biosystems, Nussloch, Germany
Leica TCS SP5	Leica Microsystems, Wetzlar, Germany
LI-COR Odyssey Fc	LI-COR GmbH, Bad Homburg, Germany
Mouse cage, Bioscape, Type 2	Zoonlab GmbH, Castrop-Rauxel, Germany
NanoDrop 2000 Spectrophotometer	Thermo Fisher Scientific Inc., Waltham, MA, USA
Noldus Pocket Observer Version 2.1.23.f	PSION Teklogix Workabout Pro
Open field arena	TSE Systems, Bad Homburg, Germany
Perfusion pump (ref. P720/66)	Instech Laboratories, Plymouth Meeting, PA, USA
SPSS	IBM, Armonk, NY, USA
Tissue Lyser II	QIAGEN, Hilden, Germany
Viia7 cycler	Applied Biosystems/Thermo Fisher Scientific Inc., Waltham, MA, USA

4 Methods

4.1 Animal experiments

4.1.1 Global Dusp8 KO and conditional Grik4-Cre;Dusp8 KO mice

Dusp8 global wild type (WT) and KO mice were generated as described (Liu et al., 2016) and shown in Figure 5A. All mice in our studies were littermates derived from heterozygous parents on a C57BL/6J background. Mice were bred and group-housed on a 12:12 h light-dark cycle (dark phase from 6 am to 6 pm) at 22°C and 50% to 60% air humidity with free access to chow diet (#1314, Altromin, Spezialfutter GmbH & Co. KG, Lage, Germany) and water. Male global Dusp8 KO mice were partially single-housed due to inter-male aggression (13 out of 29 mice). All samples for protein measurements, weight and volume calculations were taken from the colony of mice tested for behavior after completing the tests. Age of female and male mice ranked from 9 to 11 months and females tested in IntelliCage from 3 to 5 months at the start time of testing. All studies were based on power analyses to assure adequate sample sizes, and approved by the State of Bavaria, Germany (Protocol number VTA 55.2-1-54-2532-46-16). Hippocampus specific Dusp8 KO mice were bred from the transgenic mouse line C57BL/6 TG(Grik4-Cre)G32-4Stl (stock #006474, Jackson Laboratory, Bar Harbor, ME, USA; Nakazawa et al., 2002) and European Mammalian Mutant Cell Repository (EUCOMM) Dusp8tm1a mice (Figure 5B). EUCOMM Dusp8tm1a animals were generated from embryonic stem cell (ESC) clone HEPD0822-2-A10 obtained from EUCOMM. The KO first allele of Dusp8 containing a Frt-flanked LacZ reporter and neomycin selection cassette in intron 2 with a LoxP-flanked exon 3 was present in ESC HEPD0822-2-A10. Chimeric animals were generated by injecting ESCs into albino BALB/c (Charles River, Germany) and blastocysts were transferred into pseudo pregnant foster mothers. Germline transmission was obtained by breeding chimera males to wild type C57BL/6N females. KO first allele (tm1a) was converted into a conditional KO allele (tm1c) by breeding F2 animals to Gt(ROSA)26Sortm1(FLP1)Dym (MGI:2429412). The neomycin cassette and LacZ reporter were removed by Flp-recombinase. Resulting positive animals were backcrossed to wild type C57BL/6J animals to remove the tm1(FLP1)Dym cassette.

Genotyping was performed from genomic DNA isolated from ear tags. See Table 5 for respective genotyping primers purchased from Sigma-Aldrich Co., St. Louis, MO, USA.

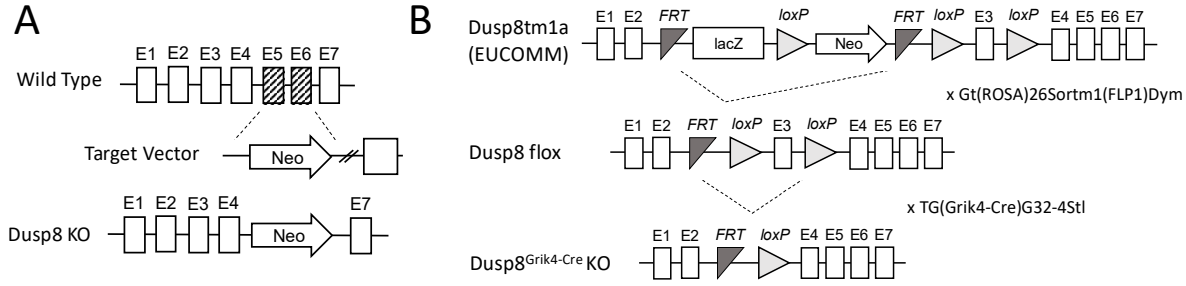

Figure 5. Global and conditional Dusp8 KO model.

(A) Generation of the global Dusp8 KO mice by replacing catalytic domains with neomycin cassette. Adapted from Liu and colleagues (2016). (B) Scheme of generation of hippocampal-specific Dusp8 KO mice by crossing Dusp8tm1a (EUCOMM) mice with Gr(ROSA)26Sortm1(FLP1)Dym and further with TG(Grik4-Cre)G32-Stl animals. E exon, neo neomycin.

Table 5. List of primers for Genotyping

PCR	Primer sequence	Transcript length
EUCOMM Dusp8tm1a WT&flox	Fwd' taaagactgagtgtgcttgggagg Rev' ttattctcccccagctcctaatgg	201 bp
EUCOMM Dusp8tm1a KO	Fwd' taaagactgagtgtgcttgggagg LAR3 cacaacgggttcttctgttagtcc	318 bp
Dusp8_FG2/loxP	Fwd' ggctatgggatgccttctct Rev' cttggtggtccctcaggtag	WT 380 bp KO 335 bp
Cre PCR	Fwd' gcg gtc tgg cag taa aaa cta tc Rev' gtg aaa cag cat tgc tgt cac tt	WT 324 bp Cre 100 bp
Global Dusp8 WT	Fwd' cgc atc gcc ttc tat cgc Rev' ctc cac cat gcc ctc ttc	370 bp
Global Dusp8 KO	Fwd' tgg gca tgt ctt ctg acg ac Rev' agt gag gtc cat cag tct gc	430 bp

Reagents for the genotyping were the following: 5x Green buffer (Go Taq flexi), magnesium chloride ($MgCl_2$; 25 mM), Polymerase (GoTaq flexi, 5U/µl) (Promega Corporation, Madison, WI, USA), Betaine (Sigma Aldrich Co.), and Deoxynucleotides (dNTPS, Life Technologies/Thermo Fisher Scientific Inc., Waltham, MA, USA).

4.1.2 Behavioral testing

4.1.2.1 Open Field Test

Open field tests were performed between 08.00 am – 02.00 pm in a sound-attenuated test room with adjustable light source. Mice were placed in the 45 cm x 45 cm x 40 cm open field arena (TSE Systems, Bad Homburg, Germany) in the middle position of the hind wall (facing the wall). The locomotor activity of the mouse was automatically

tracked for 20 min by using a light beam break ActiMot Box System (TSE ActiMot Version 08.00, TSE Systems), as previously described (Holter et al., 2015a). Prior to testing, light conditions were set to 200 lx in the middle of the arena. After each test session, the arena was wiped with Pursept A Xpress (Schülke & Mayr GmbH, Norderstedt, Germany).

4.1.2.2 Acoustic startle response / Prepulse Inhibition

Acoustic startle response (ASR) and Prepulse Inhibition (PPI) were assessed to investigate sensorimotor gating. Mice were restrained in a plastic tube placed on a fine scale within a dark sound box and had an acclimation period of 5 min. A fine scale was used to measure physical movement of the mice triggered by acoustic stimuli. A background noise of 65 dB was set for the whole session. Conducting measurements for ASR and PPI were arranged in a pseudo-random order and organized in 10 blocks, each presented 10 times. For ASR acoustic stimulus levels of 70, 80, 85, 90, 100, 110, and 120 dB were presented. PPI were assessed at an acoustic stimulus level of 110 dB with a delay of 60 ms. Inhibition was measured for prepulse levels of 67, 69, 73, and 81 dB. Each testing block began with a presentation of the startle stimulus alone (110 dB) five times. The restrainer and fine scale were cleaned with Pursept A Xpress (Schülke & Mayr GmbH).

4.1.2.3 Object recognition test

Object recognition memory test was performed between 08.00 am - 02.00 pm. Two identical objects were presented three times to the test mouse in a neutral test cage (Bioscape, Type 2, length 29.5 cm x width 18.5 cm x height 13 cm) for 5 min with an inter-trial interval of 15 min. The first test phase started 3 h after the last sample session. An unfamiliar object was presented together with one familiar object for 5 min. The second test phase was performed 24 h after the last sample session. Another unfamiliar object was presented alongside the familiar object. Interaction times with the different objects were recorded manually via a handheld computer PSION Teklogix Workabout Pro (Noldus Pocket Observer Version 2.1.23.f). Tests were performed according to a previously published protocol by Holter and colleagues (Holter et al., 2015b).

4.1.2.4 Y-maze

Spontaneous alternations in the Y-maze (in-house built, internal dimensions: arm length 29.5 cm; arm width 8 cm; height 15 cm) tested and analyzed according to Holter et al. (Holter et al., 2015b) and conducted between 08.00 am – 02.00 pm. Tested mice were introduced in a Y-shaped maze facing the wall of the starting arm. Arm entries were manually recorded for 5 min. Starting arms were alternated. Prior to testing, light conditions were set to 100 lx in the center of the arena. After each test session, Y-maze was cleaned with Pursept A Xpress (Schülke & Mayr GmbH).

4.1.2.5 Social discrimination

Social discrimination tests were performed and analyzed as described (Holter et al., 2015b), and conducted between 08.00 am – 02.00 pm. Prior to testing, experimental mice were transferred to fresh cages without food or water. Briefly, for the sample phase an ovariectomized (OVX) 129S1/SvlmJ female stimulus mouse was exposed to the test mouse in a neutral cage for 4 min at an illumination of 200 lx. After a 2 h inter-trial-interval both the familiar and a new unfamiliar stimulus mouse were placed into a neutral cage to the test mouse for another 4 min. Interactions of the test mouse with the stimulus mice were tracked manually with a handheld computer PSION Teklogix Workabout Pro (Noldus Pocket Observer Version 2.1.23.f) during both sample and test phases.

4.1.2.6 Intellicage habituation

Observer-independent tests for spatial learning in the IntelliCage system (IntelliCagePlus Version 3.3.2.0, TSE Systems) were performed with female mice only. Mice were group-housed, up to 10 animals per cage, in genotype-mixed groups. 3 d prior to the habituation in the IntelliCage, all mice were subcutaneously implanted with passive transponders that allowed distinguishing mice entering the four IntelliCage corners. Before starting the test programs, mice were allowed to habituate for 3 d in the IntelliCage with free access to food (Altromin, Spezialfutter GmbH & Co. KG) and water without a nose poke performance. Following habituation, mice were trained to get access to bottle spouts in all four corners after a nose poke action. Respective doors open to enable access to drink for 7 sec.

4.1.2.7 Place learning

Place learning was conducted by assigning each mouse to one corner of the cage for access to the drinking bottles after a nose poke (correct corner, correct nose poke). If the nose poking was performed at another corner (incorrect corner, incorrect nose poke), performance was recorded, but access was denied. Assignments were equally distributed over the cage, and nose pokes and corner visits were automatically tracked and recorded by the IntelliCage software for 5 d. Mice were not disturbed or handled during testing days. The place learning task was performed according to the published protocol of Holter and colleagues (Holter et al. 2015b).

4.1.2.8 Reversal learning

Immediately after the place learning task, mice were subjected to the reversal learning task. Briefly, each mouse was assigned to the opposite corner of the cage for access to the drinking bottles after a nose poke, and nose pokes and corner visits were monitored for 5 d. Mice were not disturbed or handled during testing days. The reversal learning test was performed according to Holter et al. (Holter et al., 2015b).

4.1.2.9 Two-bottle sucrose versus water choice test

To introduce mice to the 10% sucrose (Carl Roth GmbH + Co. KG, Karlsruhe, Germany) solution used for the sucrose wanting test, animals got access for 7 sec to sucrose solution in the respective, correct corner after nose poke performance at both drinking bottles. For a habituation period of 24 hours, no plain water, but only sucrose solution was available. After this forced sucrose period, the test program was switched to a two-bottle sucrose versus water choice test in the designated correct corner. Mice had access for 7 sec to water or sucrose at the left or right side, respectively, in the correct corner after one single nose poke performance. After each trial, mice had to leave the test corner before starting a new one. Visits in correct and incorrect corners, first choice nose pokes, and total number of nose pokes and licks at the spouts in the respective sides were monitored for five days and analyzed.

4.1.2.10 Progressive ratio set up

For measuring the motivation of tested mice for sucrose, the two-bottle sucrose versus water choice test was combined with a progressive ratio (PR)-2 paradigm for sucrose access. Animals had to perform increasing numbers of nose pokes in the respective correct corner in order to get access to the sucrose solution for 5 sec. After every 10th visit in the correct corner with a first choice for sucrose, mice had to perform two additional nose pokes (two nose pokes were added to the previous required number of nose pokes). For accessing water, the fixed ratio of 1 nose poke was kept. Mice had to give only one nose poke throughout the entire testing time to access the water bottle in the correct corner. After each trial, mice had to leave the test corner before starting a new nose poke performance. Motivation for getting access to sucrose was measured with the progressive ratio scale.

4.1.3 *In vivo* glucose sensing

Global Dusp8 WT and KO mice were fed a 45% HFD (D12451, Research diets Inc., New Brunswick, NJ, USA) for 12 weeks. Study groups were weight matched and fasted for 4 h prior to i.p. injection of 500 mg 2-deoxy-glucose (2DG) (Sigma-Aldrich Co.)/kg BW or PBS (Gibco/Life technologies/Thermo Fisher Scientific Inc., Waltham, MA, USA). Mice were sacrificed 1 h after injection. Right before sacrifice in CO_2, blood glucose from the tail vein was measured using a handheld glucometer (Freestyle freedom lite, Abbott Diabetes Care, Alameda, CA, USA). Mice were perfused and brains were processed for immunohistochemical stainings as described in 4.2.1 Tissue preparation. Cryosections of perfused brains were processed and stained for c-fos according to the given procedure in section 4.2.2 Cryosectioning.

4.1.4 Metabolic phenotyping

4.1.4.1 HFD feeding and food intake

Prior to changing the feeding from chow diet to 45 % HFD (D12451, Research diets Inc.), body weight of respective mice were measured. Body weight and food intake were measured weekly for 10 consecutive weeks. As the majority of mice were group-housed, food intake was measured once a week per cage. The food intake per single mouse was then calculated by dividing the number of animals within the respective cage.

4.1.4.2 GTT and body composition

A glucose tolerance test was performed after 12 weeks of 45 % HFD-feeding. Prior to injection, mice were fasted for 6 h. Mice were injected i.p. with 1.5 g glucose (Carl Roth GmbH + Co.)/kg body weight, and blood glucose concentrations were measured in blood collected from the tail vein before injection, and 15, 30, 60, and 120 minutes after using a handheld glucometer (Abbott Diabetes Care). Analysis of body composition was performed using the non-invasive magnetic-resonance whole-body approach with EchoMRI (EchoMRI, Houston, TX, USA).

4.2 Histology

4.2.1 Tissue preparation

Whole hippocampus microdissections were performed from fresh brain tissue. Fresh tissue was further processed for protein extraction. For preparing immunohistochemical stainings of the brain, mice were euthanized in CO_2 and perfused through the heart using a peristaltic pump. After a washing step with ice cold PBS, (Gibco) tissue was perfused with 4 % paraformaldehyde (PFA, Sigma-Aldrich Co.). Post-fixation of the brain was overnight at 4 °C in 4 % PFA. After equilibration with 30 % sucrose (Carl Roth GmbH + Co. KG), brains were maintained in PBS until further processing. Brains were cut coronally with Leica CM3050 S Cryostat (Leica Biosystems) into 20 µm sections. Brain sections were immediately mounted on glass slides, dried at RT, and then stored at -20 °C. Brain sections for immunofluorescence staining were stored in cryoprotectant buffer at -20 °C until the staining process.

4.2.2 Cryosectioning

Perfused, fixed, and sucrose-saturated brains were mounted on a tissue specimen with O.C.T. Compound (Tissue-Tek, Alphen aan den Rijn, The Netherlands) and frozen to -20°C for at least 20 min to ensure proper freezing of the entire brain tissue. With a Leica CM3050 S Cryostat (Leica Biosystems, Nussloch, Germany), slices of 20 µm were cut in a coronal orientation. Sections were collected in Tris-buffered saline (TBS) and washed 3x in TBS for 5 min to remove remaining O.C.T. compound. Sections were transferred to cryoprotectant buffer and stored at -20°C until further processing.

4.2.3 H&E staining

Hematoxylin and eosin (H&E) staining was performed on dried cryosections on glass slides. Sections were rehydrated with an ethanol dilution row of 90%, 80%, 70%, and 60%, for 2 min each. Alcohol dilution row was followed by a 2 min incubation step in deionized water. Sections were stained in filtered Mayer's solution (Hemalum solution acid acc. to Mayer, Carl Roth GmbH + Co. KG) followed by 3 x for 2 min with tap water. Two hydration steps in 90% and 100% ethanol for 2 min each were followed by an incubation in chromotrope 2R (Alfa Aesar, Haverhill, MA, USA) for 3 min. Slides were washed in 90% and 100% for 1 min each and incubated in xylol (Carl Roth GmbH + Co. KG) for 5 min. Slides were mounted immediately and dried at RT.

4.2.4 Immunohistochemistry

For immunohistochemistry, cut brain sections stored in cryoprotectant buffer at -20°C were washed 3 x 3 min and immediately mounted on glass slides, dried at room temperature, and then stored at -20°C. Slides were rehydrated with xylol, 100%, 90%, 70%, 60%, and 50% ethanol dilution with an incubation time of 2 min each. A heat induced antigen retrieval (HIER) was performed. Slides were boiled in HIER buffer 2 x for 5 min and cooled to RT in tap water. After rinsing with TBS, the slides were blocked in 10% NGS blocking solution for 1h at RT. Incubation with primary antibody was overnight at 4°C. To remove the primary antibody, slides ware washed 3 x 10 min in TBS. Secondary AB was incubated for 1 h at RT. Secondary antibody solution was removed with 3 x 10 min washing steps with TBS. The following antibodies were employed for immunohistochemistry: rabbit anti-c-fos (1:200; c-052, Santa Cruz Biotechnology), rabbit anti-Ki67 (1:1000, ab15580, Abcam), or rabbit anti-Casp3 (1:100, Cat #9664, Cell Signaling Technology) as primary antibodies or anti-rabbit (1:750, Vector BA 1000) as secondary antibody. Detections were carried out with a Discovery® DAB Map Kit (Roche Diagnostics, Switzerland / Ventana Medical Systems). Before covering the slides in mounting medium, a dehydration step of the sections was performed with 50%, 60%, 70%, 80%, 90%, and 2 x100% ethanol dilution for 2 min each and 5 min of xylol.

4.2.5 Immunofluorescence

For immunofluorescence, staining brain sections were washed 3 x 10 min in TBS and afterwards blocked in SUMI buffer for 1 h. The following antibodies were used for detecting the respective proteins: anti-phospho-c-jun polyclonal rabbit, 1:1000, Cat #9261, Cell Signaling Technology), anti-phospho-p38 polyclonal rabbit, 1:1000, Cat #9211, Cell Signaling Technology). Sections were incubated in the antibody dilutions over night at 4 °C. For immunofluorescence staining against dopamine transporter (DAT), brain sections were treated in Citrat-HIER buffer for 30 min at 85 °C. Sections were washed 3 x 5 min in PBS-Triton and blocked in PBS-Triton 1 % FBS, 2 % non-fat milk powder (AppliChem GmbH, Darmstadt, Germany). Primary antibody was rat anti-DAT (1:200, Cat. #MAB369, Merck Millipore, Burlington, MA, USA). Primary antibodies were removed and sections were washed 3 x 10 min in TBS. Goat anti-rabbit IgG (H+L) Alexa Fluor 488 antibody (Cat. #A-11008, Life technologies/Thermo Fisher Scientific Inc.) was used in the dilution 1:1000 in SUMI buffer and incubated for 1 h at room temperature. Sections were washed again 3 x 10 min in TBS, mounted on glass slides and dried at room temperature. The last washing step included DAPI in the dilution of 1:10,000. Sections were covered in Elvanol mounting medium and sealed under a coverslip. Until imaging slides were stored in the dark at 4 °C.

4.2.6 Image based manually and automated cell counting, volume calculation

Immunofluorescent stained tissue was scanned with a 10x or 20x objective using a Leica TCS SP5 (Leica Microsystems, Wetzlar, Germany) confocal laser scanner microscope. Respective brain regions and nuclei were annotated and positive cells counted manually. Number of positive cells were normalized on the area of the region of interest. Immunohistochemically stained tissue sections were scanned at 20x objective magnification using an AxioScan.Z1 digital slide scanner (Zeiss, Oberkochen, Germany). Images were evaluated using the commercially available image analysis software Definiens Developer XD 2 (Definiens AG, Munich, Germany), following a previously published procedure (Feuchtinger et al., 2015). Regions of interest, e.g. specific brain areas, were annotated manually. The calculated parameters within these defined regions were the ratio of positively immunostained cells per total cells. The annotation of hippocampal structures was performed manually according to Franklin and Paxinos using Definiens Developer XD 2 (Definiens AG)

software on H&E stained brain section scans. Every 10th section of 20 µm thick cuts was annotated resulting in 16 to 18 sections per hippocampus. Volumes were calculated with the following formula: V=(a+b)/2×200 µm, in which a and b are the areas of the annotated hippocampi of the brain slides given by the imaging software. Single volumes were added up to the total volume of the hippocampus.

4.3 Cell culture

4.3.1 Cell line maintenance

The hypothalamic cell line CLU177 were maintained in 175T cell culture flask at 37 °C and 5 % CO_2 in high glucose DMEM (Gibco) containing 10 % fetal bovine serum (FBS) (Gibco) and 1% penicillin-streptomycin (PenStrep) (Gibco) (full medium). Cells were cultivated until they reached a confluency of 80-90 %. After reaching this confluency, cells were spilt 1:20 to ensure proper cell growth. Medium was removed, and cells were washed with PBS (Gibco). For detaching from the surface, cells were incubated for 5 min in 5 % Trypsin-EDTA (Gibco) at 37 °C. Trypsinization was halted by the addition of full medium to the detached cells. Cells were spun down for 5 min at 500 x g and resuspended in full medium before seeding them in a fresh 175T cell culture flask.

4.3.2 Transfection of CLU177 cells

For overexpression of CLU177, cells were seeded in a 6-well plate with 25,000 cells per well, one day prior to transfection (60 % confluency). Lipofectamine 2000 (Thermo Fisher Scientific Inc.) was used as a transfection reagent. 6 µl of Lipofectamine 2000 (Thermo Fisher Scientific Inc.) and 4 µg plasmid DNA were diluted in 100 µl plain high glucose DMEM (Gibco) medium, respectively. Dilutions were inverted three times and incubated for 5 min at RT. Next, plasmid dilution and Lipofectamine 2000 dilutions were combined and incubated again for 10 min at RT. Transfection medium was then added dropwise to the cells. After 6 h 500 µl of full medium was added to the wells. The pCMV6-GFP plasmid (insert GFP, origene, kanamycin (25 µg/ml), G418) was transfected as control, and the pCMV6-Dusp8 plasmid (insert Dusp8, origene, kanamycin (25 µg/ml), G418) was used to overexpress Dusp8 specifically.

4.3.3 2DG treatment of CLU177 cells

For the glucose restriction and 2DG stimulation experiments, 75 000 cells per well were seeded into a 6-well plate. Cells were cultivated for one day until they reached confluency of 80%. 2DG treatment procedure was identical for naïve or CLU177 cells transfected with pCMV6-GFP or pCMV6-Dusp8, respectively. Prior to the treatment, cells were incubated for 3 h in starvation medium (high glucose DMEM (Gibco), 1% FBS (Gibco), 1% PenStrep (Gibco)). The treatment with increasing 2DG concentrations and the negative glucose control were performed in isosmotic conditions as mannitol (Carl Roth GmbH + Co. KG) was added in indicated concentrations to always reach a final concentration of 25 mM sugar: control = 25 mM glucose, 2.5 mM 2DG + 22.5 mM mannitol, 10 mM 2DG + 15 mM mannitol, 25 mM 2DG, - glucose = 25 mM mannitol. Cells were treated for 1 h, medium was removed and cells were washed with ice cold PBS (Gibco). After removing the PBS, cells were immediately frozen in dry ice and kept at -80°C for further processing.

4.4 Protein extraction and transcriptional analysis

4.4.1 Protein extraction from brain tissue

Hippocampus tissue was lysed in Radioimmunoprecipitation assay buffer (RIPA, Thermo Fisher Scientific Inc.) containing Halt Phosphatase and Protease Inhibitor Cocktail (Thermo Fisher Scientific) and 1 mM phenyl-methane-sulfonylfluorid (PMSF, Carl Roth GmbH + Co. KG) in a Tissue Lyser II (QIAGEN, Hilden, Germany) for 2 min in pre-cooled racks. Samples were then centrifuged (12,000 x g, 7 min) and supernatants were collected. Until further processing, samples were stored at -80 °C.

4.4.2 Protein extraction from cells

6-well plates with frozen cells were carefully thawed on ice and cells were scraped off the wells in 100 µl of RIPA buffer containing Halt Phosphatase and Protease Inhibitor Cocktail and 1 mM PMSF and transferred in a 1.5 ml Eppendorf reaction tube. Cell lysates of two wells were pooled to get a decent amount of protein concentration for SDS page and western blotting. Samples were then centrifuged (12,000 x g, 7 min) and supernatants were collected.

4.4.3 SDS page and western blot

Protein concentrations of isolated samples were measured using Pierce BCA Protein Assay Kit (Thermo Fisher Scientific Inc.). Samples were diluted in lysis buffer for equal concentrations and 4x NuPage buffer (Thermo Fisher Scientific Inc.) + 50 µM dithiothreitol (DTT, Sigma-Aldrich Co.) were added. After denaturation at 95 °C for 10 min samples were loaded and separated on a 4 - 20 % gradient Criterion™ TGX™ Precast Gels (cat. 5671094, Bio-Rad, Munich, Germany) and then transferred to a PVDF membrane (cat. 1704157, Bio-Rad). Membranes were blocked in TBS with 0.05 % Tween20 (Sigma-Aldrich Co.) (TBS-T) containing 5 % BSA (VWR International LLC., Randor, PA, USA) for 1 h. Proteins were detected by the following primary antibodies diluted in blocking buffer: anti-phospho-SAPK/JNK (polyclonal rabbit, 1:1000, Cat #9251, Cell Signaling Technology, Danvers, MA, USA), anti-JNK1 (monoclonal mouse, 1:1000, Cat #3708, Cell Signaling Technology), anti-phospho-Erk (polyclonal rabbit, 1:1000, Cat #9101, Cell Signaling Technology), anti-Erk (polyclonal rabbit, 1:1000, Cat #9102, Cell Signaling Technology) anti-phospho-p38 polyclonal rabbit, 1:1000, Cat #4511, Cell Signaling Technology), anti-p38 (polyclonal rabbit, 1:1000, Cat #9212, Cell Signaling Technology), and anti-GAPDH (monoclonal mouse, 1:10,000, Cat sc166545; Santa Cruz Biotechnology, Dallas, TX, USA). Secondary antibodies anti-rabbit HRP (goat anti-rabbit IgG-HRP, Cat sc-2004, Santa Cruz Biotechnology) and anti-mouse HRP (mIgGk BP-HRP, Cat sc-516102, Santa Cruz Biotechnology) were diluted 1:10,000. ECL Clarity (Cat# 170-5060, Biorad) was used for detection of HRP-induced chemiluminescence with Amersham Hyperfilm ECL (#28906836, GE Healthcare Limited, Little Chalfont, UK) or with the Fluorescence-chemiluminescence system LI-COR Odyssey Fc (LI-COR GmbH, Bad Homburg, Germany) and imaging software iS Version 5.2. Densitometric analyses were performed with ImageJ (2.0.0-rc-68/1.52f). For the detection of multiple antibodies, membranes were stripped with Restore PLUS Western Blot Stripping Buffer (Thermo Fisher Scientific Inc.) followed by blocking for 1 h.

4.4.4 RNA isolation from cells

RNA of CLU177 cells was extracted using the NucleoSpin RNA extraction kit (Macherey-Nagel GmbH + Co. KG, Düren, Germany) according to the manufacturers protocol. Cells were scraped from the wells in 150 µl RIPA containing 1 %

Protease/Phosphatase inhibitor, 1 % EDTA (Thermo Fisher Scientific Inc.), 1 % PMSF and 0.5 % RNasin Plus (Cat. N261, Promega). 300 µl of RA1 buffer containing 2 % DTT buffer was added to 50 µl of cell lysate and either processed immediately or stored at -80 °C. For precipitation of RNA 350 µl of ethanol (70 %) were added to the lysate and mixed properly. Lysates were transferred to NucleoSpin RNA columns and spun down for 30 s at 11,000 x g. The binding membrane of the column was desalted using 350 µl of provided membrane desalting buffer and centrifuged for 1 min at 11,000 x g. Bound DNA was digested using 95 µl provided DNase reaction mix, incubated for 15 min and inactivated with 200 µl RAW2 buffer. Buffer was removed by spinning 11,000 x g for 30 s. Membrane was washed two times using 600 µl RA3 and 250 µl RA3 buffer, respectively. Washing buffer was removed by spinning at 11,000 x g for 30 s and 2 min respectively. RNA was eluted in 40 µl pre-warmed provided RNase-free water. Concentration of RNA was measured immediately using NanoDrop 2000 (Thermo Fisher Scientific Inc.) or stored at -80 °C.

4.4.5 Quantitative polymerase chain reaction

QuantiTec Reverse Transcription Kit (Qiagen N.V., Hilden, Germany) was used to transcribe 0.2 µg of extracted RNA to complementary DNA (cDNA). cDNA was diluted 1:5 and 2µl diluted cDNA was used for quantitative polymerase chain reactions using TaqMan Assay (Applied Biosystems/Fisher Scientific Inc.). Samples were run in a 384-well plate containing 2.5 µl master mix, 0.25 µl water, 0.25 µl TaqMan Assay, and 2 µl diluted cDNA (total volume 5 µl). TaqMan universal master mix II was used for the reaction. Following TaqMan Assay probes were used: Dusp8 (Mm01158980_m1) and HPRT (Mm01545399_m1). The delta-delta cycle threshold (Ct) was used for evaluating the expression levels. Hypoxanthine phosphoribosyltransferase 1 (HPRT) expression level was used as a reference housekeeping gene. Reaction and measurement were conducted with a Viia7 cycler (Applied Biosystems/Thermo Fisher Scientific Inc.).

4.5 Statistical analysis

For statistical analyses, GraphPad Prism 8.0.1c, JMP 13 (SAS Institute, Cary, NC), or SPSS (IBM, Armonk, NY, USA) were used. Multiple comparisons were performed by Two-way ANOVA with ad hoc Sidak’s multiple comparison tests. Two-tailed unpaired

Student’s t-tests were used to compare two groups. Murine hippocampal weights and volumes were further assessed by Analysis of Co-Variance (ANCOVA) with skull length and/or body weight as covariates. P-values ≤ 0.05 were considered as statistically significant. Unless stated otherwise, all results are presented as means $\pm$ SEM.

5 Results

5.1 Dusp8 is a modulator of hippocampus morphology and signaling in mice

5.1.1 Reduced hippocampal volume of Dusp8 KO mice

Dusp8 is highly expressed in the CNS, and especially in the limbic system of the brain. We therefore investigated the influence of Dusp8 on brain morphology taking advantage of a global Dusp8 KO mouse model. Microdissection of different brain areas was performed from fresh tissue of chow fed body weight matched animals. We found comparable weights of the hypothalamus, the amygdala, and the prefrontal cortex in male and female mice. Only the hippocampus weight was significantly reduced in Dusp8 KO mice compared to WT littermates (Fig. 6A,C). To confirm this finding we performed sequential cuts through fixed brain tissue and calculated the volume of the hippocampus from H&E stained sections. We found a reduced hippocampal volume in both sexes of mice deficient for Dusp8 (Fig. 6B,D).

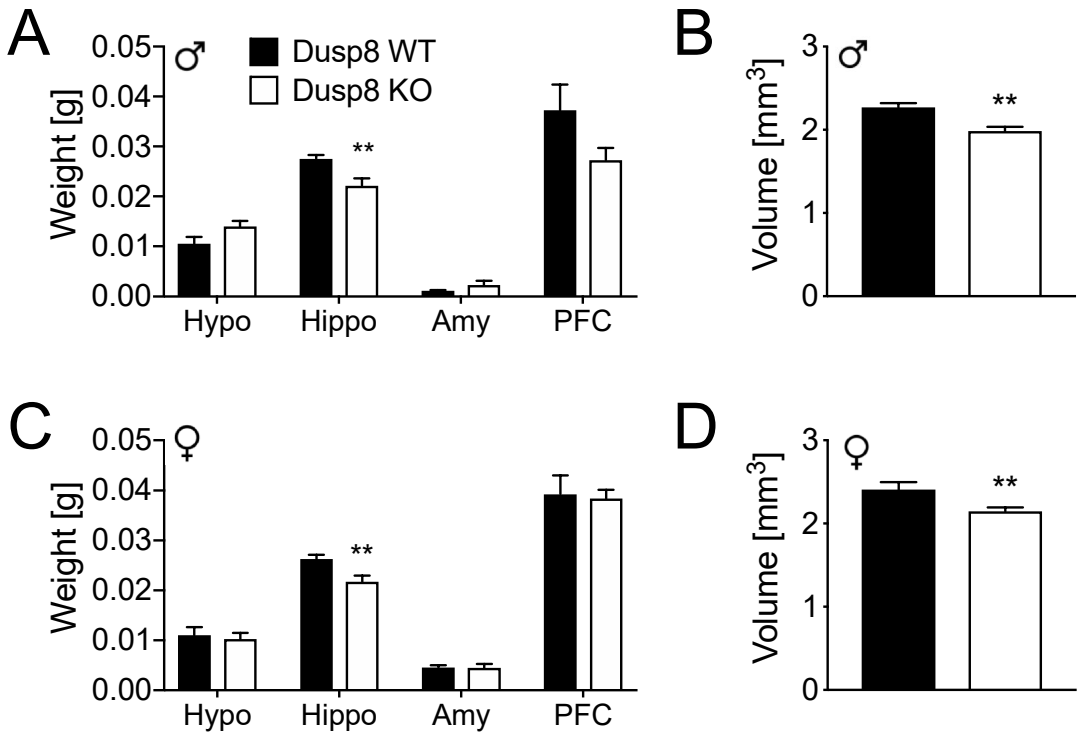

Figure 6. Brain microdissection and hippocampal volume of male and female Dusp8 WT and KO mice.

Tissue weights were recorded from freshly microdissected hypothalamic (Hypo), hippocampi (Hippo), amygdales (Amy) and prefrontal cortices (PFC) (A,C) Male WT: n=7, male KO: n=6-7; female WT: n=7-8, female KO: n=7-8. Hippocampus volume calculations from sequential cryosections (B,D). Male WT: n=5, male KO: n=7, female WT: n=4, female KO: n=6. Means ± SEM. ** $p < 0.01$.

Both hippocampal weight and hippocampal volume were reduced in Dusp8 deficient mice compared to WT littermates.

5.1.2 Unperturbed cellular proliferation in the hippocampus

As both male and female mice deficient for Dusp8 showed a reduced hippocampal volume and weight, we next performed stainings for cellular apoptosis and proliferation with markers Ki67 and Casp3, respectively. We distinguished between the dorsal and ventral part, as well as three subregions of the hippocampus (Fig. 7A). We found similar levels of Ki67 positive cells per total cells within the investigated subregions CA1, CA3, and DG in Dusp8 WT and Dusp8 KO male (Fig. 7B,C) and female (Fig. 7D,E) mice compared to WT controls. Comparable levels of Ki67 positive cells were found within the investigated subregions CA1, CA3, and DG. For the apoptosis marker, Casp3, we could not detect any positive cells in the brain sections of all investigated mice.

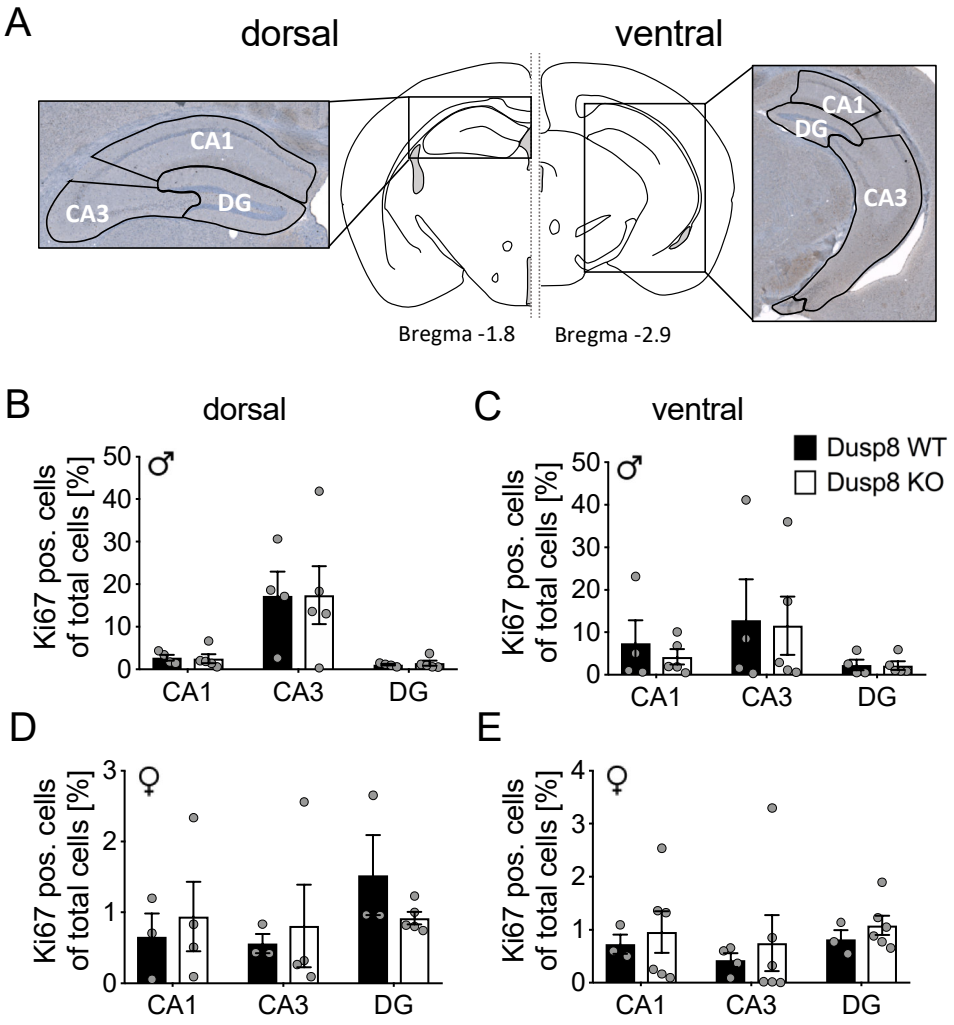

Figure 7. Neuronal proliferation in hippocampal CA1, CA3 and DG regions.

Respective regions were manually assigned (A). Immunohistochemical detection of Ki67-positive cells in in the dorsal (B,D) and ventral (C,E) hippocampus of male (B,C) and female (D,E) Dusp8 WT and KO mice. Male WT: n=4, male KO: n=5; female WT: n=3, female KO: n=4-6. Means ± SEM.

Our results indicate that neither cellular proliferation, nor apoptosis within the hippocampus of global Dusp8 KO male and female mice compared the WT control mice, is the underlying cause of the altered hippocampus morphology.

5.1.3 Increased MAPK Erk-signaling in hippocampal structure of Dusp8 KO mice

Since Dusp8 is a physiological inhibitor of MAPKs Jnk, p38, and Erk, we investigated the activation levels of these MAPKs in hippocampal protein lysates of Dusp8 KO mice compared to WT controls. Phosphorylation levels of Jnk and p38 were not altered in the hippocampus of male and female mice deficient for the phosphatase (Fig. 8A-D). However, for the MAPK Erk, an increased phosphorylation level relative to the total

protein and the loading control was found in the hippocampus of Dusp8 KO mice. This increase in P-ERK levels were borderline significant ($p=0.0806$, Fig. 8E) in male and significant in female Dusp8 KO mice ($p<0.01$, Fig. 8F) relative to their WT littermates.

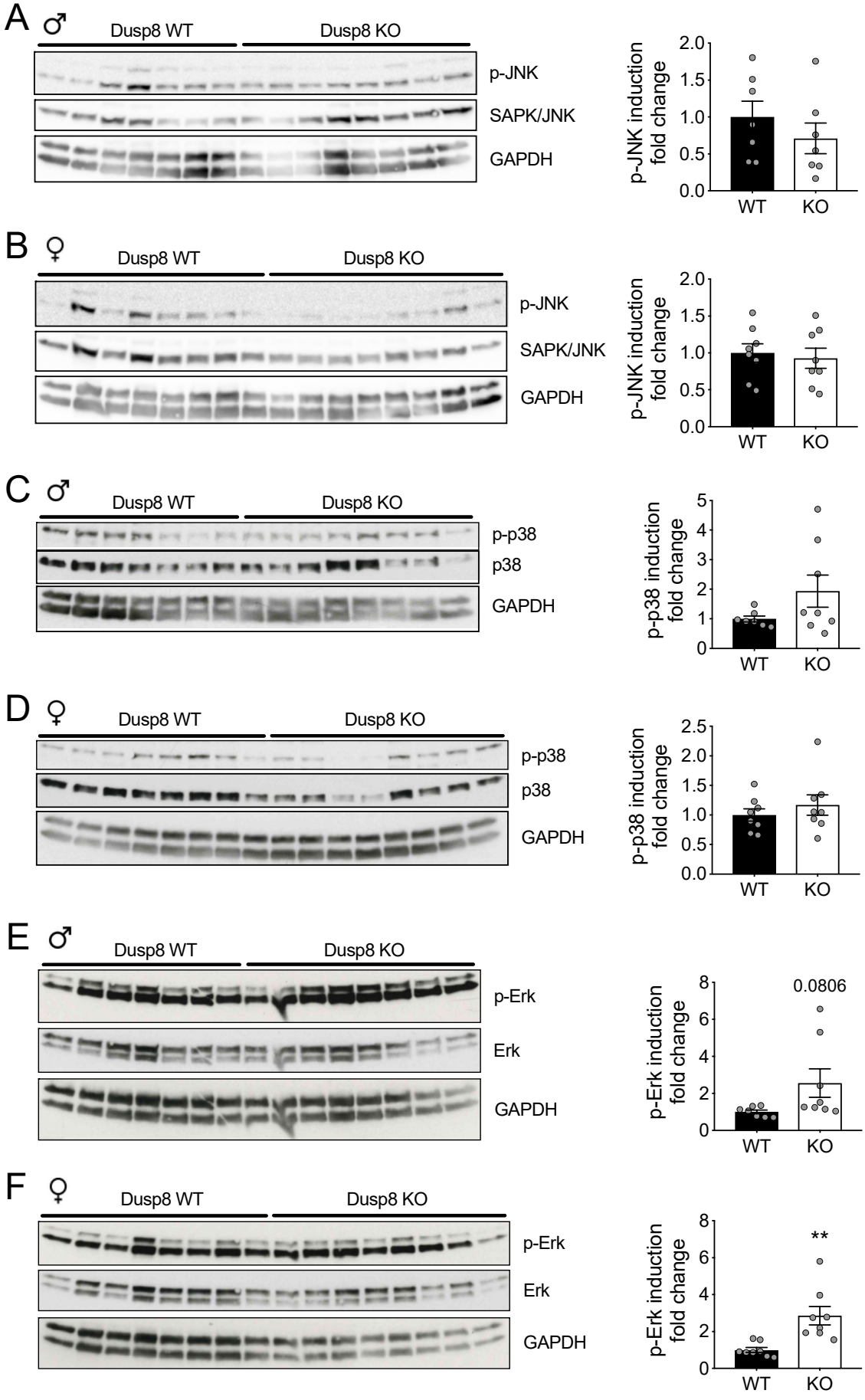
A ♂
Dusp8 WT
Dusp8 KO
p-JNK
SAPK/JNK
GAPDH
p-JNK induction fold change
2.0
1.5
1.0
0.5
0.0
WT
KO
B ♀
Dusp8 WT
Dusp8 KO
p-JNK
SAPK/JNK
GAPDH
p-JNK induction fold change
2.0
1.5
1.0
0.5
0.0
WT
KO
C ♂
Dusp8 WT
Dusp8 KO
p-p38
p38
GAPDH
p-p38 induction fold change
5
4
3
2
1
0
WT
KO
D ♀
Dusp8 WT
Dusp8 KO
p-p38
p38
GAPDH
p-p38 induction fold change
2.5
2.0
1.5
1.0
0.5
0.0
WT
KO
E ♂
Dusp8 WT
Dusp8 KO
p-Erk
Erk
GAPDH
p-Erk induction fold change
0.0806
8
6
4
2
0
WT
KO
F ♀
Dusp8 WT
Dusp8 KO
p-Erk
Erk
GAPDH
p-Erk induction fold change
**
8
6
4
2
0
WT
KO

Figure 8. MAPK activity in the hippocampus of Dusp8 KO and WT mice.

Western blots and densitometric analysis for phosphorylated and non-phosphorylated MAPKs are shown. JNK-signaling in male (A) and female (B) Dusp8 WT and Dusp8 KO mice. Activity of p38-signaling pathway in male (C) and female (D) Dusp8 WT and Duso8 KO mice. Western blot analysis of Erk-signaling in the hippocampus of male (E) and female (F) Dusp8 WT and Dusp8 KO mice. Fold change of phosphorylation was calculated relative to respective total protein and GAPDH as loading control. 30 µg of hippocampus protein was loaded per animal. Male WT: n=7, male KO: n=8; female WT: n=8, female KO: n=8. Means ± SEM. ** $p < 0.01$.

Taken together, the Dusp8 deficient mice showed unperturbed phosphorylation of Jnk and p38 MAPK in the hippocampus, whereas phosphorylation of Erk was increased. This suggests a hippocampus-specific selectivity of Dusp8 for Erk rather than for Jnk or p38.

5.2 Dusp8 is a rheostat for social and cognitive behaviors in mice

5.2.1 Assessing cognition in Dusp8-deficient mice

The hippocampus is one of the main centers for learning and memory, spatial orientation, as well as emotional control. Prompted by the reduced hippocampal mass and volume, we wanted to investigate whether this morphological alteration has any influence on hippocampus-dependent behavior such as learning and memory, as well as cognition in Dusp8 deficient mice.

5.2.1.1 Intact sensory motor gating and increased anxiety in Dusp8 KO mice

The protocol for the cognition pipeline included a basic test for sensorimotor gating by exposing mice to an acoustic stimulus. We measured the startle response to respective increasing acoustic stimuli. Startle responses to acoustic stimuli were comparable between Dusp8 KO and WT mice in both male (Fig. 9A) and female (Fig. 9B) animals. To get more insight into the basis of potential gating deficits in forebrain circuitry of Dusp8 KO mice we conducted a prepulse inhibition test. We could not find any differences in inhibition response to an acoustic stimulus evoked startle response between Dusp8 KO mice and Dusp8 WT littermates (Fig. 9C,D).

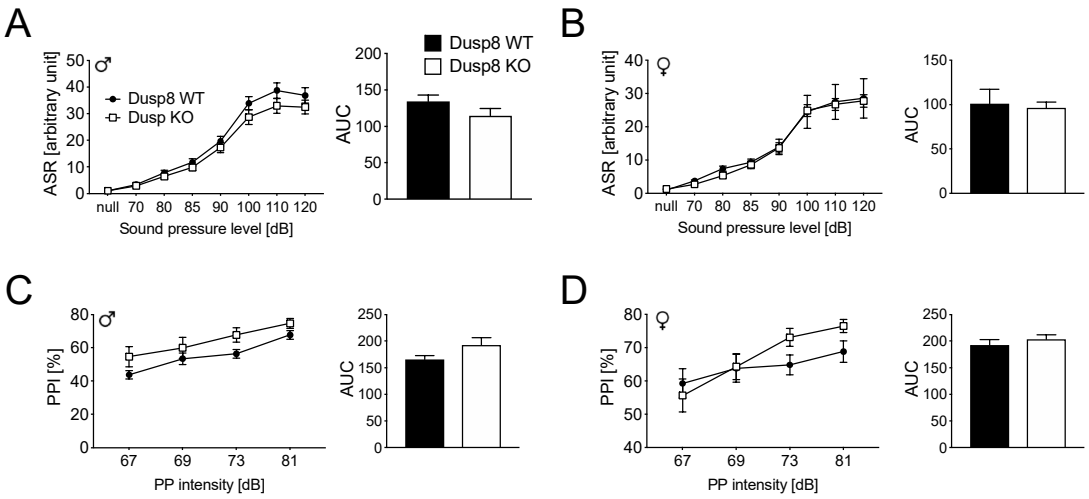

Figure 9. Acoustic Startle Response and Prepulse Inhibition in Dusp8 KO and WT mice.

Acoustic startle response (ASR) was measured at increasing levels of stimuli varying from 70 dB to 120 dB with a background level of 65 dB. Neither Dusp8 KO male (A) nor female (C) mice show differences in the ASR compared to their WT littermates. Prepulse inhibition (PPI) was conducted with prepulse stimuli ranging from 67 dB to 81 dB with an inter-stimulus interval of 50 ms. PPI is unperturbed in Dusp8 KO mice compared to WT littermates (B,D). Male WT: n=15, male KO: n=15; female WT: n=8, female KO: n=12. Means ± SEM.

Taken together, Dusp8 KO animals do not show any alteration in sensorimotor gating, neither in an ASR test nor in the PPI test indicating an intact integrating network.

Basic cognitive phenotyping includes test for anxiety-related behavior. We therefore performed an open field test and introduced the mice into an open field arena (Fig. 10A) for twenty minutes and monitored localization and movement. For male Dusp8 KO mice we found an increased anxiety-related behavior reflected by a significantly reduced time spent (Fig. 10B) and distance travelled in the center (Fig. 10C) of the arena. Surprisingly, accompanying this was a longer overall distance travelled in the entire arena (Fig 10D). The number of rearing events did not significantly differ between Dusp8 KO and Dusp8 WT males (Fig. 10E). In contrast to male Dusp8 KO mice, female Dusp8 KO mice did not show elevated anxiety-related behavior, reflected by differences in the time spent (Fig. 10F) and distance travelled in the center (Fig. 10G). However, a trend towards a longer distance travelled in the entire arena was consistent with the observation for male Dusp8 KO mice (Fig. 10H). This increase in horizontal activity was at the cost of the vertical investigation of the arena, as the number of rearing events was diminished in female Dusp8 KO mice compared to Dusp8 WT mice (Fig. 10I).

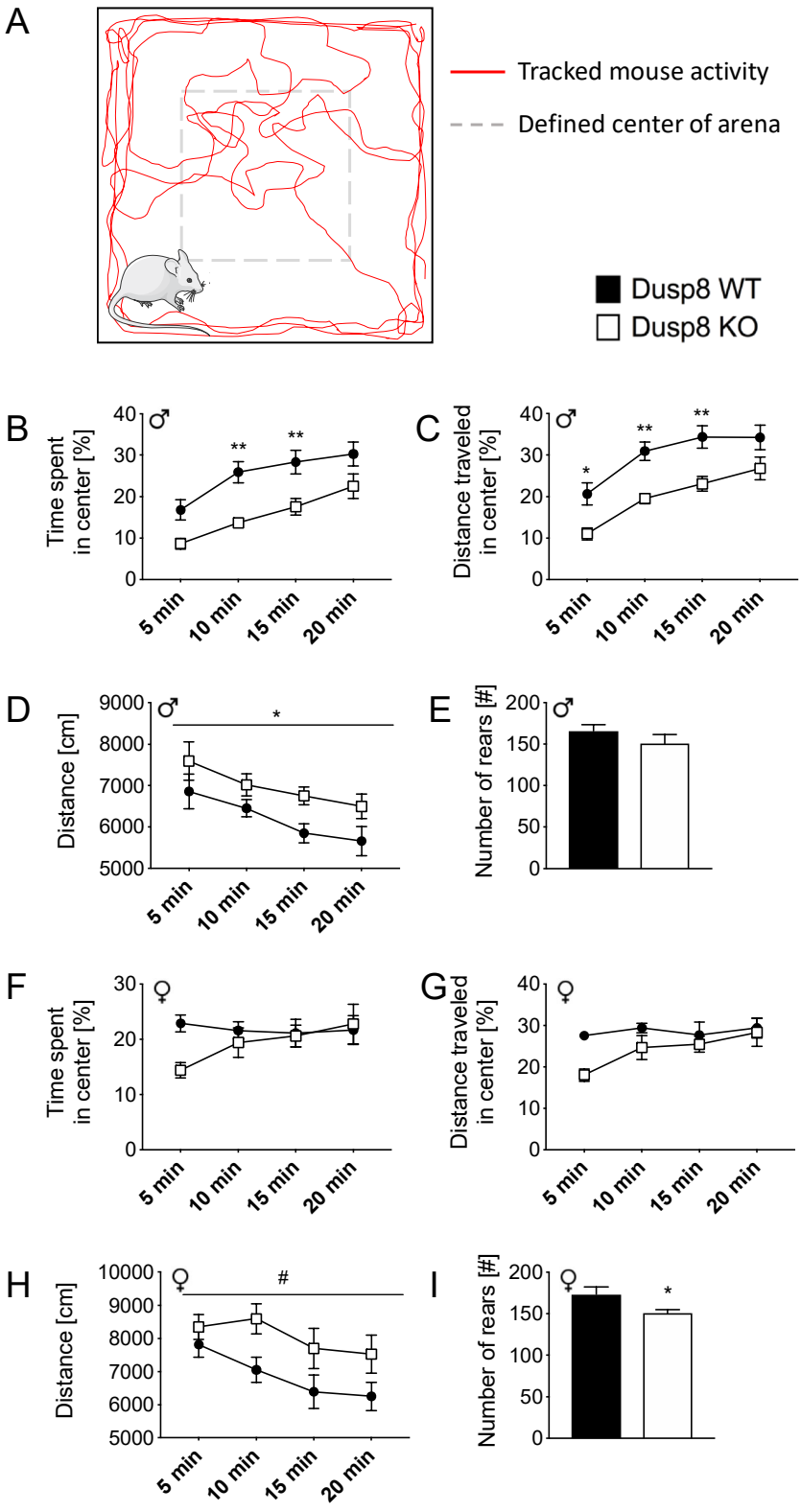

Figure 10. Open Field Test in female and male Dusp8 WT and KO mice.

Mice were able to freely explore the arena (A). Percentage of time spent (B,F) and percentage of distance travelled (C,G) in the center of the open field during the test time of 20 minutes in male and female Dusp8 WT and KO mice was calculated. Total activity of male (D,E) and female (H,I) Dusp8 WT and KO mice is shown as distance travelled in the entire arena during the test time

(D,H) and the total number of rearing events (E,I). Male WT: n=15, male KO: n=14; female WT: n=8, female KO: n=12. Means ± SEM. # p < 0.1; * p < 0.05; ** p < 0.01.

In the open field test, we identified an increased anxiety-related behavior for male mice deficient for Dusp8. In both sexes we found a hyperactivity regarding horizontal, on the extent of vertical investigation.

5.2.1.2 Retrograde working memory, social discrimination, and object recognition are intact in Dusp8 KO animals

As the hippocampus is specifically involved in retrograde working memory, we next assessed hippocampus-specific cognition in Dusp8 KO mice by testing retrograde working memory in a Y-Maze arena (Fig. 11A) and tracked the entries into the freely accessible arms of the setup.

For male and female Dusp8 KO mice, we did not find any differences in the percentage of spontaneous alternation entries compared to WT controls (Fig. 11A,D). However, for male Dusp8 KO mice, an increased number of total entries into the arms were recorded (Fig. 11C), thus reflecting a higher activity of Dusp8 KO males compared to WT controls. A similar behavior was observed for the Dusp8 KO females, however here the difference in entry numbers did not reach significance (Fig. 11E).

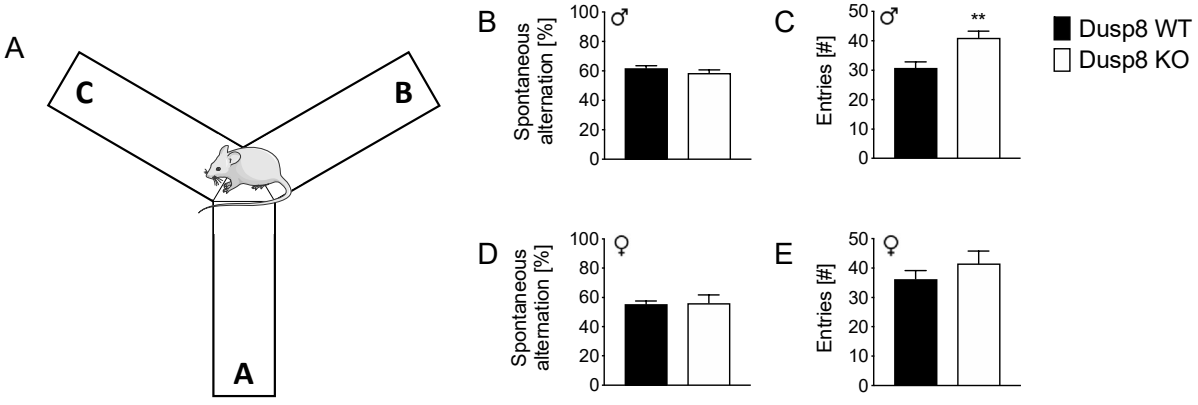

Figure 11. Spatial working memory of male and female Dusp8 WT and KO mice in a Y-Maze.

(A) Mice were allowed to freely explore the Y-Maze arena during the test phase. Arms were assigned with letters A to C to record the respective arm entries. (B-E) Orientation and horizontal investigation performance in the arena is shown as percentage of spontaneous alternations between arms in male (B) and female (D) mice, and as total number of arm entries in male (C) and female (E) mice. Male WT: n=15, male KO: n=12; female WT: n=8, female KO: n=12. Means ± SEM. ** p < 0.01.

Overall, the results of the Y-Maze test showed intact spatial orientation but higher locomotion in Dusp8 KO mice, and suggested increased exploratory behavior of novel environments.

The higher exploratory activity of Dusp8 KO mice in the Y-Maze test prompted us to perform an object recognition test (Fig 12A). This test assesses the short- and long-term working memory and exploratory behavior of KO mice exposed to inanimate objects.

Animals performed three habituation phases in the test cage with two identical objects. All male animals showed a habituation behavior to the objects throughout the sample phases (Fig 12B). In females, Dusp8 KO mice did not reduce their interaction time with the objects over the habituation sessions (Fig 12C). Regardless of sex, Dusp8 KO animals spent significantly more time interacting with the objects compared to WT littermate controls (Fig 12B,C). In the test phase for short-term memory after 3 h, male Dusp8 WT and Dusp8 KO animals showed the expected higher interaction time with the novel object in the cage (Fig. 12D). However, Dusp8 KO males spent significantly more time for investigation of familiar and unfamiliar objects compared to Dusp8 WT males. The calculated recognition index did not differ between Dusp8 WT and Dusp8 KO animals (Fig. 12E). Female Dusp8 WT and Dusp8 KO animals spent significantly more time investigating the novel object in the test cage during the short-term memory-testing interval (Fig. 12F). Similar to the male Dusp8 KO mice, females also showed a longer investigation time with both objects in the cage compared to WT littermates, however this only reached borderline statistical significance. The recognition index for female Dusp8 KO mice did not differ from WT controls (Fig. 12G).

In the following long-term memory assessment 24 h after the last habituation phase, male WT mice showed a trend towards higher interaction time with the novel object, whereas male Dusp8 KO mice spent significantly more time investigating the novel object (Fig. 12H). However, during the test phase, male Dusp8 KO mice spent significantly more time investigating objects in the cage compared to the WT control mice. Although male Dusp8 KO mice show differences in investigation times, the calculated recognition index did not differ from Dusp8 WT males (Fig. 12I). Both groups of female mice showed a longer investigation time for the novel object at the time point for long-term memory, however Dusp8 KO females spent significantly more time investigating both of the presented objects in the cage compared to Dusp8 WT female

mice (Fig. 12J). Nevertheless, object recognition indices were again comparable, and point in the direction of an unperturbed long-term memory of females deficient for Dusp8 (Fig. 12K).

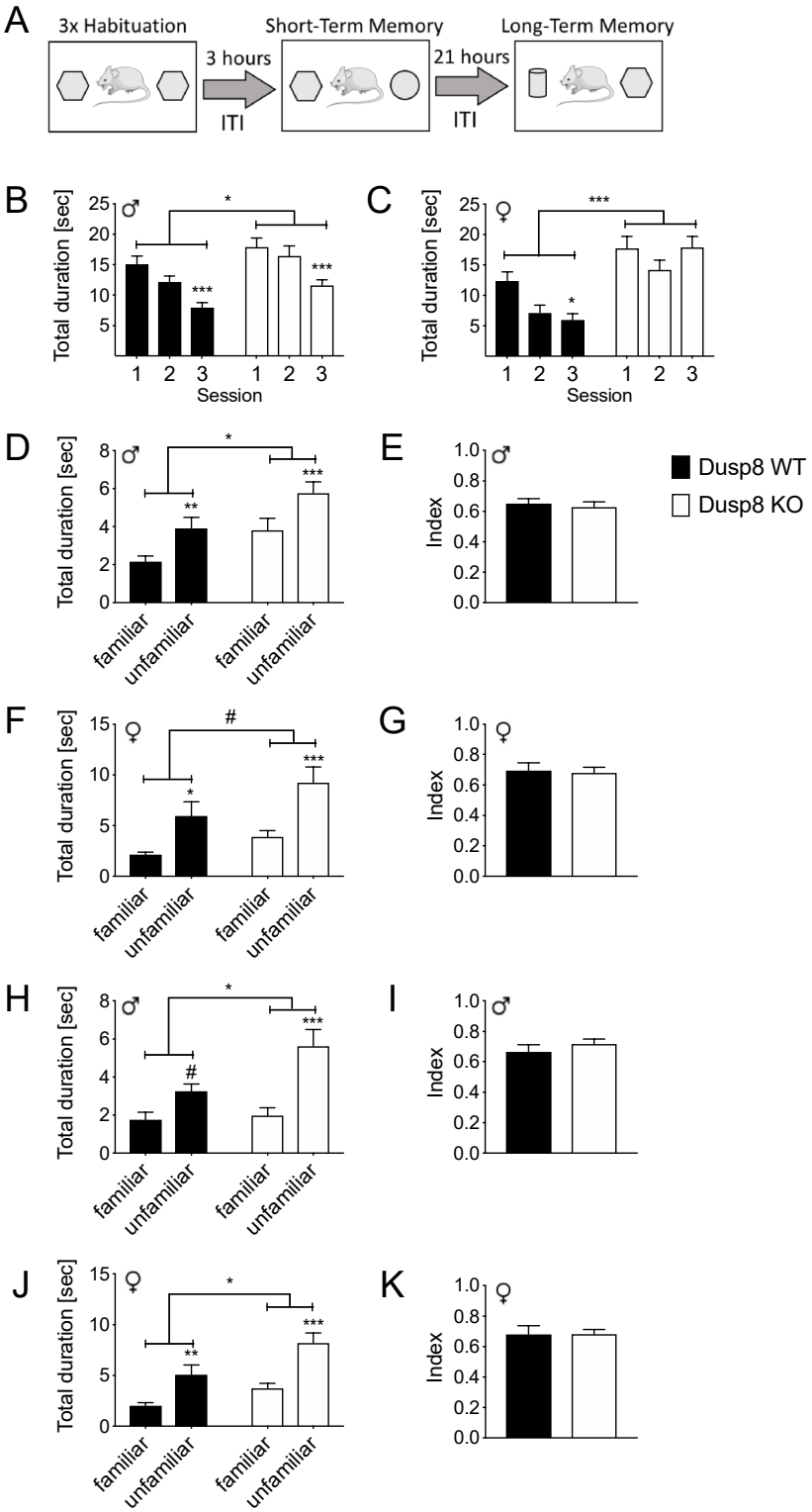

Figure 12. Object Recognition Test in female and male Dusp8 WT and KO mice.

(A) Protocol of the object recognition task with three habituation sessions 1-3 followed by a short and a long-term memory test after a 3-hour or 24-hour inter-trial interval (ITI), respectively. (B,C) Interaction times with identical objects in the testing arena for the habituation sessions 1-3 in male (B) and female (C) mice, respectively. (D-G) Short-term memory recognition measures after the 3h-ITI for the familiar and a novel object, shown as total duration spent with the familiar and unfamiliar object, or as object recognition index in male (D,E) or female (F,G) mice. (H-K) depicts the corresponding long-term memory recognition measures after the 24h-ITI with the familiar and a novel unfamiliar object. Male WT: n=14, male KO: n=15; female WT: n=8, female KO: n=11. Means ± SEM. # $p < 0.1$; * $p < 0.05$; ** $p < 0.01$; *** $p < 0.001$.

The object recognition memory test thus revealed that short- and long-term object recognition memory is unperturbed in male and female Dusp8 KO mice. The longer time spent on investigation of the objects in the test cage reflects the previously observed hyperactivity and perhaps an increased salience in incentive stimuli of Dusp8 KO mice.

To uncover social aspects of cognition and memory performance, we conducted interaction data in a social discrimination test (Fig. 13A). In the sample phase, both sexes of Dusp8 KO mice showed trends towards a shorter investigation time with the first unfamiliar mouse, although the difference did not reach significance (Fig. 13B,D). Notably and contrary to usually observed higher interaction time with the unfamiliar mouse, the interaction time in the test phase did not differ between the familiar and unfamiliar mouse for all animals (Fig. 13C,E). The calculated social recognition index was comparable between both genotypes (Fig. 13F,G).

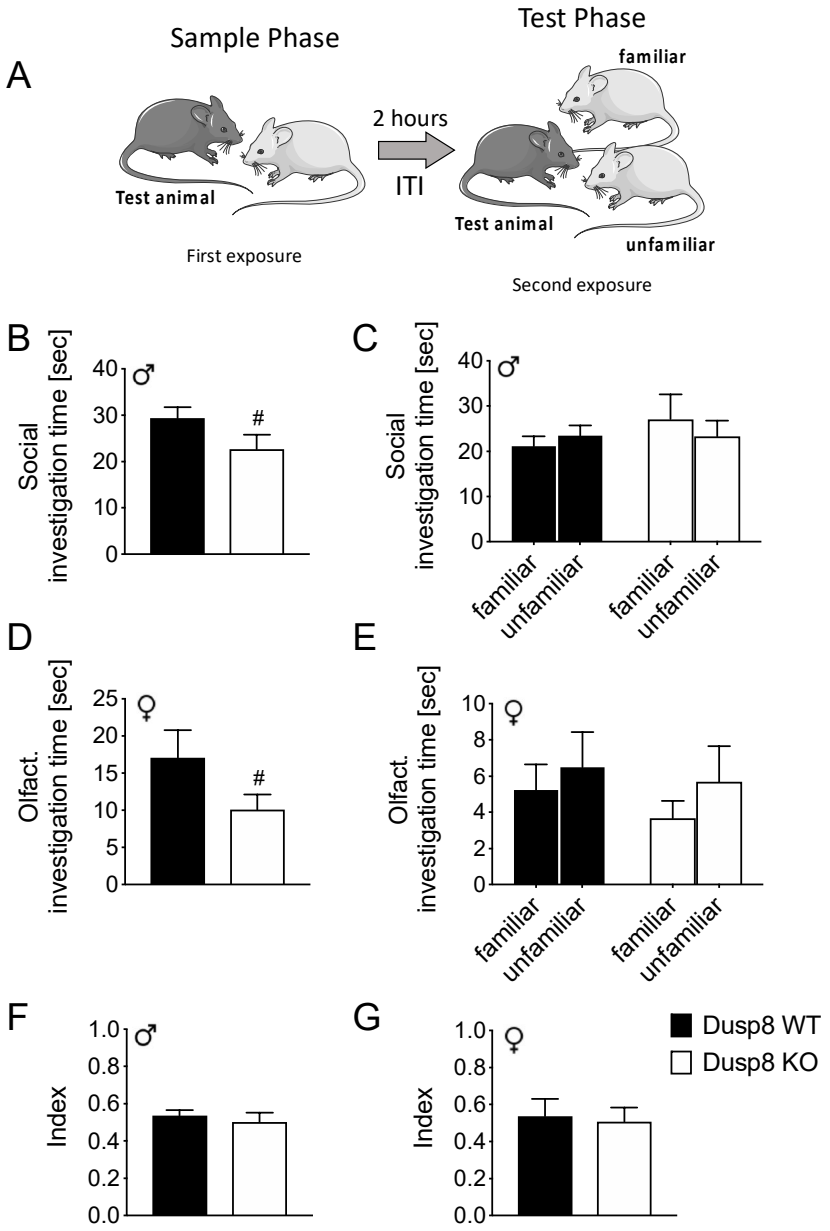

Figure 13. Social Discrimination Test in female and male Dusp8 WT and KO mice.

(A) Schematic overview of test animals (dark grey) exposed to an unfamiliar OVX female (light grey). Mice were allowed to freely interact for 4 min, followed by a 2-hour inter-trial interval (ITI). Subsequently, the same now familiar mouse and a new unfamiliar OVX female were introduced to the test mouse for 4 min, and the interaction times were recorded. The interaction time of male Dusp8 WT or KO mice with the unfamiliar animals is depicted in the sample phase (B) or the test phase (C). The olfactory interaction times of female Dusp8 WT and KO mice are depicted in the sample (D) and test phase (E). Social investigation times included mounting behavior of male mice in addition to olfactory interactions. (F) shows the social discrimination index of male and (G) female Dusp8 WT and KO mice, respectively, calculated as ratio of interaction time with the unfamiliar mouse and the total interaction time with both mice. Male WT: n=15, male KO: n=14; female WT: n=8, female KO: n=12. Means ± SEM. # $p < 0.1$.

Overall, these data demonstrate a comparable performance in a social recognition task in male and female Dusp8 WT and KO mice, but a trend towards an increased social

anxiety when exposed to an unfamiliar ovariectomized female mouse. It has to be noted, that the results for the testing phase interacting with a familiar and an unfamiliar mouse remain inconclusive.

5.2.1.3 Place and reversal learning

Since the hippocampal structure is not only involved in emotional gate keeping and memory formation, but also essential for spatial orientation and memory, we used the TSE Systems IntelliCage as observer-independent tracking system to assess spatial orientation in a home cage environment. Due to inter-subject aggression between male mice, we could only test female mice in this group-house set up.

After a habituation phase, a place learning program was started and limited the mice to one randomly assigned single corner to get access to water after a single nose poke against the respective door in the test corner (Fig. 14A).

Behavioral tracking in the first dark phase of the test paradigm revealed a significantly higher error rate for performed nose pokes of Dusp8 deficient females compared to control WT controls (Fig. 14B). Additionally, we found a higher number of visits at the beginning of the dark phase (Fig. 14C), as well as a higher number of total visits (Fig. 14D) and an increased number of performed total nose pokes (Fig. 14E). By the second dark phase of the place learning paradigm, error rate of nose poke performance of Dusp8 KO mice did not differ from WT mice anymore (Fig. 14F). The observed hyperactivity of the first dark phase was consistent during the second night, reflected by increased number of visits in the first hours of the dark phase (Fig. 14G), increased number of total visits (Fig. 14H), and elevated number of total nose pokes (Fig. 14I). The results of the place learning task suggest an impaired spatial memory formation during the 1st dark phase and an overall increased locomotor activity in female Dusp8 KO mice.

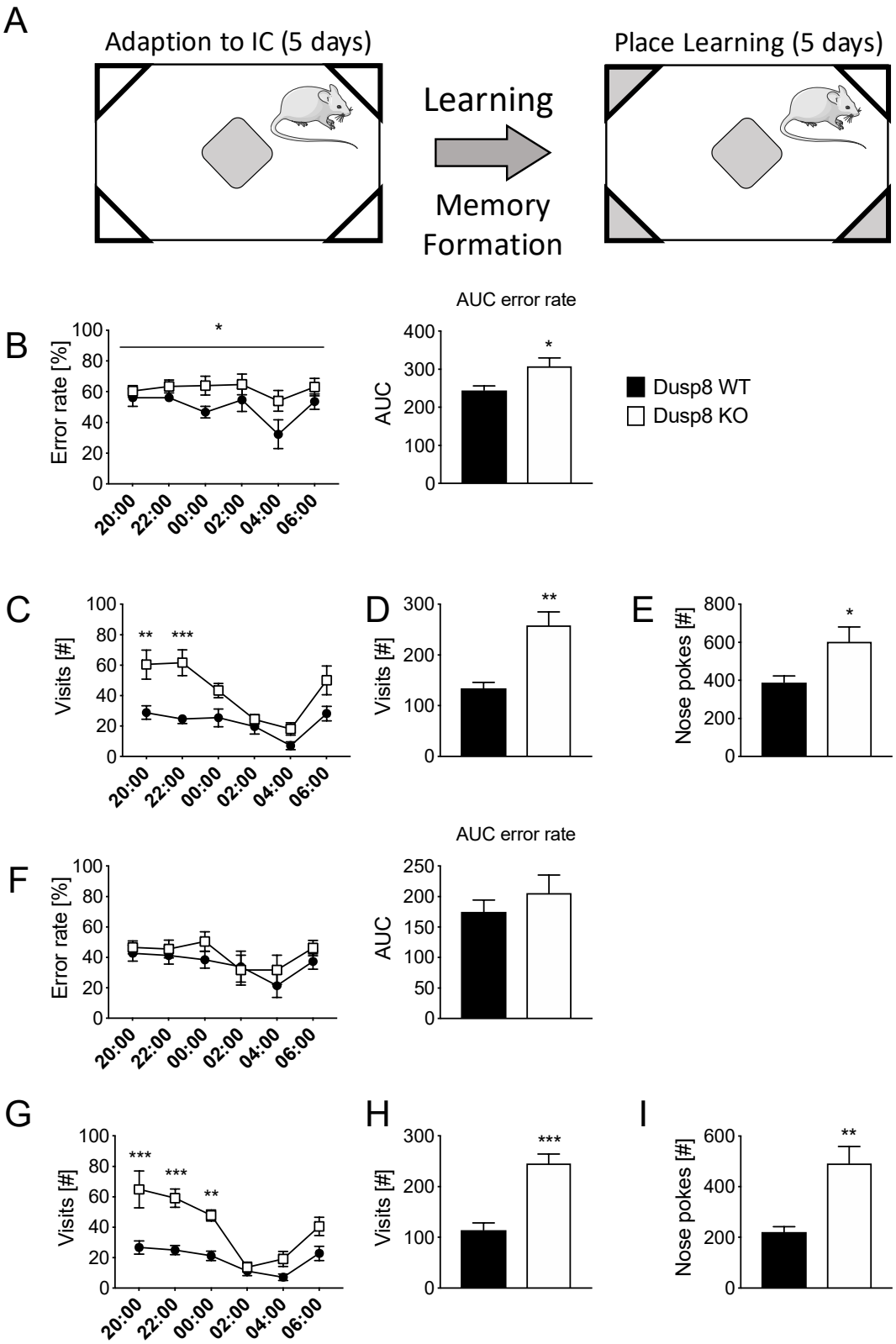

Figure 14. Place Learning Test of female Dusp8 WT and KO mice group-housed in the automated IntelliCage behavioral monitoring system.

(A) Schematic of the place learning task. White corners contain water bottles freely accessible after a nose poke during the adaption phase (first 5 days). In the subsequent place learning task phase (duration 5 days), corners with blocked access to the water bottles after a nose poke are shown in

grey. (B) Percentage of erroneous nose pokes in the first night phase as measure for the learning performance. Overall activity of the mice in the first night phase is monitored as bi-hourly number of corner visits (C), average number of corner visits (D) and average number of nose pokes (E). (F-I) depict the corresponding values from the second night of the place learning task. IC IntelliCage. WT: n=8, KO: n=9. Means ± SEM. * $p < 0.05$; ** $p < 0.01$; *** $p < 0.001$.

To test spatial memory flexibility, mice were challenged with a reversal learning task, where the correct corner with access to water after nose poke was switched to the opposite corner of the cage (Fig. 15A).

Analysis of nose poke performances revealed a comparable error rate in Dusp8 KO and Dusp8 WT mice during the first dark phase (Fig. 15B). Consistent with the results of the place learning task, Dusp8 deficient mice showed an increased number of visits in the first hours of the dark phase (Fig. 15C). This finding was strengthened by the observation of an increased number of visits (Fig. 15D) and a trend towards a higher number of performed nose pokes of Dusp8 KO mice compared to WT controls (Fig. 15E).

Analysis of the collected data for the second dark phase of the reversal learning task revealed similar behavioral results. All mice showed a comparable error rate of nose poking in the correct corner of the IntelliCage (Fig. 15F). Temporal analysis again showed a higher number of visits in the test corner during the first hours of the dark phase (Fig. 15G) and in the total number of visits during the dark phase (Fig. 15H), with a trend to a higher number of nose pokes of mice lacking Dusp8 compared to wild type littermates (Fig. 15I).

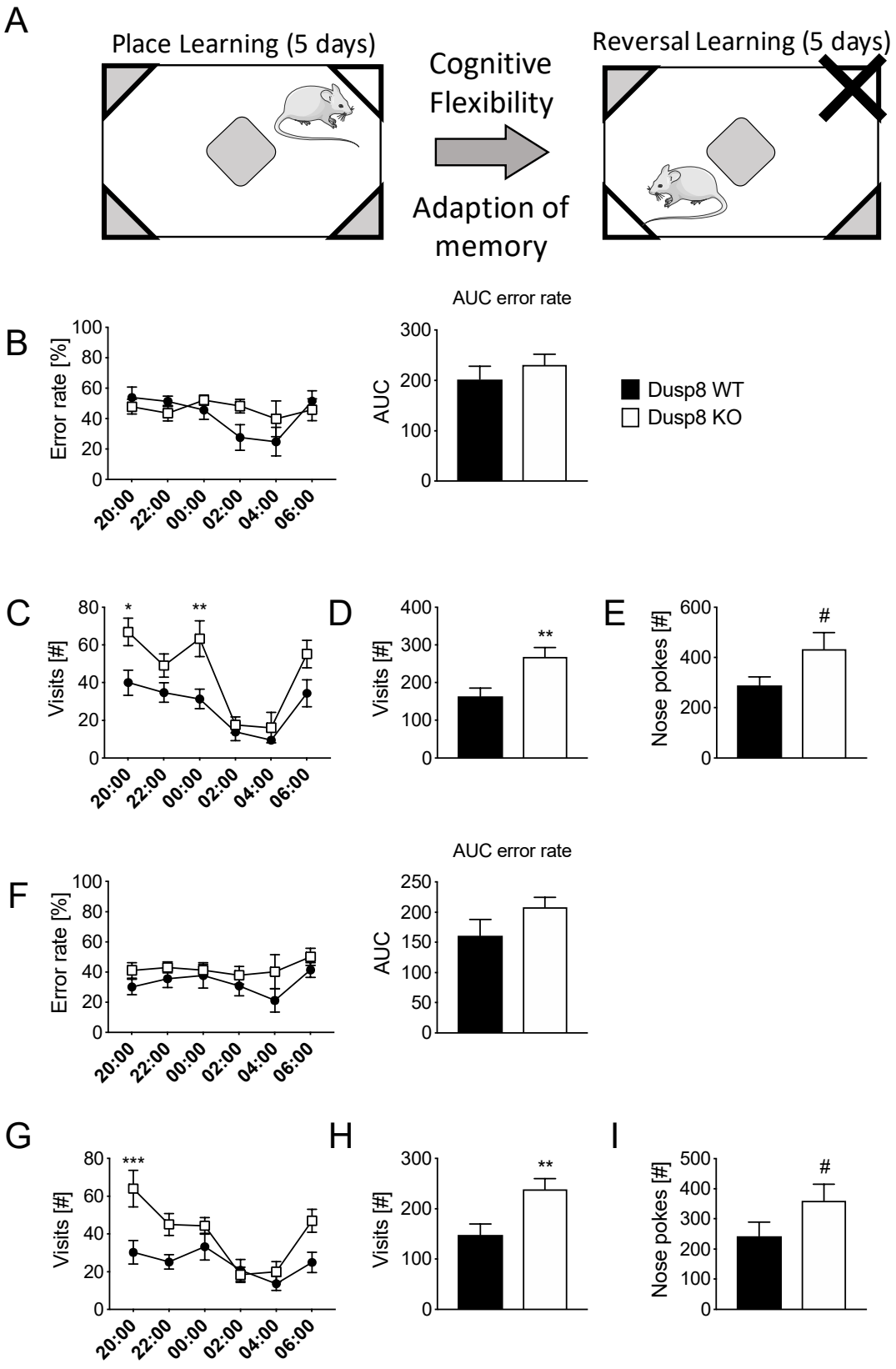

Figure 15. Reversal Learning Test of female Dusp8 WT and KO mice group-housed in an automated IntelliCage behavioral monitoring system.

(A) Schematic of the reversal learning task. In the initial place learning test, one corner (labeled in white) contains a water bottle with free access after a nose poke; the other three (grey) corners

contain bottles with blocked access. To induce reversal learning, the accessible bottle in the (white) corner is switched to the opposing corner, which will now grant access to water after a nose poke. Subsequently, (B) the number of erroneous nose pokes in the first night phase as measure for the reversal learning performance, and (C-E) the overall activity of the mice in the first night phase, monitored as bi-hourly number of corner visits (C), average number of corner visits (D) and average number of nose pokes (E), were recorded. (F-I) depict the corresponding values from the second night of the reversal learning task. WT: n=8, KO: n=9. Means ± SEM. # $p < 0.1$; * $p < 0.05$; ** $p < 0.01$, *** $p < 0.001$. Elements of artwork were provided by Servier medical art under the creative commons license 3.0.

Dusp8 KO mice showed a mild impairment in the spatial learning task in the IntelliCage set up, but no impairment in a reversal learning task. Throughout both tests, Dusp8 deficient animals showed a hyperactive phenotype reflected by a higher number of corner visits and higher number of total performed nose pokes.

Taken together, these data indicate that Dusp8 has no influence on memory flexibility, but contributes to an increased locomotor drive in female Dusp8 KO mice.

5.3 Dusp8 and the control of sucrose reward behavior

5.3.1 Comparable sucrose preference but increased sucrose seeking in Dusp8 KO mice

Prompted by the finding that female Dusp8 KO mice were hyperactive and showed a mild impairment in spatial memory, we wanted to further investigate the impact of Dusp8 on activity, seeking behavior, and motivation in response to a hedonic incentive stimulus that is influenced by the reward system and can influence cognitive performance. We used sucrose as a hedonic stimulus and monitored sucrose consumption, as well as motivational behavior of the animals, in a two-bottle water vs. sucrose choice test in the IntelliCage set up.

5.3.1.1 Increased sucrose consumption of Dusp8 KO animals in a two-bottle water vs. sucrose choice test

After the forced sucrose habituation phase, animals could choose between sucrose solution or plain water after one nose poke on the respective side in the correct test corner (Fig. 16A).

We observed an increasing preference for sucrose during the first dark phase of all animals (Fig. 16B, left panel) and a respective decrease of preference for water (Fig.16C, left panel) in both WT and Dusp8 KO females. The preference for performing

nose pokes in the incorrect corner remained stable for both genotypes throughout the dark phase (Fig. 16D, left panel). The levels of the respective preference remained stable during the second dark phase (Fig. 16B-D, right panels). Consistent with the previous observations in the IntelliCage, Dusp8 deficient females showed a significantly higher number of visits in the test corners during the second dark phase compared to WT littermates (Fig. 16E). Furthermore, Dusp8 KO mice performed significantly more licks at the drinking bottles than WT control mice (Fig. 16F). Interestingly, this increase in total number of licks in Dusp8 KO females was only driven by a significantly increased number of licks at the sucrose bottles, not at the accessible water bottles.

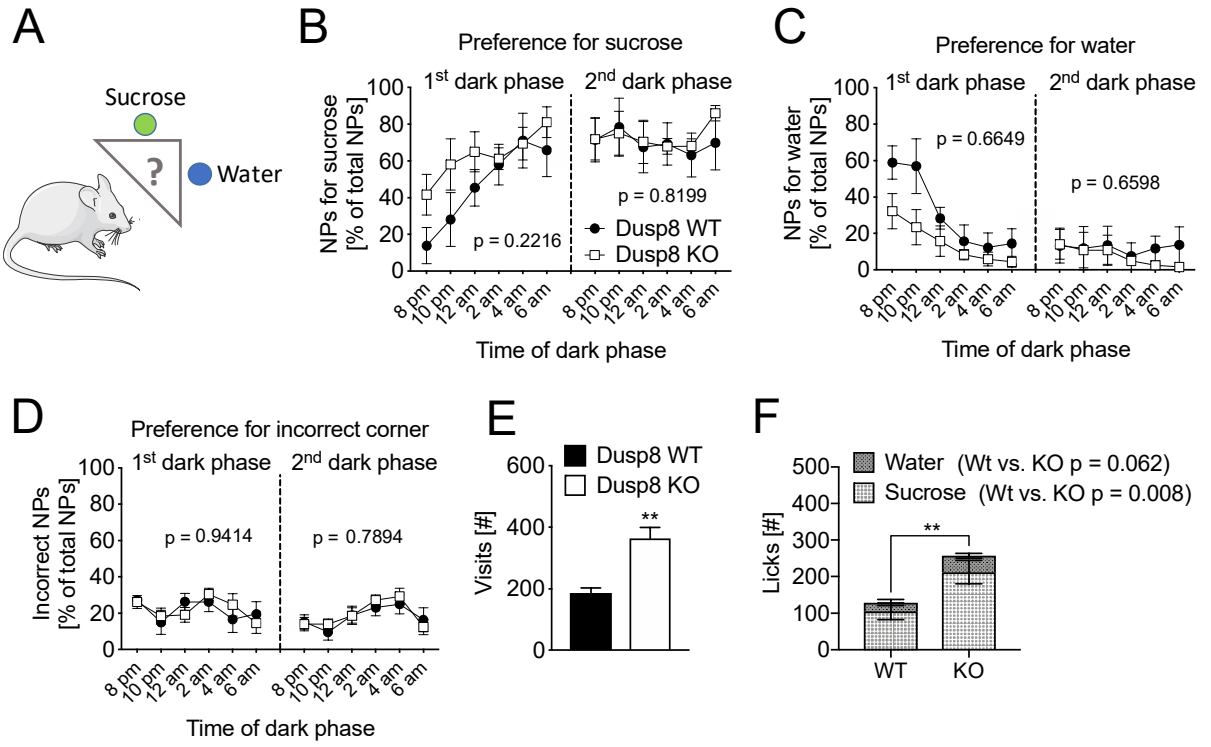

Figure 16. Two-bottle sucrose vs. water choice test of female, chow-fed Dusp8 WT & KO mice.

(A) Mice were able to choose between sucrose solution and water after one nose poke (NP) in the correct test corner. (B) Preference for sucrose in the first and second dark phase. (C) Preference for water in the first and second dark phase. (D) Preference for performing NPs in incorrect corners in the first and second dark phase. (E) Total number of corner visits of mice in the second dark phase. (F) Total consumption of water and sucrose in the second dark phase. Female WT: n=6, female KO: n=8. Means ± SEM. ** $p < 0.01$.

Taken together, female Dusp8 KO mice showed a comparable preference for sucrose in a two-bottle choice test relative to WT controls. Interestingly, Dusp8 deficient mice showed a higher sucrose consumption compared to WT animals.

5.3.1.2 Randomly distributed corner visits of Dusp8 mice in a progressive ratio task for sucrose

Prompted by our observation that Dusp8 KO mice display higher sucrose consumption, we were interested in the question whether this higher consumption is caused by a higher drive and motivation for sucrose. We added a progressive ratio task for accessing the sucrose bottle to the two-bottle water vs sucrose choice test setup. Therefore, access to the drinking bottle with plain water was given after performing one single nose poke at the respective side, but mice had to perform an increasing number of nose pokes to get access to the preferred sucrose solution (Fig. 17A).

Introducing the progressive ratio task resulted in an enormous drop in the preference for sucrose in the first dark phase for all animals (Fig. 17B). Preference for performing nose pokes for water access increased in both genotypes during the first dark phase (Fig. 17C). When we compared the Dusp8 KO females with their WT controls, we observed a significantly lower preference for water in the Dusp8 KO mice on day 2. This difference persisted over the entire eight-day testing period, and was accompanied by a higher preference for performing nose pokes in the incorrect corner with no access to any drinking bottle (Fig. 17D). Interestingly, the maximal number of performed motivated nose pokes for sucrose in the last night of testing was comparable between both groups of mice (Fig. 17E). As observed in the previous test setups, we again monitored a high activity reflected by the increased number of corner visits of Dusp8 KO mice compared to WT controls (Fig. 17F). The most interesting difference between Dusp8 KO and WT mice was the random distribution of performed nose pokes by Dusp8 KO mice between all four corners (1/4 of nose pokes in correct, 3/4 of nose pokes in incorrect corners). In contrast, WT mice preferred nose poking in the correct rather than incorrect corners (1/2 of nose pokes in correct corner, 1/2 of nose pokes in incorrect corners) (Fig. 17G). This observation points towards a different seeking strategy behavior for mice lacking Dusp8 compared to WT controls when challenged with a progressive ratio task.

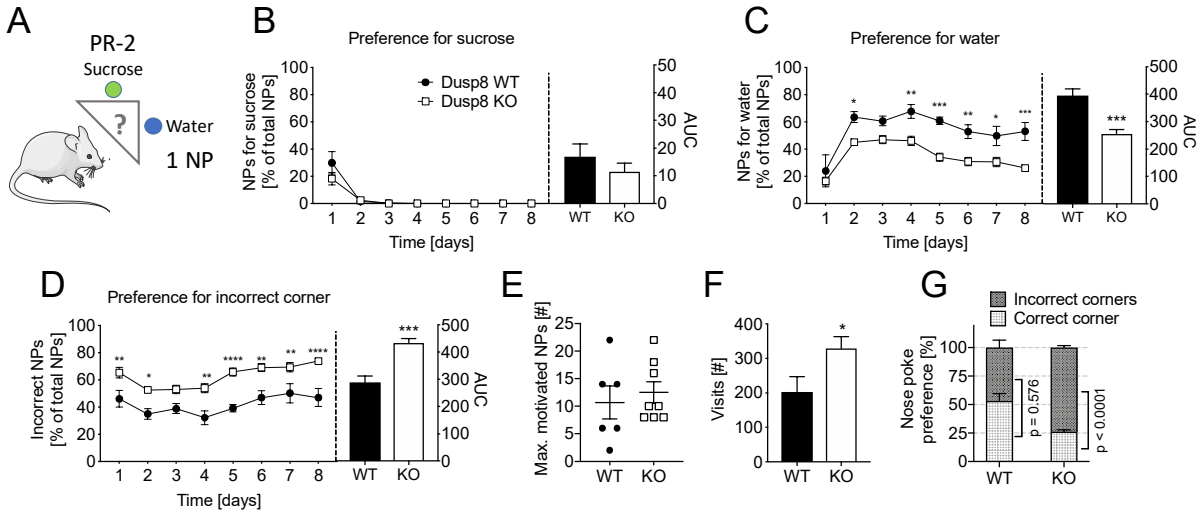

Figure 17. Progressive ratio setup of two-bottle choice test for sucrose vs. water test of female chow-fed Dusp8 WT and KO mice.

(A) Mice had to perform increasing number of nose pokes to access sucrose solution, whereas water was accessible after single nose poke performance at the respective side. Preference for (B) sucrose and (C) water during the 8 days of testing, measured by the number of nose pokes in the correct corner. (D) Nose pokes in the incorrect corner of the IntelliCage set up during the 8 days of testing. (E) Motivational levels reflected by nose pokes for sucrose in the progressive ratio schedule during the 8th dark phase of testing. Increased foraging and random investigation behavior in Dusp8 KO mice was reflected by (F) higher total numbers of corner visits and (G) a random 25% distribution of nose poke preference for the assigned correct vs. incorrect corners during the 8th dark phase. Female WT: n=6, female KO: n=8. Means ± SEM. * $p < 0.05$, ** $p < 0.01$, *** $p < 0.001$.

When confronted with a progressive ratio task, Dusp8 KO mice showed a higher preference for performing incorrect nose pokes. This was at costs of correct nose pokes for water, which resulted in a random like distribution between all four corners in the IntelliCage. Besides this different sucrose seeking strategy between Dusp8 KO and WT mice the general motivational performance level did not differ.

5.3.1.3 Unperturbed dopamine transporter expression in Dusp8 KO mice indicates an intact dopamine reward system

Seeking behavior is mainly driven by dopaminergic neurons in the reward system network of the NAcc and the VTA of the brain. We investigated the integrity of this system for seeking and reward by performing immunofluorescent stainings in cryosections against the DAT (Fig. 18A). We found similar levels of DAT signal in both Dusp8 WT and Dusp8 KO females in the NAcc (Fig. 18B) and a comparable number of DAT positive cells in the VTA (Fig 18C). Thus, our data provide evidence for an intact and unperturbed dopaminergic reward system in mice deficient for Dusp8.

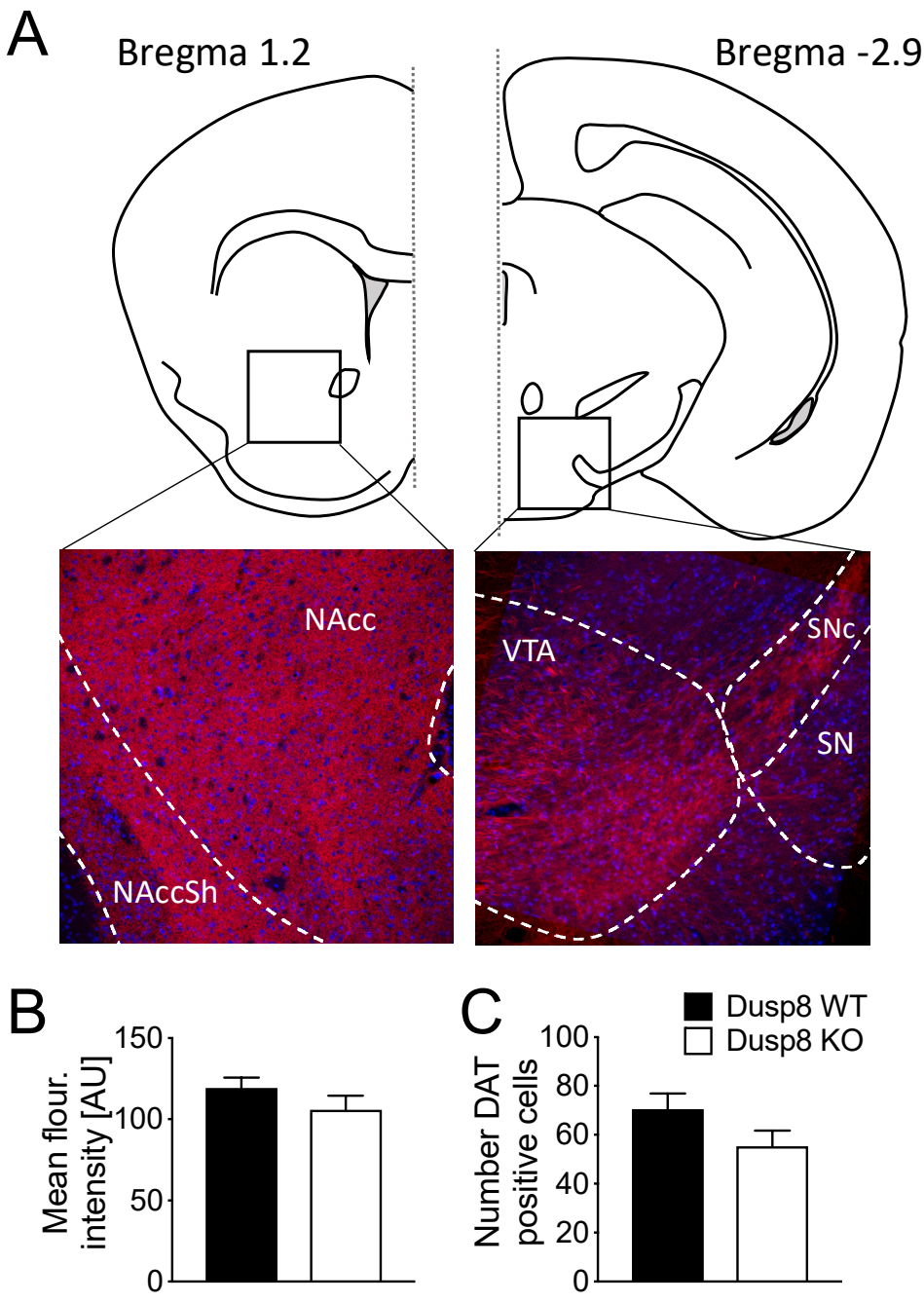

Figure 18. Dopamine transporter in the reward system nucleus accumbens and ventral tegmental area of female mice.

Representative immunofluorescent staining against DAT of the NAcc and VTA (A). DAT staining in red and DAPI positive nuclei in blue. Mean fluorescent intensity of the staining in the defined regions of interest in the NAcc (B) and number of DAT positive cells in the VTA (C). NAcc nucleus accumbens, NAccSh nucleus accumbens shell, SN substantia nigra, SNc substantia nigra pars compacta, VTA ventral tegmental area. Means ± SEM.

5.3.2 Dusp8 deficiency alters the cellular response to glucose *in vitro* in neuronal cells and in vivo in glucose sensing brain areas

Dusp8 KO mice showed elevated sucrose seeking compared to wild type littermates, but the central mechanisms involved in converting the external stimulus of sweetness to the altered behavioral output remain elusive. We hypothesized that glucose sensing by neurons would be altered in Dusp8 KO mice, thus triggering the increased sucrose wanting behavior. The role of Dusp8 in neuronal glucose sensing was assessed by measuring Dusp8 expression and MAPK phosphorylation in a cellular *in vitro* model, as well as by measuring MAPK-signaling and neuronal activity *in vivo* in brain centers known to be involved in glucose homeostasis and sensing in Dusp8 KO mice injected with 2DG. 2DG is a non-metabolizable analogue to glucose that raises blood glucose, is taken up by the cells, and phosphorylated, but cannot be further metabolized, and is thus a well-established tool to study glucose sensing and counter-regulatory mechanisms *in vitro* and *in vivo* (Mizuno and Oomura 1984, Zhang et al. 2006, Ogunnowo-Bada et al. 2014, Verberne et al. 2014).

5.3.2.1 2DG-induced reduction in Erk phosphorylation and increased Dusp8 expression in CLU177 cells

To gain primary insight into the role of Dusp8 and glucose sensing, we used the murine hypothalamic cell line CLU177, immortalized neurons and broadly used for *in vitro* studies for CNS diseases and disorders. Stimulation of CLU177 cells with increasing 2DG concentrations (Fig. 19A) revealed comparable levels of phosphorylated c-jun (Fig. 19B) and p38 (Fig. 19C). Interestingly, 2DG treatment with all three concentrations 2.5 mM, 10 mM, and 25 mM lead to a significant reduction in Erk phosphorylation (Fig. 19D). Since no changes in Erk phosphorylation were seen in the glucose-negative control, this effect seems to be specific to 2DG and not induced by a general lack of glucose in the treatment medium. p-MAPK levels were normalized to the loading control, ß-actin. Due to the specificity of the antibodies against phosphorylated and non-phosphorylated MAPK, it was not possible to assess MAPK levels on the same membrane itself. Since there is no specific antibody against Dusp8 available, we analyzed Dusp8 mRNA expression in the 2DG stimulated CLU177 cells and showed a concentration dependent upregulation of Dusp8 expression (Fig. 19E). The Dusp8 expression levels were highest with the lowest treatment concentration.

This indicates a highly sensitive intracellular regulation within a narrow range of stimuli presentation.

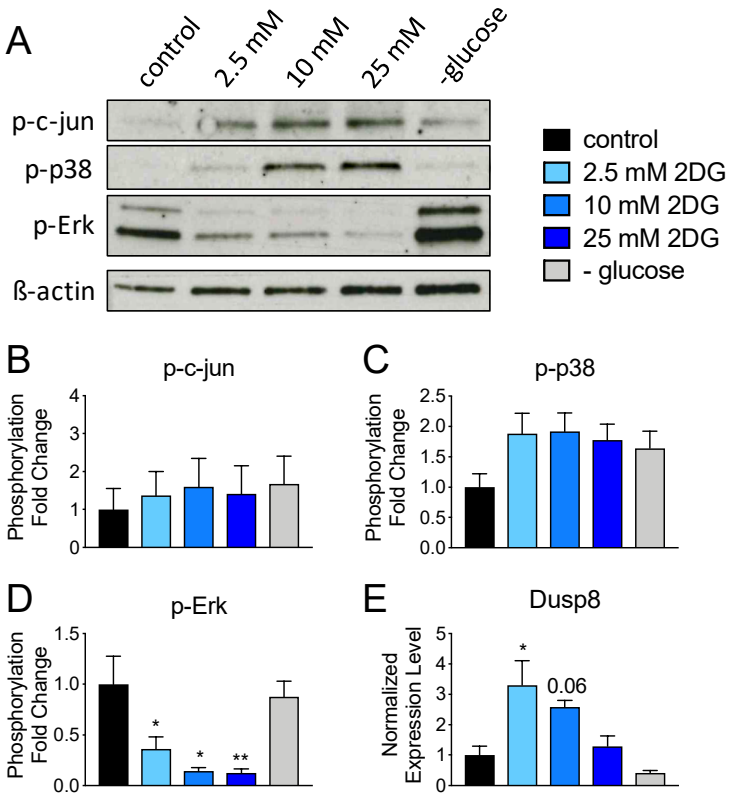

Figure 19. MAPK phosphorylation and Dusp8 expression in 2DG stimulated CLU177 cells.

(A) Western blot pf phosphorylated MAPKs of 2DG stimulated CLU177 cell lysates. Densitometric analysis of western blots for p-c-jun (B), p-p38 (C), and p-Erk (D) normalized on ß-actin loading control. (E) Dusp8 expression level of 2DG stimulated respective CLU177 cell lysates relative to Hprt expression. n=4. Means ± SEM. * $p < 0.05$, ** $p < 0.01$.

We found an upregulation of Dusp8 expression in 2DG-stimulated cells, and in parallel, a reduction in Erk phosphorylation compared to control conditions. To investigate whether this reduction is indeed a Dusp8 dependent effect, we induced an overexpression of Dusp8 in CLU177 cells. Unfortunately, we could not reproduce the 2DG-induced downregulation of p-Erk in control cells. Therefore, we were not able to interpret the impact of Dusp8 overexpression on the phosphorylation status of MAPK in 2DG treated cells.

5.3.2.2 Increased 2DG stimulated c-jun phosphorylation in hypothalamic nuclei of Dusp8 KO mice

Prompted by our finding of unperturbed Jnk and p38 activity, yet impaired Erk phosphorylation *in vitro*, we next performed stainings against p-Erk, p-c-jun, and p-p38 in cryosections of 2DG and saline injected Dusp8 KO and Dusp8 WT mice. First, we focused on the Arc and the ventromedial hypothalamus (VMH), two hypothalamic nuclei containing glucose sensitive neurons.

We found a significant upregulation of p-c-jun positive cells in the Arc in Dusp8 KO mice (Fig 20A) and in the VMH (Fig 20B) after 2DG stimulation. For MAPK-p38, the phosphorylation pattern in the Arc did not significantly differ (Fig 20C). We did not see any 2DG-induced upregulation of p-p38 positive cells and both genotypes were comparable regarding their number of p-p38 positive cells. A similar result was observed in the VMH (Fig 20D). Unfortunately, it was not feasible to generate stainings for phosphorylated Erk. This was most likely not due to a lack of Erk-signaling in the hypothalamus, but a non-suitable antibody against p-Erk for *ex vivo* brain sections. Changes in the staining protocol did not improve the staining signal or were too harsh and harmed the integrity of the brain sections. However, the phosphorylation status of MAPK-Erk in glucose sensing brain regions remains an interesting topic since Erk seemed to be the 2DG sensing MAPK *in vitro*.

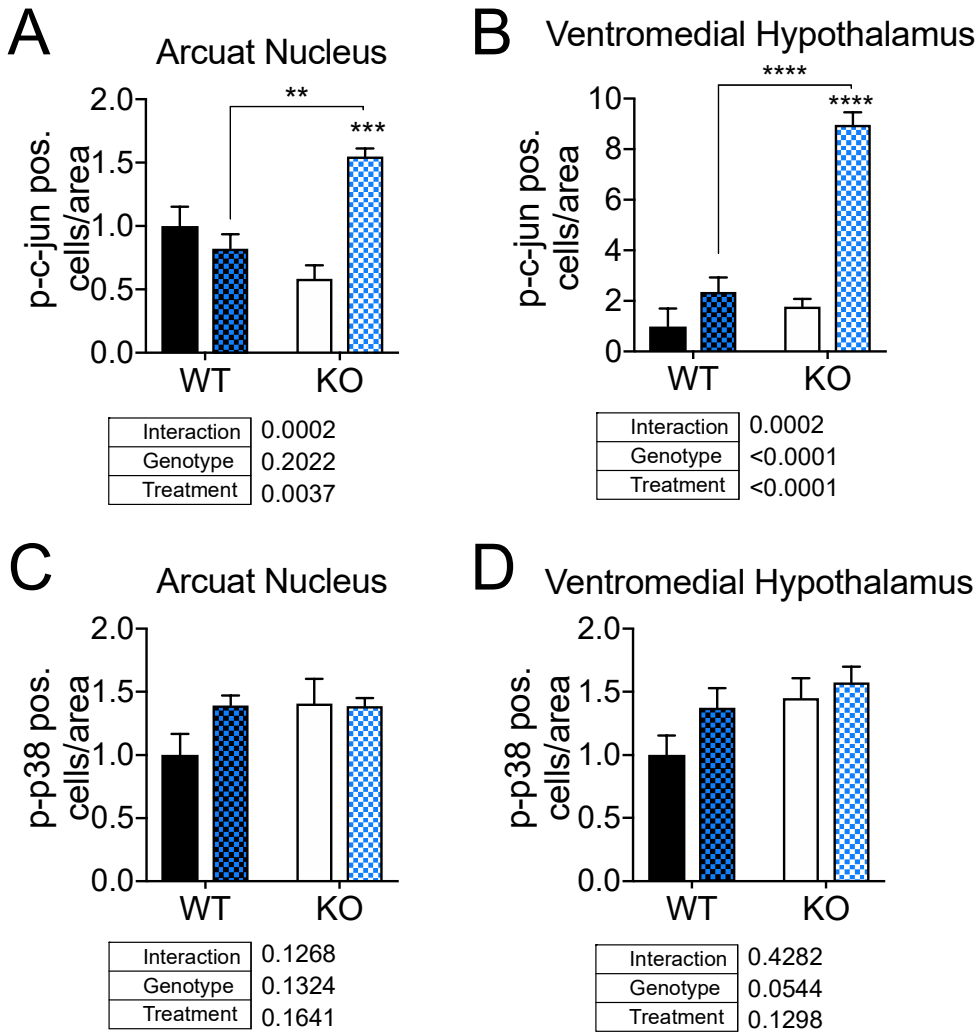

Figure 20. Phosphorylation of c-jun and p38 in the hypothalamus after 2DG injection.

Dusp8 WT and Dusp8 KO mice were i.p. injected with 2DG. Stainings for p-c-jun show a 2DG-induced upregulation in Dusp8 KO mice after injection in the Arc (A) and VMH (B). Stainings for p-p38 do not show any difference between Dusp8 KO and Dusp8 WT mice in the Arc (C) or the VMH (B)., Dusp8 WT PBS: n=5, Dusp8 WT 2DG: n=6, Dusp8 KO PBS: n=4 Dusp8 KO 2DG: n=4. Means ± SEM. ** $p < 0.01$, *** $p < 0.001$, **** $p < 0.0001$.

5.3.2.3 Cellular activation in various metabolic and glucose sensing centers in the brain

The 2DG-induced upregulation of Jnk-signaling in the Arc of Dusp8 KO mice raised the question of whether the increased MAPK activity can lead to a higher neuronal activity in this center and other glucose sensitive nuclei in the brain. To evaluate neuronal activity, brain sections of 2DG injected Dusp8 KO mice were stained for c-fos and analyzed relative to WT controls and PBS injected littermates. Therefore, we focused not only on the hypothalamus, but also analyzed parts of the limbic and reward system, brainstem, and cortex (Fig. 21A).

We found a 2DG-induced, but Dusp8 independent upregulation of c-fos positive cells in the Arc, VMH, and PVN of the hypothalamus (Fig. 21B), which reached statistical significance in the PVN of Dusp8 KO mice.

Regarding reward behavior, the observed reduction in hippocampus size and the close connection in the limbic system led us to investigate the neural activity in the respective critical brain centers NAcc, Hippocampus, and the basolateral amygdala (BLA). An induction of neuronal activity in the NAcc and BLA after 2DG injection did not reach statistical significance in either group (Fig. 21C). In the hippocampus we found a borderline significantly higher number of c-fos positive cells in Dusp8 KO 2DG injected mice compared to Dusp8 KO PBS control mice ($p=0.0506$) and a significantly higher level compared to Dusp8 WT 2DG stimulated mice (Fig. 21C).

Extra-hypothalamic glucose sensing centers in the brainstem showed significant treatment differences. We found a significant c-fos induction fold change in the PAG and the raphe nuclei after 2DG induction in Dusp8 KO mice compared to PBS injected mice (Fig. 21D). Cortical area insula and lateral septum in the striatum did not respond to 2DG i.p. injection (Fig. 21D). We found comparable levels of c-fos positive cells in the lateral septum and the insula of Dusp8 WT and Dups8 KO mice injected with 2DG and PBS.

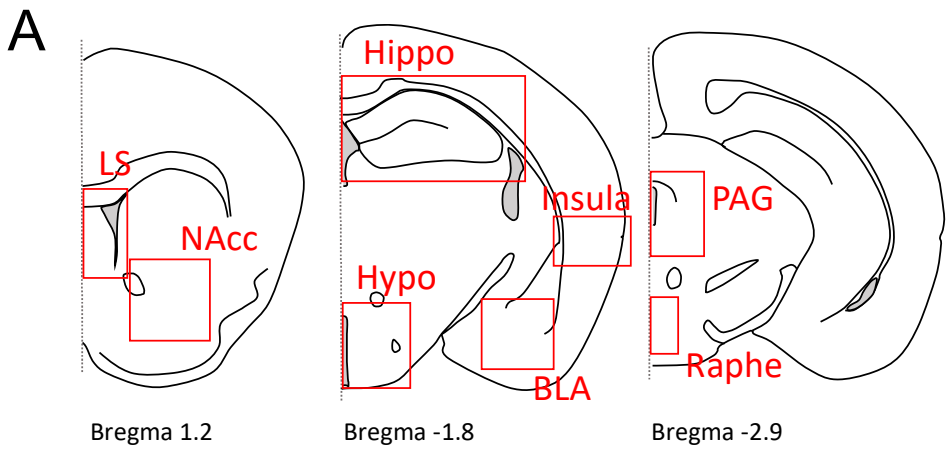
A
LS
NAcc
Hippo
Insula
Hypo
BLA
PAG
Raphe
Bregma 1.2
Bregma -1.8
Bregma -2.9

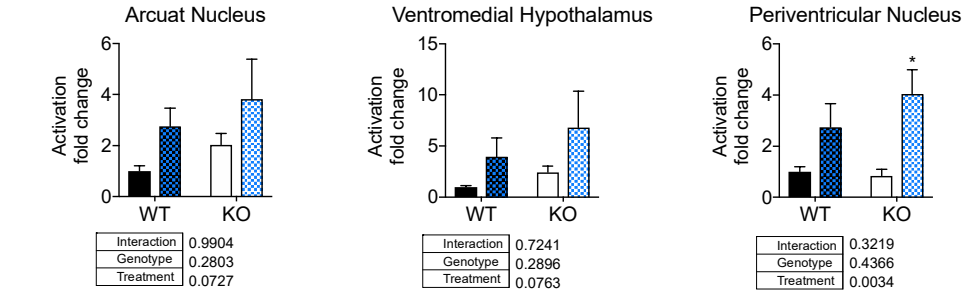
B
Arcuat Nucleus
Activation fold change
WT
KO
Interaction 0.9904
Genotype 0.2803
Treatment 0.0727
Ventromedial Hypothalamus
Interaction 0.7241
Genotype 0.2896
Treatment 0.0763
Periventricular Nucleus
*
Interaction 0.3219
Genotype 0.4366
Treatment 0.0034

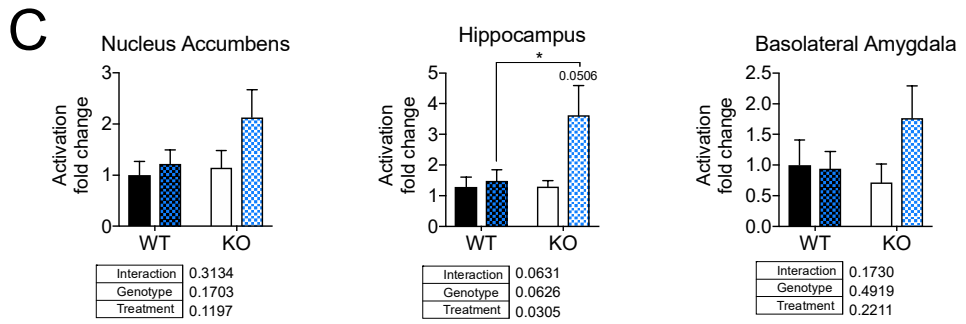
C
Nucleus Accumbens
Activation fold change
WT
KO
Interaction 0.3134
Genotype 0.1703
Treatment 0.1197
Hippocampus
*
0.0506
Interaction 0.0631
Genotype 0.0626
Treatment 0.0305
Basolateral Amygdala
Interaction 0.1730
Genotype 0.4919
Treatment 0.2211

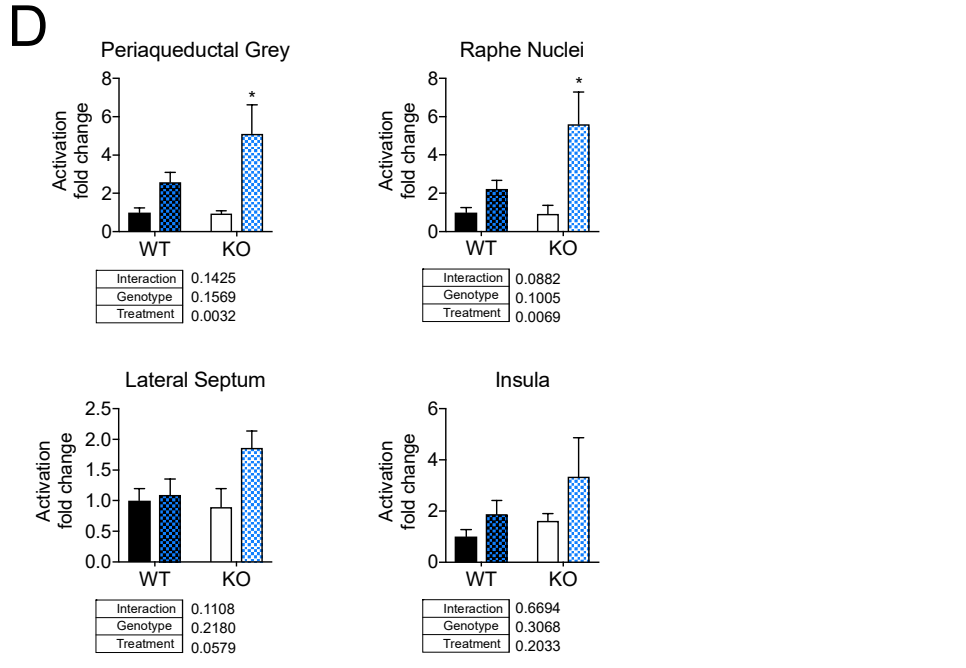
D
Periaqueductal Grey
Activation fold change
WT
KO
*
Interaction 0.1425
Genotype 0.1569
Treatment 0.0032
Raphe Nuclei
*
Interaction 0.0882
Genotype 0.1005
Treatment 0.0069
Lateral Septum
Interaction 0.1108
Genotype 0.2180
Treatment 0.0579
Insula
Interaction 0.6694
Genotype 0.3068
Treatment 0.2033

Figure 21. Neuronal activation in the glucose sensing centers of Dusp8 KO and WT mice after 2DG injection.

(A) Schematic overview of brain centers analyzed for neuronal activation after i.p. injection of 2DG. Induction of neuronal action after 2DG injection compared to WT PBS of (B) hypothalamic nuclei, (C) brain centers for reward behavior (nucleus accumbens) and limbic system (hippocampus, basolateral amygdala) and (D) extra-hypothalamic glucose sensing centers in the brainstem (periaqueductal grey and raphe nuclei), the lateral septum and insula. Dusp8 WT PBS: n=5-11, Dusp8 WT 2DG: n=5-12, Dusp8 KO PBS: n=4-8, Dusp8 KO 2DG: n=4-10. LS latera septum, NAcc nucleus accumbens, Hippo hippocampus, Hypo hypothalamus, BLA basolateral amygdala, PAG periaqueductal grey. Means ± SEM. * $p < 0.05$.

Taken together, we found a significant increase in neuronal activity indicated by a higher number of c-fos positive cells in Dusp8 KO 2DG injected mice in the hypothalamic PVN, the limbic hippocampus, as well as in the PAG, and the Raphe nuclei of the brainstem compared to the Dusp8 KO PBS group. This 2DG dependent effect was absent in WT mice indicating a higher responsiveness to sucrose when Dusp8 is ablated. Our results further point to a different MAPK activation pattern in defined brain centers, i.e. hypothalamus and hippocampus when Dusp8 KO mice are stimulated with 2DG. Overall, we reveal an impact of Dusp8 on glucose sensing in an *in vivo* global Dusp8 KO mouse model as well as in an *in vitro* system using murine hypothalamic CLU177 cells.

We found a hyperactive behavior and a mild impairment of spatial orientation of mice deficient for Dusp8, as well as a different seeking strategy for sweet sucrose solution. Our results point in the direction of a different 2DG stimulated MAPK activation pattern and neuronal activity pattern in defined brain centers. The predominant neuronal activation differences in the hippocampus indicates not only a role in the regulation of behavior, but that it might also influence glucose and energy metabolism.

5.4 Unperturbed energy and glucose homeostasis after the ablation of Dusp8 from the hippocampus of mice

To interrogate the role of hippocampal Dusp8 in glucose and energy metabolism, we generated hippocampus specific Dusp8 KO mice by crossing the commercially available Grik4-Cre mice with EUCOMM $Dusp8^{flox/flox}$ mice. Mice carrying both the Grik4-Cre and the Dusp8-flox allele show a tissue-specific knock out of Dusp8 in the CA1 and CA3 subregion (further referred to as $Dusp8^{Grik4\text{-}Cre}$ KO).

5.4.1 Hippocampus-specific Dusp8 KO mice show intact metabolic homeostasis

Animals lacking Dusp8 in the hippocampus showed comparable body weight (Fig. 22A) and body weight gain (Fig. 22B) as the Dusp8$^{Grik4\text{-}Cre}$ WT control mice throughout a 10 week exposure to HFD. The Dusp8$^{Grik4\text{-}Cre}$ KO mice displayed no difference in the cumulative food intake during that time (Fig. 22C) compared to Dusp8$^{Grik4\text{-}Cre}$ WT controls, indicating a similar propensity towards diet induced obesity. This was corroborated by a similar body composition at the end of the HFD exposure (Fig. 22D).

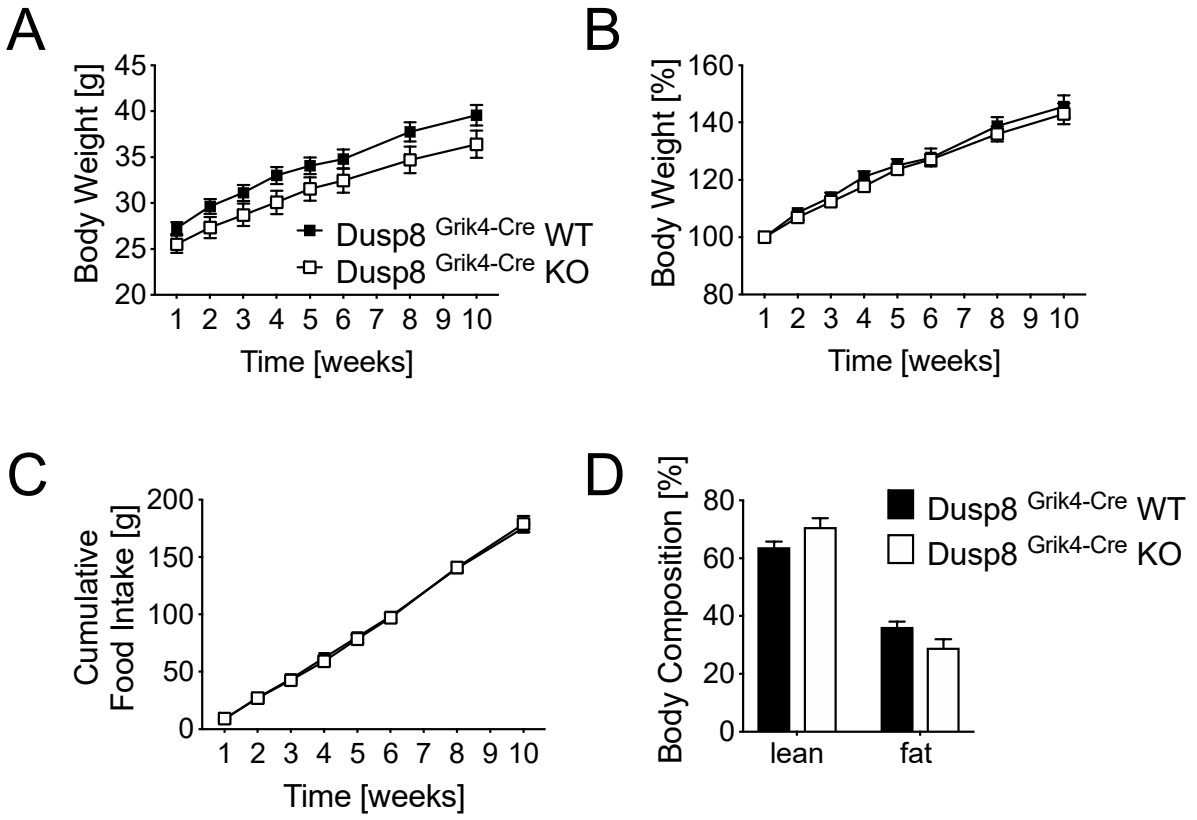

Figure 22. Weight gain, food intake and body composition of Dusp8 $^{Grik4\text{-}Cre}$ KO and WT mice on 45% HFD.

Monitoring of body weight for 10 weeks after diet switch from chow to 45 % HFD. (A) Body weight and (B) body weight in percent from starting weight over 10 weeks. (C) Cumulative food intake of 45 % HFD over 10 weeks. (D) Body composition after 10 weeks of 45 % HFD exposure. Dusp8$^{Grik4\text{-}Cre}$ WT: n=16, Dusp8$^{Grik4\text{-}Cre}$ KO: n=13. Means ± SEM.

Taken together, hippocampus-specific deletion of Dusp8 does not affect HFD-induced changes in energy metabolism.

5.4.2 Intact glucose tolerance in hippocampus-specific Dusp8 KO mice

We investigated the role of hippocampus-specific Dusp8 on glucose homeostasis and therefore performed a glucose tolerance test (GTT) in HFD-fed fed Dusp8$^{Grik4\text{-}Cre}$ KO and WT mice and measured basal blood glucose levels.

Dusp8$^{Grik4\text{-}Cre}$ KO showed no difference in glucose sensitivity compared to Dusp8$^{Grik4\text{-}Cre}$ WT control mice in a GTT after a 1.5 g glucose/kg body weight bolus i.p. injection (Fig. 23A). However, we found a significantly reduced basal glucose level after 6 h of fasting (Fig. 23B).

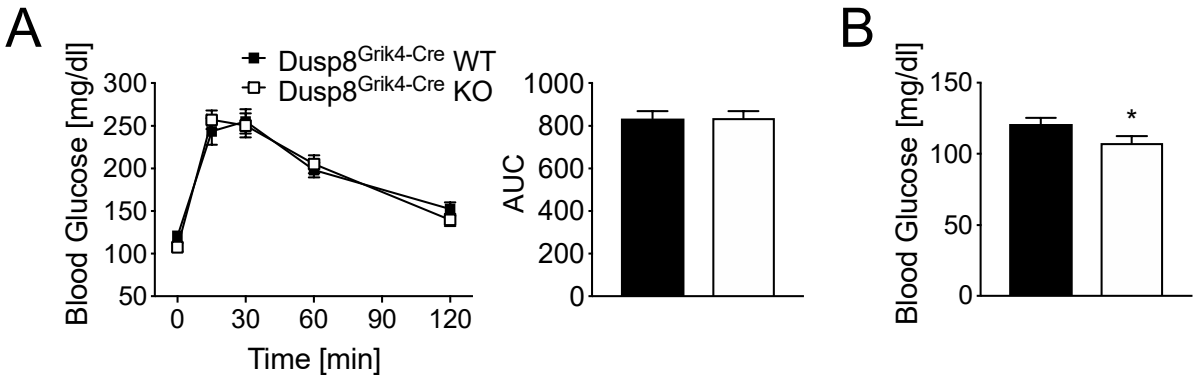

Figure 23. Glucose tolerance and basal blood glucose of hippocampus specific Dusp8 KO mice.

(A) Glucose sensitivity in an i.p. GTT (1.5 g/kg BW). Dusp8$^{Grik4\text{-}Cre}$ KO mice show comparable response to glucose bolus injection than control animals over the time and in the area under the curve (AUC). (B) Basal blood glucose levels after 6 h of fasting. Dusp8$^{Grik4\text{-}Cre}$ KO animals showed significantly reduced blood glucose levels compared to Dusp8$^{Grik4\text{-}Cre}$ WT animals. Dusp8$^{Grik4\text{-}Cre}$ WT: n=16, Dusp8$^{Grik4\text{-}Cre}$ KO: n=13. Means ± SEM. * $p < 0.05$.

Overall, hippocampal Dusp8 does not seem to regulate glucose metabolism, but might still play a role in glucose sensing since basal glucose levels were reduced in mice deficient for Dusp8 in the hippocampus. It would be interesting to investigate hippocampal Dusp8 expression and neuronal activity after fasting in this animal model.

6 Discussion

In the first part of this study, we aimed to characterize the influence of dual-specificity phosphatase 8, a physiological inhibitor of MAPK-signaling that is mainly expressed in the brain (Muda et al., 1996), on brain morphology, cognitive performance, and learning and memory in mice. We found a significantly reduced hippocampus size in Dusp8 KO mice, a hyperactivity phenotype, as well as a mild impairment of spatial memory. The second part of this study characterized the role of Dusp8 in sucrose reward behaviors and in central glucose sensing. We could show altered sucrose seeking behavior and different neuronal activity in various brain centers involved in glucose sensing and behavior when the mice were in a state of glucose deprivation. We could last show that hippocampal Dusp8 is not involved in regulating food intake, body weight gain, or glucose tolerance. Overall, aberrations in morphology and behavior in Dusp8 KO mice point to a novel role of Dusp8 in hippocampal function. Dusp8 plays a part in the glucose sensing network of the brain and might modulate sucrose seeking behavior.

6.1 Dusp8 has a tissue- and context-dependent MAPK specificity

Contrary to previous reports on a structure-specificity of Dusp8 for Jnk (Theodosiou and Ashworth 2002b) and a close bidirectional modulation of Dusp8 and Jnk (Theodosiou and Ashworth 2002a, Patterson et al. 2009), we found similar Jnk activity in the hippocampus of global Dusp8 KO mice compared to control mice. Furthermore, despite other literature suggesting an equal affinity and specificity of Dusp8 to p38 and Jnk (Caunt and Keyse 2013), p-p38 levels also did not differ between Dusp8 KO and WT mice. This might be due to compensatory mechanisms of other Jnk-mediating Dusps with a widespread specificity to MAPKs. To our surprise, we found increased levels of p-Erk in hippocampal lysates of Dusp8 KO mice. Literature supporting this finding is by Liu and colleagues (Liu et al. 2016), who showed a Dusp8-mediated remodeling of cardiomyocytes via Erk activity. The observed specificity of Dusp8 to Erk shown in the heart and the hippocampus might be tissue specific, as it is not in line with structural analysis of binding motifs and stimulated cell culture models. As both brain tissue and cardiomyocytes are electrically excitable, this shared feature might be an explanation for the specificity of Dusp8 towards Erk differing from previously investigated tumor cell models. The question of whether Dusp8 is acting specifically

on Erk in a tissue-dependent manner or whether its binding all three regular MAPKs in the hippocampus needs to be further addressed.

The increased activity of the Erk-signaling pathway seems to not have any impact on cellular proliferation, as we did not find any difference in the amount of positive cells labeled for the proliferation marker Ki67 in the hippocampus of Dusp8 KO mice. This is quite surprising since activated Erk-signaling pathway is contributing to the activation of the cell cycle and cell proliferation (Zhang and Liu 2002). However, Rai and colleagues (Rai et al. 2019) recently reviewed an ambivalent role of activated Erk in cell signaling. They provided evidence that activated Erk-signaling might contribute to cell death in neurodegenerative disease like Parkinson's and Alzheimer's, but also show a neuroprotective effect in ROS-induced cellular stress. However, we did not find any induction of apoptosis using the marker casp3 in our Dusp8 KO mouse model. We therefore conclude that elevated Erk-signaling in the hippocampus of Dusp8 KO mice does not contribute to cell proliferation or cell death. Furthermore, we conclude from this data that the reduced hippocampus weight and volume found in Dusp8 deficient animals is not based on elevated Erk-signaling, which is modulating various cellular functions. Reasons for the reduced hippocampus size in animals deficient for Dusp8 remain elusive. So far, we cannot exclude a developmental aspect of the site reduction since Martell and colleagues (Martell et al. 1995) already showed a high expression of Dusp8 in differentiating as well as differentiated cells of embryos at E16.5. Examination of hippocampus sizes in young animals (P21) might give more insights in the impact during development.

6.2 Are behavioral alterations of Dusp8 KO mice reminiscent of the bipolar disorder in humans?

Since an interesting GWAS study identified a risk-variant in the DUSP8 locus located on the short arm of chromosome 11 at position 15.5 that was previously linked to the susceptibility of type 2 diabetes (Kong et al., 2009), we were wondering whether there are more physiological roles of Dusp8 regulated in the CNS. Prompted by a report of Serretti and Mandelli (Serretti and Mandelli 2008), which showed a potential association of the Dusp8 locus 11p15.5 and bipolar disorder (BD), we hypothesized a bipolar disorder-like phenotype in our global Dusp8 KO model. BD is a diagnostically heterogeneous psychiatric disorder that is characterized by fluctuations with manic and

depressive episodes (Diagnostic and Statistical Manual of Mental Disorders (DSM) Association, 2013). In general, the typical BD symptoms mania and hypomania lead to impairments in social functioning, elevated motor drive, and mood as well as mood-incongruent psychotic features. The depressive episodes usually show a rapid onset and offset and occur at early age (Grande et al., 2016).

Currently available BD mouse models such as CLOCK or GRIK2/Glut6 mutants are characterized i.e. by increased locomotion and energy in a temporal pattern, which is quite similar to the behavioral phenotype of our global Dusp8 mouse model that displayed a mild perturbation in spatial orientation, increased anxiety, and hyperactivity. The hypothesis that our Dusp8 KO mice have a BD-like phenotype is further supported by findings in murine BD models of sleep deprivation that show comparable symptoms such as increased anxiety and increased exploratory behavior. Along this line of evidence, mice with psychostimulant-induced BD also showed increased locomotion and anxiety levels (Beyer and Freund, 2017). Notably, BD has recently been linked to a decreased volume of specific hippocampal subfields, which was directly correlated with the disease progression (Cao et al., 2017). However, these parallels to BD animal models are limited to those mouse models only. Key features, such as increased risk-taking like behavior, increased hedonia, and reduced depression like behavior, were either not present or not tested. The observed hyperactivity phenotype of global Dusp8 KO mice is rather insufficient to support a mania-like behavior. Furthermore, the reduced hippocampus size observed might be in line with some observations in patients with BD, but in fact, reduced hippocampal volumes are more specifically observed in models of schizophrenia, depression, posttraumatic stress disorder (PTSD), and attention deficit hyperactivity disorder (ADHD) and each is associated with hyperactivity (Malykhin and Coupland 2015, O'Doherty et al. 2015, Kalmady et al. 2017, Al-Amin et al. 2018). However, together with collaborators from the university of Tübingen, we show that human carriers of the Dusp8 lead SNP rs2334499:C>T have a reduced hippocampus size (Baumann et al. 2019; in submission *Sci. Rep.*). This finding, which is in line with the global Dusp8 KO mouse model, is quite intriguing. Unfortunately, there are no data available that provides evidence for impaired cognition or increased risk for psychiatric disorders in the human Dusp8 SNP carriers. Thus, open questions remain regarding the translational phenotype of Dusp8 mediated BD-like symptoms.

Our results do not provide enough evidence to connect the observed hippocampal morphology and the behavioral alterations to bipolar disorder. It is well known, that dopamine is playing a central role in BD (Cousins et al. 2009). The dopamine hypothesis of bipolar affective disorder is a controversially discussed topic, which includes the involvement of dopamine receptor content, as well as alterations in dopamine transport (Ashok et al. 2017). The hypothesis suggests that manic episodes occur with the elevation of D2/3 receptors in the striatum, increasing the dopaminergic transmission and depressive symptoms with increased DAT levels, resulting in reduced dopaminergic signaling. Although the critical enzyme for dopamine synthesis, tyrosine hydroxylase (TH), is not included in the dopamine hypothesis of BD, there is some evidence that hyperactivation of TH is involved in manic rapid mood cycling (Sidor et al. 2015). The observation that the gene encoding for TH, the critical enzyme for catecholamine synthesis, is also located on the locus 11p15.5 (Chitbangonsyn et al. 2003), and the fact that dopamine is playing a central role in BD (Cousins et al. 2009), might give a sufficient explanation for the observed association of the Dusp8 and bipolar disorder (Serretti and Mandelli 2008). Our contribution to the behavioral characterization of Dusp8 in the global knockout mouse model give hints to an involvement of the TH in the dopamine hypothesis and less of a contribution of the Dusp8 locus to BD. However, the involvement of TH and the effects of unbalanced dopamine transmission due to reduced/increased synthesis in BD require further investigations.

6.3 Contribution of the dopamine system to Dusp8-mediated sucrose seeking behavior

The increased sucrose consumption and the hyperactivity phenotype of the mice deficient for Dusp8 in the two-bottle choice test might be a consequence of the reduced hippocampus volume since experiments in rats provided evidence that functional hippocampus signaling in the postprandial period is controlling the initiation of food consumption (Henderson et al. 2013). In the IntelliCage setup we did not monitor food intake, as the mice had free access to *ad libitum* chow food in a rack provided in the middle of the cage. However, it might be reasonable to suggest an increased consumption of sucrose due to an impaired signaling of the reduced hippocampus volume. This impaired signaling might be reasonable for an increased sucrose

consumption due to a lack of meal onset regulation. The fact that we could only record the increased consumption of sucrose during the general program, but not in the period of forced sucrose, might point towards an involvement of the hippocampus as the overconsumption only appeared in the behavioral spectrum of the mice once a spatial cue was coupled to the hedonic stimulus. This might indicate that mice lacking Dusp8 have stronger attention toward an attractive stimulus and therefore a higher consumption of sucrose. However, this increased incentive salience effect caused by a perturbed integration of hippocampal-relayed afferent input.

The “trial-and-error” strategy of foraging for sucrose observed in the Dusp8 deficient mice in the progressive ratio task in the two-bottle water vs sucrose choice test might be a dopamine dependent behavior. Motivational, goal directed, and predictive behavior is known to be largely depending on the mesoaccumbal dopamine pathway (Pennartz et al. 2011). DAT knock out mice were shown to have a higher motivational level for sucrose progressive ratio task (Davis et al., 2018), strengthening the results of an involvement of the dopamine system in controlling motivational level in reward-seeking behavior.

However, we did not find any evidence that Dusp8 might be a developmental factor in the maturation of the dopaminergic system. The integrity and functionality is given by the fact that we did not find differences in the amount of DAT in the nucleus accumbens or the number of DAT-positive cells in the VTA of Dusp8 KO and Dusp8 WT mice. However, immunofluorescent labeling of DAT might not be the ideal way to verify an intact dopaminergic system in the brain. Evaluating the physiological level of neuronal activity in dopaminergic neurons of the reward system might have given a more valuable output. Unfortunately, the brains of Dusp8 KO and WT were harvested without a prior acute reward stimulus. Another reliable factor to evaluate the functionality of the dopaminergic system would have been the evaluation of the presence and activity of dopamine receptors as well as DARPP-32 especially since these have been linked to Erk signaling. Literature provides evidence that D1R is mediating Erk-signaling by DARPP-32 phosphorylation and indirect interaction with NMDA glutamate receptor. D2R is mediating Erk activity, i.e. via G protein-coupling (Baik 2013). Together with our finding that p-Erk levels are elevated in hippocampal lysates, it might not be too implausible for Erk-signaling to be elevated in other brain areas such as the dopaminergic striatum. This might be connected to the differences in the performed

sucrose seeking strategy of Dusp8 KO mice. A connection linking the reduced hippocampus size to the differences during the progressive ratio task remains an open question. There is a close network of glutamatergic and GABAergic neurons connecting the prefrontal cortex and the hippocampus via different dopaminergic centers of the basal ganglia of bidirectional and unidirectional projections, respectively (Thierry et al., 2000), that we have yet to study.

The generated data cannot conclusively answer the question of whether the observed “trial-and-error” strategy of Dusp8 KO mice during the progressive ratio task in the IntelliCage setup is caused by an altered dopamine-dependent reward system in the brain, stereotyped behavior, negatively reinforcing, or displacement activity due to observed hyperactivity.

6.4 Deregulation of glucose sensing by Dusp8 deficiency

Diabetes is characterized by an impairment in glucose tolerance and blood glucose homeostasis, which can lead to hyper- or hypoglycemia. Glucose sensing centers in the brain react to changes in blood glucose levels and induce counter-regulatory responses to keep the homeostatic state (Lopez-Gambero et al., 2018). Since Kong and colleagues (Kong et al. 2009) identified DUSP8 as a potential novel type 2 diabetes risk gene, we hypothesized that Dusp8 might play a role in glucose sensing. High sucrose consumption and sucrose seeking behavior pointed towards Dusp8-dependent perturbation of glucose sensing due to increased MAPK-signaling, and unbalanced neuronal activity in central homeostatic, glucose sensing, and connected areas.

Since a 2DG induced upregulation of Dusp8 in a widely glucose dependent glioma cell line was previously reported (Heminger et al. 2006), we used stimulation experiments with this glucose analogue that accumulates in the cell, and therefore blocks glycolysis to get deeper insights into the role of Dusp8 in glucose sensing and counter-regulatory responses. The upregulation of Dusp8 by 2DG treatment, coupled with a downregulation of Erk phosphorylation, was in line with the specificity of Dusp8 for Erk that we observed in hippocampal brain tissue lysates. Whether the observed downregulation of p-Erk after 2DG treatment is cause, consequence, or independent of Dusp8 still needs further investigation.

As the brain is crucially dependent on glucose for energy generation, a shutdown of glycolysis leads to a huge stress response, which in turn leads to activation of Erk signaling and might be related to c-fos expression. In the absence of Dusp8, increased Erk phosphorylation might be the reason for the increased level of c-fos observed after 2 DG injection in Dusp8 KO mice. Therefore, we postulate that Dusp8 might be involved in ending or modulating Erk activity to prevent an overshoot in the response to glucose deprivation. A similar feedback loop coupled to Erk activity has already been described for Dusp6 (Perez-Sen et al. 2019). Following this hypothesis, a quick activation or expression of Dusp8 in response to Erk activity would be required, which is exactly what we saw with the low dose 2DG stimulation *in vitro*. The literature regarding this inducibility is conflicting since recent literature states that Dusp8 is a non-inducible and non-early response gene (Patterson et al. 2009), whereas the first description of Dusp8 indicates a role as inducible-early gene (Martell et al. 1995). Our findings point rather to a role of Dusp8 in rapid signal modulation of Erk activity.

Furthermore, it was shown that 2DG is able to reduce levels of BDNF and its receptor trkB in hippocampi of rats (Garriga-Canut et al. 2006). BDNF and trk require a functional MAPK pathway to induce hippocampal neuronal signaling (Gottschalk et al. 1999). A 2DG-induced reduction of BDNF and a lack of Dusp8-inhibited MAPK phosphorylation might explain the increased neuronal activity in Dusp8 KO mice after 2DG stimulation via an overreacting network, especially in the hippocampus. This might be an additional aspect adding onto the potential effect of a downregulation of the Erk stress response.

Increased neuronal activity in the PAG of 2DG injected Dusp8 KO mice is in line with the increased activity in the PVN of the same mice as projections of various PAG neurons to the PVN have been described (Floyd et al. 1996). These glutamatergic projections might be involved in an excitatory influence of the HPA-axis (Ziegler et al. 2012). As opposed to the PAG, the raphe nuclei send serotonergic efferences to the PVN of the hypothalamus, which is also suggested to stimulate the HPA-axis and trigger stress responses in the body (Hanley and Van de Kar 2003). A hyperactivation of the raphe nuclei might thus contribute to the increased neuronal activity of the PVN after glycolysis blockade. What we show here hints to a regulatory involvement of Dusp8 in the HPA-axis in brain centers after systemic glycolytic stress. However, there

are more nuclei of the brainstem involved in integrating ascending stress stimuli (Myers et al. 2017).

Whether this paralleled neuronal activity in the dense PVN-brainstem network after 2DG injection is cause, consequence, or direct effect of the 2DG stimulation still remains to be determined. We did not collect direct data measuring HPA-axis activity or other PAG and raphe nuclei-dependent behavior, e.g. fear reaction, defensive behavior, or aggression.

6.5 No direct metabolic control by hippocampal Dusp8

The hippocampus might only play a minor role in the regulation of energy metabolism, but is embedded in a complex neuronal network. There is evidence that the hippocampus is able to influence food intake and food preference, which is beyond the nutritional needs of the animal and that metabolic dysfunction is able to influence this regulatory influence. The hippocampal formation receives sensory input from olfactory, gustatory, and visuospatial centers, mnemonic, cognitive information, as well as gastrointestinal signals and relays this information of different aspects (Kanoski and Grill 2017).

Motivated by the influence of the hippocampus on food intake and our findings of increased hippocampal neuronal activity in 2DG injected Dusp8 KO mice, we investigated the impact of hippocampal Dusp8 deletion on energy and glucose metabolism under obesogenic conditions. As we did not find an effect of a Grik4-driven hippocampus specific deletion of Dusp8 on food intake, body weight gain, or glucose tolerance; a lack of Dusp8 function in the CA1 subregion does not seem to be perturbing the above described complex regulatory homeostatic system. However, it would be interesting to test how hippocampal Dusp8 is influencing metabolic homeostasis on a chow diet. It is possible that the specific lack of Dusp8 in this subregion is compensated during development, and that challenging the system with a diet switch is blunting the basic impairment.

7 Conclusion and Outlook

Dual-specificity phosphatase 8 is expressed in the CNS, predominantly in the hippocampus, and regulates MAPK-signaling. The hippocampus is a major center for learning, memory, and cognition with increasing evidence describing it as a relay center for integration of homeostatic, cognitive, and associative information, particularly but not exclusively in the control of ingestive behavior. In our Dusp8 KO mouse model, we found a reduced hippocampus volume, and specificity of Dusp8 toward Erk-MAPK in this brain region. Mice deficient for Dusp8 showed only mild impairments in hippocampus-dependent spatial memory, but increased activity and anxiety-related behaviors. Sucrose consumption was increased in Dusp8 KO mice, whereas motivational behavior was unperturbed. In line with the literature, we found a network of brain areas differentially responding to 2DG injections of Dusp8 WT and KO mice. Cell culture experiments revealed a potentially indirect upregulation of Dusp8 expression after glucose deprivation by 2DG.

Built upon the known association of the Dusp8 locus 11q15.5 with bipolar disorder, we interrogated whether Dusp8 plays a role in this psychiatric disorder. Global KO mice displayed increased locomotion with mild cognitive and mood behavior alterations, but no clear alteration that would allow for a conclusive involvement of Dusp8 in the etiology of BD. To provide evidence for such a claim, tests for risk taking, depression, and impaired impulsivity would be necessary.

Next, we found unperturbed motivational behavior for sucrose, whereas consumption was increased. As we only performed a progressive ratio test, more evidence could be collected by challenging mice with aversive conditioning for the preferred sucrose. Similarly, further investigations of Dusp8 and the dopaminergic reward network are needed to unravel the rationale for the “trial-and-error” strategy of Dusp8 KO mice, i.e. a switch from directed behavior to uncontrolled behavior that is mainly built upon choice. Future studies should clarify whether the stimulation or inhibition of the dopaminergic system can rescue the observed phenotype seen in the progressive ratio task. It might be of further interest to test whether hedonic-related behavior is in general more prominent in mice lacking Dusp8. Tests for hedonic pleasure with high palatable food, i.e. not only sucrose, might be a way to shed light on this question.

The promising findings of increased neuronal activity in Dusp8 KO mice after glycolysis shutdown point to a role for Dusp8 in glucose sensing. To gain more insight into the specific involvement of the CNS in glucose sensing and to avoid feedback mechanisms from the periphery, performing i.c.v. 2DG injection and direct injections in the core nuclei involved in glucose sensing might be an interesting approach. These experiments could then be combined with electrophysiological measurements to corroborate our findings.

We did not find any indication that Dusp8 in the hippocampus is involved in the maintenance of glucose homeostasis. Nonetheless, we aimed to shed new light on the role of Dusp8 specifically in the hippocampus on the regulation of glucose and energy homeostasis. We did not measure a battery of murine behaviors in Dusp8Grik4-Cre KO animals, e.g. in a cognition pipeline. Additional tasks for spatial orientation (Morris Water Maze) and spatial working memory (patrolling task in the IntelliCage), as well as memory retrieval, could be included.

Overall, Dusp8 was shown to influence hippocampus morphology, and it had a mild but significant role in memory and cognition. It also plays a role in glucose sensing in a complex network of brain centers, including the hippocampus. However, further studies need to be done to clarify the mechanistic underpinnings of metabolic homeostasis and behavior changes driven by Dusp8.

8 References

Al-Amin, M., Zinchenko, A. and Geyer, T., 2018. Hippocampal subfield volume changes in subtypes of attention deficit hyperactivity disorder. Brain Res 1685: 1-8. DOI: 10.1016/j.brainres.2018.02.007

Alessi, D. R., Cuenda, A., Cohen, P., Dudley, D. T. and Saltiel, A. R., 1995. PD 098059 is a specific inhibitor of the activation of mitogen-activated protein kinase kinase in vitro and in vivo. J Biol Chem 270(46): 27489-27494. DOI: 10.1074/jbc.270.46.27489

Andermann, M. L. and Lowell, B. B., 2017. Toward a Wiring Diagram Understanding of Appetite Control. Neuron 95(4): 757-778. DOI: 10.1016/j.neuron.2017.06.014

Ashok, A. H., Marques, T. R., Jauhar, S., Nour, M. M., Goodwin, G. M., Young, A. H. and Howes, O. D., 2017. The dopamine hypothesis of bipolar affective disorder: the state of the art and implications for treatment. Mol Psychiatry 22(5): 666-679. DOI: 10.1038/mp.2017.16

Association, A. P., 2013. Diagnostic and Statistical Manual of Mental Disorders (DSM-5), American Psychiatric Publishing, Washington. ISBN:

Avruch, J., 2007. MAP kinase pathways: the first twenty years. Biochim Biophys Acta 1773(8): 1150-1160. DOI: 10.1016/j.bbamcr.2006.11.006

Baik, J. H., 2013. Dopamine signaling in reward-related behaviors. Front Neural Circuits 7: 152. DOI: 10.3389/fncir.2013.00152

Bannerman, D. M., Rawlins, J. N., McHugh, S. B., Deacon, R. M., Yee, B. K., Bast, T., Zhang, W. N., Pothuizen, H. H. and Feldon, J., 2004. Regional dissociations within the hippocampus--memory and anxiety. Neurosci Biobehav Rev 28(3): 273-283. DOI: 10.1016/j.neubiorev.2004.03.004

Banzhaf-Strathmann, J., Benito, E., May, S., Arzberger, T., Tahirovic, S., Kretzschmar, H., Fischer, A. and Edbauer, D., 2014. MicroRNA-125b induces tau hyperphosphorylation and cognitive deficits in Alzheimer's disease. Embo j 33(15): 1667-1680. DOI: 10.15252/embj.201387576

Barker, G. R. I. and Warburton, E. C., 2011. When Is the Hippocampus Involved in Recognition Memory? The Journal of Neuroscience 31(29): 10721-10731. DOI: 10.1523/jneurosci.6413-10.2011

Bendotti, C., Tortarolo, M. and Borsello, T., 2006. Targeting stress activated protein kinases, JNK and p38, as new therapeutic approach for neurodegenerative diseases. Central Nervous System Agents in Medicinal Chemistry (Formerly Current Medicinal Chemistry-Central Nervous System Agents) 6(2): 109-117.

Bermudez, O., Pages, G. and Gimond, C., 2010. The dual-specificity MAP kinase phosphatases: critical roles in development and cancer. Am J Physiol Cell Physiol 299(2): C189-202. DOI: 10.1152/ajpcell.00347.2009

Beyer, D. K. E. and Freund, N., 2017. Animal models for bipolar disorder: from bedside to the cage. Int J Bipolar Disord 5(1): 35. DOI: 10.1186/s40345-017-0104-6

Biessels, G. J. and Despa, F., 2018. Cognitive decline and dementia in diabetes mellitus: mechanisms and clinical implications. Nature Reviews Endocrinology 14(10): 591-604. DOI: 10.1038/s41574-018-0048-7

Bodai, L. and Marsh, J. L., 2012. A novel target for Huntington's disease: ERK at the crossroads of signaling. The ERK signaling pathway is implicated in Huntington's disease and its upregulation ameliorates pathology. Bioessays 34(2): 142-148.

Borg, M. A., Sherwin, R. S., Borg, W. P., Tamborlane, W. V. and Shulman, G. I., 1997. Local ventromedial hypothalamus glucose perfusion blocks counterregulation during systemic hypoglycemia in awake rats. J Clin Invest 99(2): 361-365. DOI: 10.1172/jci119165

Boulton, T. G., Yancopoulos, G. D., Gregory, J. S., Slaughter, C., Moomaw, C., Hsu, J. and Cobb, M. H., 1990. An insulin-stimulated protein kinase similar to yeast kinases involved in cell cycle control. Science 249(4964): 64-67. DOI: 10.1126/science.2164259

Brewster, J. L., de Valoir, T., Dwyer, N. D., Winter, E. and Gustin, M. C., 1993. An osmosensing signal transduction pathway in yeast. Science 259(5102): 1760-1763. DOI: 10.1126/science.7681220

Brunstrom, J. M., Burn, J. F., Sell, N. R., Collingwood, J. M., Rogers, P. J., Wilkinson, L. L., Hinton, E. C., Maynard, O. M. and Ferriday, D., 2012. Episodic memory and appetite regulation in humans. PLoS One 7(12): e50707. DOI: 10.1371/journal.pone.0050707

Cao, B., Passos, I. C., Mwangi, B., Amaral-Silva, H., Tannous, J., Wu, M. J., Zunta-Soares, G. B. and Soares, J. C., 2017. Hippocampal subfield volumes in mood disorders. Mol Psychiatry 22(9): 1352-1358. DOI: 10.1038/mp.2016.262

Cargnello, M. and Roux, P. P., 2011. Activation and function of the MAPKs and their substrates, the MAPK-activated protein kinases. Microbiol Mol Biol Rev 75(1): 50-83. DOI: 10.1128/mmbr.00031-10

Caunt, C. J. and Keyse, S. M., 2013. Dual-specificity MAP kinase phosphatases (MKPs): shaping the outcome of MAP kinase signalling. Febs j 280(2): 489-504. DOI: 10.1111/j.1742-4658.2012.08716.x

Chen, R. H., Sarnecki, C. and Blenis, J., 1992. Nuclear localization and regulation of erk- and rsk-encoded protein kinases. Mol Cell Biol 12(3): 915-927. DOI: 10.1128/mcb.12.3.915

Chen, Z., Gibson, T. B., Robinson, F., Silvestro, L., Pearson, G., Xu, B., Wright, A., Vanderbilt, C. and Cobb, M. H., 2001. MAP kinases. Chem Rev 101(8): 2449-2476.

Chitbangonsyn, S. W., Mahboubi, P., Walker, D., Rana, B. K., Diggle, K. L., Timberlake, D. S., Parmer, R. J. and O'Connor, D. T., 2003. Physical mapping of autonomic/sympathetic candidate genetic loci for hypertension in the human genome: a somatic cell radiation hybrid library approach. J Hum Hypertens 17(5): 319-324. DOI: 10.1038/sj.jhh.1001550

Coulombe, P. and Meloche, S., 2007. Atypical mitogen-activated protein kinases: structure, regulation and functions. Biochim Biophys Acta 1773(8): 1376-1387. DOI: 10.1016/j.bbamcr.2006.11.001

Cousins, D. A., Butts, K. and Young, A. H., 2009. The role of dopamine in bipolar disorder. Bipolar Disord 11(8): 787-806. DOI: 10.1111/j.1399-5618.2009.00760.x

Cuadrado, A. and Nebreda, A. R., 2010. Mechanisms and functions of p38 MAPK signalling. Biochem J 429(3): 403-417. DOI: 10.1042/bj20100323

Davis, G. L., Stewart, A., Stanwood, G. D., Gowrishankar, R., Hahn, M. K. and Blakely, R. D., 2018. Functional coding variation in the presynaptic dopamine transporter associated with neuropsychiatric disorders drives enhanced motivation and context-dependent impulsivity in mice. Behav Brain Res 337: 61-69. DOI: 10.1016/j.bbr.2017.09.043

Davis, R. J., 2000. Signal transduction by the JNK group of MAP kinases. Cell 103(2): 239-252.

De Jaeger, X., Courtey, J., Brus, M., Artinian, J., Villain, H., Bacquie, E. and Roullet, P., 2014. Characterization of spatial memory reconsolidation. Learn Mem 21(6): 316-324. DOI: 10.1101/lm.033415.113

Deng, W., Aimone, J. B. and Gage, F. H., 2010. New neurons and new memories: how does adult hippocampal neurogenesis affect learning and memory? Nature Reviews Neuroscience 11: 339. DOI: 10.1038/nrn2822

Dudley, D. T., Pang, L., Decker, S. J., Bridges, A. J. and Saltiel, A. R., 1995. A synthetic inhibitor of the mitogen-activated protein kinase cascade. Proc Natl Acad Sci U S A 92(17): 7686-7689. DOI: 10.1073/pnas.92.17.7686

Duric, V., Banasr, M., Licznerski, P., Schmidt, H. D., Stockmeier, C. A., Simen, A. A., Newton, S. S. and Duman, R. S., 2010. A negative regulator of MAP kinase causes depressive behavior. Nat Med 16(11): 1328-1332. DOI: 10.1038/nm.2219

Eichenbaum, H., 2013. Memory on time. Trends Cogn Sci 17(2): 81-88. DOI: 10.1016/j.tics.2012.12.007

Enslen, H., Raingeaud, J. and Davis, R. J., 1998. Selective activation of p38 mitogen-activated protein (MAP) kinase isoforms by the MAP kinase kinases MKK3 and MKK6. J Biol Chem 273(3): 1741-1748. DOI: 10.1074/jbc.273.3.1741

Erlanson-Albertsson, C., 2005. How palatable food disrupts appetite regulation. Basic Clin Pharmacol Toxicol 97(2): 61-73. DOI: 10.1111/j.1742-7843.2005.pto_179.x

Fanselow, M. S. and Dong, H. W., 2010. Are the dorsal and ventral hippocampus functionally distinct structures? Neuron 65(1): 7-19. DOI: 10.1016/j.neuron.2009.11.031

Feuchtinger, A., Stiehler, T., Jutting, U., Marjanovic, G., Luber, B., Langer, R. and Walch, A., 2015. Image analysis of immunohistochemistry is superior to visual scoring as shown for patient outcome of esophageal adenocarcinoma. Histochem Cell Biol 143(1): 1-9. DOI: 10.1007/s00418-014-1258-2

Floyd, N. S., Keay, K. A., Arias, C. M., Sawchenko, P. E. and Bandler, R., 1996. Projections from the ventrolateral periaqueductal gray to endocrine regulatory subdivisions of the paraventricular nucleus of the hypothalamus in the rat. Neurosci Lett 220(2): 105-108. DOI: 10.1016/s0304-3940(96)13240-7

Franklin, K. B. J. and Paxinos, G., 2007. The Mouse Brain in Stereotaxic Coordinates, Elsevier Inc. ISBN: 978-0-12-369460-7.

Fuchs, S. Y., Adler, V., Buschmann, T., Yin, Z., Wu, X., Jones, S. N. and Ronai, Z., 1998. JNK targets p53 ubiquitination and degradation in nonstressed cells. Genes Dev 12(17): 2658-2663. DOI: 10.1101/gad.12.17.2658

Garriga-Canut, M., Schoenike, B., Qazi, R., Bergendahl, K., Daley, T. J., Pfender, R. M., Morrison, J. F., Ockuly, J., Stafstrom, C., et al., 2006. 2-Deoxy-D-glucose reduces epilepsy progression by NRSF-CtBP-dependent metabolic regulation of chromatin structure. Nat Neurosci 9(11): 1382-1387. DOI: 10.1038/nn1791

González, J. A., Jensen, L. T., Fugger, L. and Burdakov, D., 2008. Metabolism-Independent Sugar Sensing in Central Orexin Neurons. Diabetes 57(10): 2569-2576. DOI: 10.2337/db08-0548

Gottschalk, W. A., Jiang, H., Tartaglia, N., Feng, L., Figurov, A. and Lu, B., 1999. Signaling mechanisms mediating BDNF modulation of synaptic plasticity in the hippocampus. Learn Mem 6(3): 243-256.

Grande, I., Berk, M., Birmaher, B. and Vieta, E., 2016. Bipolar disorder. Lancet 387(10027): 1561-1572. DOI: 10.1016/s0140-6736(15)00241-x

Hanley, N. R. and Van de Kar, L. D., 2003. Serotonin and the neuroendocrine regulation of the hypothalamic--pituitary-adrenal axis in health and disease. Vitam Horm 66: 189-255.

Heminger, K., Jain, V., Kadakia, M., Dwarakanath, B. and Berberich, S. J., 2006. Altered gene expression induced by ionizing radiation and glycolytic inhibitor 2-deoxy-glucose in a human glioma cell line: implications for radio sensitization. Cancer Biol Ther 5(7): 815-823. DOI: 10.4161/cbt.5.7.2812

Henderson, Y. O., Smith, G. P. and Parent, M. B., 2013. Hippocampal neurons inhibit meal onset. Hippocampus 23(1): 100-107. DOI: 10.1002/hipo.22062

Higgs, S., 2008. Cognitive influences on food intake: the effects of manipulating memory for recent eating. Physiol Behav 94(5): 734-739. DOI: 10.1016/j.physbeh.2008.04.012

Holter, S. M., Einicke, J., Sperling, B., Zimprich, A., Garrett, L., Fuchs, H., Gailus-Durner, V., Hrabe de Angelis, M. and Wurst, W., 2015a. Tests for Anxiety-Related Behavior in Mice. Curr Protoc Mouse Biol 5(4): 291-309. DOI: 10.1002/9780470942390.mo150010

Holter, S. M., Garrett, L., Einicke, J., Sperling, B., Dirscherl, P., Zimprich, A., Fuchs, H., Gailus-Durner, V., Hrabe de Angelis, M., et al., 2015b. Assessing Cognition in Mice. Curr Protoc Mouse Biol 5(4): 331-358. DOI: 10.1002/9780470942390.mo150068

Jeanneteau, F., Deinhardt, K., Miyoshi, G., Bennett, A. M. and Chao, M. V., 2010. The MAP kinase phosphatase MKP-1 regulates BDNF-induced axon branching. Nat Neurosci 13(11): 1373-1379. DOI: 10.1038/nn.2655

Ji, D. and Wilson, M. A., 2007. Coordinated memory replay in the visual cortex and hippocampus during sleep. Nat Neurosci 10(1): 100-107. DOI: 10.1038/nn1825

Kalmady, S. V., Shivakumar, V., Arasappa, R., Subramaniam, A., Gautham, S., Venkatasubramanian, G. and Gangadhar, B. N., 2017. Clinical correlates of hippocampus volume and shape in antipsychotic-naive schizophrenia. Psychiatry Res Neuroimaging 263: 93-102. DOI: 10.1016/j.pscychresns.2017.03.014

Kang, L., Dunn-Meynell, A. A., Routh, V. H., Gaspers, L. D., Nagata, Y., Nishimura, T., Eiki, J., Zhang, B. B. and Levin, B. E., 2006. Glucokinase Is a Critical Regulator of Ventromedial Hypothalamic Neuronal Glucosensing. Diabetes 55(2): 412-420. DOI: 10.2337/diabetes.55.02.06.db05-1229

Kang, L., Routh, V. H., Kuzhikandathil, E. V., Gaspers, L. D. and Levin, B. E., 2004. Physiological and Molecular Characteristics of Rat Hypothalamic Ventromedial Nucleus Glucosensing Neurons. Diabetes 53(3): 549-559. DOI: 10.2337/diabetes.53.3.549

Kanoski, S. E. and Grill, H. J., 2017. Hippocampus Contributions to Food Intake Control: Mnemonic, Neuroanatomical, and Endocrine Mechanisms. Biol Psychiatry 81(9): 748-756. DOI: 10.1016/j.biopsych.2015.09.011

Karlsson, M. P. and Frank, L. M., 2009. Awake replay of remote experiences in the hippocampus. Nat Neurosci 12(7): 913-918. DOI: 10.1038/nn.2344

Kim, S. H., Shin, S. Y., Lee, K. Y., Joo, E. J., Song, J. Y., Ahn, Y. M., Lee, Y. H. and Kim, Y. S., 2012. The genetic association of DUSP6 with bipolar disorder and its effect on ERK activity. Prog Neuropsychopharmacol Biol Psychiatry 37(1): 41-49. DOI: 10.1016/j.pnpbp.2011.11.014

Kohno, D., 2017. Sweet taste receptor in the hypothalamus: a potential new player in glucose sensing in the hypothalamus. The Journal of Physiological Sciences 67(4): 459-465. DOI: 10.1007/s12576-017-0535-y

Komorowski, R. W., Manns, J. R. and Eichenbaum, H., 2009. Robust Conjunctive Item–Place Coding by Hippocampal Neurons Parallels Learning What Happens

Where. The Journal of Neuroscience 29(31): 9918-9929. DOI: 10.1523/jneurosci.1378-09.2009

Kong, A., Steinthorsdottir, V., Masson, G., Thorleifsson, G., Sulem, P., Besenbacher, S., Jonasdottir, A., Sigurdsson, A., Kristinsson, K. T., et al., 2009. Parental origin of sequence variants associated with complex diseases. Nature 462(7275): 868-874. DOI: 10.1038/nature08625

Krishna, M. and Narang, H., 2008. The complexity of mitogen-activated protein kinases (MAPKs) made simple. Cell Mol Life Sci 65(22): 3525-3544. DOI: 10.1007/s00018-008-8170-7

Kropff, E., Carmichael, J. E., Moser, M. B. and Moser, E. I., 2015. Speed cells in the medial entorhinal cortex. Nature 523(7561): 419-424. DOI: 10.1038/nature14622

Kyriakis, J. M. and Avruch, J., 2012. Mammalian MAPK signal transduction pathways activated by stress and inflammation: a 10-year update. Physiol Rev 92(2): 689-737. DOI: 10.1152/physrev.00028.2011

Lavenex, P. and Amaral, D. G., 2000. Hippocampal-neocortical interaction: a hierarchy of associativity. Hippocampus 10(4): 420-430. DOI: 10.1002/1098-1063(2000)10:4<420::aid-hipo8>3.0.co;2-5

Lawler, S., Fleming, Y., Goedert, M. and Cohen, P., 1998. Synergistic activation of SAPK1/JNK1 by two MAP kinase kinases in vitro. Curr Biol 8(25): 1387-1390.

Lee, I. and Kesner, R. P., 2002. Differential contribution of NMDA receptors in hippocampal subregions to spatial working memory. Nat Neurosci 5(2): 162-168. DOI: 10.1038/nn790

Lee, J. K. and Kim, N. J., 2017. Recent Advances in the Inhibition of p38 MAPK as a Potential Strategy for the Treatment of Alzheimer's Disease. Molecules 22(8). DOI: 10.3390/molecules22081287

Liu, R., van Berlo, J. H., York, A. J., Vagnozzi, R. J., Maillet, M. and Molkentin, J. D., 2016. DUSP8 Regulates Cardiac Ventricular Remodeling by Altering ERK1/2 Signaling. Circ Res 119(2): 249-260. DOI: 10.1161/circresaha.115.308238

Lopez-Gambero, A. J., Martinez, F., Salazar, K., Cifuentes, M. and Nualart, F., 2018. Brain Glucose-Sensing Mechanism and Energy Homeostasis. Mol Neurobiol. DOI: 10.1007/s12035-018-1099-4

Magnuson, M. A., 1990. Glucokinase Gene Structure: Functional Implications of Molecular Genetic Studies. Diabetes 39(5): 523-527. DOI: 10.2337/diab.39.5.523

Malykhin, N. V. and Coupland, N. J., 2015. Hippocampal neuroplasticity in major depressive disorder. Neuroscience 309: 200-213. DOI: 10.1016/j.neuroscience.2015.04.047

Martell, K. J., Seasholtz, A. F., Kwak, S. P., Clemens, K. K. and Dixon, J. E., 1995. hVH-5: A Protein Tyrosine Phosphatase Abundant in Brain that Inactivates Mitogen-Activated Protein Kinase. J Neurochem 65(4): 1823-1833. DOI: 10.1046/j.1471-4159.1995.65041823.x

Martin, S. J. and Clark, R. E., 2007. The rodent hippocampus and spatial memory: from synapses to systems. Cellular and Molecular Life Sciences 64(4): 401. DOI: 10.1007/s00018-007-6336-3

Mathiasen, M. L., Hansen, L. and Witter, M. P., 2015. Insular projections to the parahippocampal region in the rat. J Comp Neurol 523(9): 1379-1398. DOI: 10.1002/cne.23742

Mehan, S., Meena, H., Sharma, D. and Sankhla, R., 2011. JNK: a stress-activated protein kinase therapeutic strategies and involvement in Alzheimer's and various neurodegenerative abnormalities. J Mol Neurosci 43(3): 376-390. DOI: 10.1007/s12031-010-9454-6

Mietlicki-Baase, E. G., Reiner, D. J., Cone, J. J., Olivos, D. R., McGrath, L. E., Zimmer, D. J., Roitman, M. F. and Hayes, M. R., 2014. Amylin Modulates the Mesolimbic Dopamine System to Control Energy Balance. Neuropsychopharmacology 40: 372. DOI: 10.1038/npp.2014.180

Miller, A. A. and Spencer, S. J., 2014. Obesity and neuroinflammation: a pathway to cognitive impairment. Brain Behav Immun 42: 10-21. DOI: 10.1016/j.bbi.2014.04.001

Mizuno, Y. and Oomura, Y., 1984. Glucose responding neurons in the nucleus tractus solitarius of the rat: in vitro study. Brain Res 307(1-2): 109-116. DOI: 10.1016/0006-8993(84)90466-9

Mohammad, H., Marchisella, F., Ortega-Martinez, S., Hollos, P., Eerola, K., Komulainen, E., Kulesskaya, N., Freemantle, E., Fagerholm, V., et al., 2018. JNK1 controls adult hippocampal neurogenesis and imposes cell-autonomous control of anxiety behaviour from the neurogenic niche. Mol Psychiatry 23(2): 487. DOI: 10.1038/mp.2017.21

Morris, A. P., Voight, B. F., Teslovich, T. M., Ferreira, T., Segre, A. V., Steinthorsdottir, V., Strawbridge, R. J., Khan, H., Grallert, H., et al., 2012. Large-scale association analysis provides insights into the genetic architecture and pathophysiology of type 2 diabetes. Nat Genet 44(9): 981-990. DOI: 10.1038/ng.2383

Morris, R. G., Garrud, P., Rawlins, J. N. and O'Keefe, J., 1982. Place navigation impaired in rats with hippocampal lesions. Nature 297(5868): 681-683. DOI: 10.1038/297681a0

Moser, E. I., Kropff, E. and Moser, M. B., 2008. Place cells, grid cells, and the brain's spatial representation system. Annu Rev Neurosci 31: 69-89. DOI: 10.1146/annurev.neuro.31.061307.090723

Moser, M. B. and Moser, E. I., 1998. Functional differentiation in the hippocampus. Hippocampus 8(6): 608-619. DOI: 10.1002/(sici)1098-1063(1998)8:6<608::aid-hipo3>3.0.co;2-7

Muda, M., Theodosiou, A., Rodrigues, N., Boschert, U., Camps, M., Gillieron, C., Davies, K., Ashworth, A. and Arkinstall, S., 1996. The dual specificity phosphatases M3/6 and MKP-3 are highly selective for inactivation of distinct mitogen-activated protein kinases. J Biol Chem 271(44): 27205-27208. DOI: 10.1074/jbc.271.44.27205

Mudgett, J. S., Ding, J., Guh-Siesel, L., Chartrain, N. A., Yang, L., Gopal, S. and Shen, M. M., 2000. Essential role for p38alpha mitogen-activated protein kinase in placental angiogenesis. Proc Natl Acad Sci U S A 97(19): 10454-10459. DOI: 10.1073/pnas.180316397

Murray, E. A. and Mishkin, M., 1998. Object recognition and location memory in monkeys with excitotoxic lesions of the amygdala and hippocampus. J Neurosci 18(16): 6568-6582.

Myers, B., Scheimann, J. R., Franco-Villanueva, A. and Herman, J. P., 2017. Ascending mechanisms of stress integration: Implications for brainstem regulation of neuroendocrine and behavioral stress responses. Neurosci Biobehav Rev 74(Pt B): 366-375. DOI: 10.1016/j.neubiorev.2016.05.011

Nakazawa, K., Quirk, M. C., Chitwood, R. A., Watanabe, M., Yeckel, M. F., Sun, L. D., Kato, A., Carr, C. A., Johnston, D., et al., 2002. Requirement for hippocampal CA3 NMDA receptors in associative memory recall. Science 297(5579): 211-218. DOI: 10.1126/science.1071795

O'Doherty, D. C., Chitty, K. M., Saddiqui, S., Bennett, M. R. and Lagopoulos, J., 2015. A systematic review and meta-analysis of magnetic resonance imaging measurement of structural volumes in posttraumatic stress disorder. Psychiatry Res 232(1): 1-33. DOI: 10.1016/j.pscychresns.2015.01.002

O'Keefe, J. and Dostrovsky, J., 1971. The hippocampus as a spatial map. Preliminary evidence from unit activity in the freely-moving rat. Brain Res 34(1): 171-175. DOI: 10.1016/0006-8993(71)90358-1

Ogunnowo-Bada, E. O., Heeley, N., Brochard, L. and Evans, M. L., 2014. Brain glucose sensing, glucokinase and neural control of metabolism and islet function. Diabetes Obes Metab 16 Suppl 1: 26-32. DOI: 10.1111/dom.12334

Olton, D. S. and Papas, B. C., 1979. Spatial memory and hippocampal function. Neuropsychologia 17(6): 669-682.

Patterson, K. I., Brummer, T., O'Brien, P. M. and Daly, R. J., 2009. Dual-specificity phosphatases: critical regulators with diverse cellular targets. Biochem J 418(3): 475-489. DOI: 10.1042/BJ20082234

Pearson, G., Robinson, F., Beers Gibson, T., Xu, B. E., Karandikar, M., Berman, K. and Cobb, M. H., 2001. Mitogen-activated protein (MAP) kinase pathways:

regulation and physiological functions. Endocr Rev 22(2): 153-183. DOI: 10.1210/edrv.22.2.0428

Pennartz, C. M., Ito, R., Verschure, P. F., Battaglia, F. P. and Robbins, T. W., 2011. The hippocampal-striatal axis in learning, prediction and goal-directed behavior. Trends Neurosci 34(10): 548-559. DOI: 10.1016/j.tins.2011.08.001

Perez-Sen, R., Queipo, M. J., Gil-Redondo, J. C., Ortega, F., Gomez-Villafuertes, R., Miras-Portugal, M. T. and Delicado, E. G., 2019. Dual-Specificity Phosphatase Regulation in Neurons and Glial Cells. Int J Mol Sci 20(8). DOI: 10.3390/ijms20081999

Pfuhlmann, K., Pfluger, P. T., Schriever, S. C., Muller, T. D., Tschop, M. H. and Stemmer, K., 2017. Dual specificity phosphatase 6 deficiency is associated with impaired systemic glucose tolerance and reversible weight retardation in mice. PLoS One 12(9): e0183488. DOI: 10.1371/journal.pone.0183488

Preston, A. R. and Eichenbaum, H., 2013. Interplay of hippocampus and prefrontal cortex in memory. Curr Biol 23(17): R764-773. DOI: 10.1016/j.cub.2013.05.041

Rai, S. N., Dilnashin, H., Birla, H., Singh, S. S., Zahra, W., Rathore, A. S., Singh, B. K. and Singh, S. P., 2019. The Role of PI3K/Akt and ERK in Neurodegenerative Disorders. Neurotox Res 35(3): 775-795. DOI: 10.1007/s12640-019-0003-y

Raman, M., Chen, W. and Cobb, M. H., 2007. Differential regulation and properties of MAPKs. Oncogene 26(22): 3100-3112. DOI: 10.1038/sj.onc.1210392

Routh, V. H., Hao, L., Santiago, A. M., Sheng, Z. and Zhou, C., 2014. Hypothalamic glucose sensing: making ends meet. Front Syst Neurosci 8: 236. DOI: 10.3389/fnsys.2014.00236

Serretti, A. and Mandelli, L., 2008. The genetics of bipolar disorder: genome 'hot regions,' genes, new potential candidates and future directions. Mol Psychiatry 13(8): 742-771. DOI: 10.1038/mp.2008.29

Seternes, O. M., Kidger, A. M. and Keyse, S. M., 2019. Dual-specificity MAP kinase phosphatases in health and disease. Biochim Biophys Acta Mol Cell Res 1866(1): 124-143. DOI: 10.1016/j.bbamcr.2018.09.002

Shiozaki, K. and Russell, P., 1995. Cell-cycle control linked to extracellular environment by MAP kinase pathway in fission yeast. Nature 378(6558): 739-743. DOI: 10.1038/378739a0

Sidor, M. M., Spencer, S. M., Dzirasa, K., Parekh, P. K., Tye, K. M., Warden, M. R., Arey, R. N., Enwright, J. F., 3rd, Jacobsen, J. P., et al., 2015. Daytime spikes in dopaminergic activity drive rapid mood-cycling in mice. Mol Psychiatry 20(11): 1406-1419. DOI: 10.1038/mp.2014.167

Song, Z., Levin, B. E., McArdle, J. J., Bakhos, N. and Routh, V. H., 2001. Convergence of Pre- and Postsynaptic Influences on Glucosensing Neurons in the Ventromedial Hypothalamic Nucleus. Diabetes 50(12): 2673-2681. DOI: 10.2337/diabetes.50.12.2673

Steckler, T., Drinkenburg, W. H., Sahgal, A. and Aggleton, J. P., 1998. Recognition memory in rats--I. Concepts and classification. Prog Neurobiol 54(3): 289-311.

Steele, R. J. and Morris, R. G., 1999. Delay-dependent impairment of a matching-to-place task with chronic and intrahippocampal infusion of the NMDA-antagonist D-AP5. Hippocampus 9(2): 118-136. DOI: 10.1002/(sici)1098-1063(1999)9:2<118::aid-hipo4>3.0.co;2-8

Stranahan, A. M., 2015. Models and mechanisms for hippocampal dysfunction in obesity and diabetes. Neuroscience 309: 125-139. DOI: 10.1016/j.neuroscience.2015.04.045

Sweatt, J. D., 2004. Hippocampal function in cognition. Psychopharmacology (Berl) 174(1): 99-110. DOI: 10.1007/s00213-004-1795-9

Taube, J. S., Muller, R. U. and Ranck, J. B., Jr., 1990. Head-direction cells recorded from the postsubiculum in freely moving rats. I. Description and quantitative analysis. J Neurosci 10(2): 420-435.

Theodosiou, A. and Ashworth, A., 2002a. Differential effects of stress stimuli on a JNK-inactivating phosphatase. Oncogene 21(15): 2387-2397. DOI: 10.1038/sj.onc.1205309

Theodosiou, A. and Ashworth, A., 2002b. MAP kinase phosphatases. Genome Biol 3(7): Reviews3009. DOI: 10.1186/gb-2002-3-7-reviews3009

Thierry, A. M., Gioanni, Y., Degenetais, E. and Glowinski, J., 2000. Hippocampo-prefrontal cortex pathway: anatomical and electrophysiological characteristics. Hippocampus 10(4): 411-419. DOI: 10.1002/1098-1063(2000)10:4<411::aid-hipo7>3.0.co;2-a

Timper, K. and Bruning, J. C., 2017. Hypothalamic circuits regulating appetite and energy homeostasis: pathways to obesity. Dis Model Mech 10(6): 679-689. DOI: 10.1242/dmm.026609

Verberne, A. J., Sabetghadam, A. and Korim, W. S., 2014. Neural pathways that control the glucose counterregulatory response. Front Neurosci 8: 38. DOI: 10.3389/fnins.2014.00038

Wang, Z., Harkins, P. C., Ulevitch, R. J., Han, J., Cobb, M. H. and Goldsmith, E. J., 1997. The structure of mitogen-activated protein kinase p38 at 2.1-A resolution. Proc Natl Acad Sci U S A 94(6): 2327-2332. DOI: 10.1073/pnas.94.6.2327

Waterson, M. J. and Horvath, T. L., 2015. Neuronal Regulation of Energy Homeostasis: Beyond the Hypothalamus and Feeding. Cell Metab 22(6): 962-970. DOI: 10.1016/j.cmet.2015.09.026

WHO (2018). "Obesity and overweight." Retrieved July, 17th 2019, from https://www.who.int/news-room/fact-sheets/detail/obesity-and-overweight.

Widmann, C., Gibson, S., Jarpe, M. B. and Johnson, G. L., 1999. Mitogen-activated protein kinase: conservation of a three-kinase module from yeast to human. Physiol Rev 79(1): 143-180. DOI: 10.1152/physrev.1999.79.1.143

Williams, R. H., Alexopoulos, H., Jensen, L. T., Fugger, L. and Burdakov, D., 2008. Adaptive sugar sensors in hypothalamic feeding circuits. Proceedings of the National Academy of Sciences 105(33): 11975-11980. DOI: 10.1073/pnas.0802687105

Wu, J. J., Roth, R. J., Anderson, E. J., Hong, E. G., Lee, M. K., Choi, C. S., Neufer, P. D., Shulman, G. I., Kim, J. K., et al., 2006. Mice lacking MAP kinase phosphatase-1 have enhanced MAP kinase activity and resistance to diet-induced obesity. Cell Metab 4(1): 61-73. DOI: 10.1016/j.cmet.2006.05.010

Xia, Y., Wu, Z., Su, B., Murray, B. and Karin, M., 1998. JNKK1 organizes a MAP kinase module through specific and sequential interactions with upstream and downstream components mediated by its amino-terminal extension. Genes Dev 12(21): 3369-3381. DOI: 10.1101/gad.12.21.3369

Xu, S. and Cobb, M. H., 1997. MEKK1 binds directly to the c-Jun N-terminal kinases/stress-activated protein kinases. J Biol Chem 272(51): 32056-32060. DOI: 10.1074/jbc.272.51.32056

Yoon, S. and Seger, R., 2006. The extracellular signal-regulated kinase: multiple substrates regulate diverse cellular functions. Growth Factors 24(1): 21-44. DOI: 10.1080/02699050500284218

Zemla, R. and Basu, J., 2017. Hippocampal function in rodents. Curr Opin Neurobiol 43: 187-197. DOI: 10.1016/j.conb.2017.04.005

Zhang, S., Han, J., Sells, M. A., Chernoff, J., Knaus, U. G., Ulevitch, R. J. and Bokoch, G. M., 1995. Rho family GTPases regulate p38 mitogen-activated protein kinase through the downstream mediator Pak1. J Biol Chem 270(41): 23934-23936. DOI: 10.1074/jbc.270.41.23934

Zhang, W. and Liu, H. T., 2002. MAPK signal pathways in the regulation of cell proliferation in mammalian cells. Cell Research 12(1): 9-18. DOI: 10.1038/sj.cr.7290105

Zhang, X. D., Deslandes, E., Villedieu, M., Poulain, L., Duval, M., Gauduchon, P., Schwartz, L. and Icard, P., 2006. Effect of 2-deoxy-D-glucose on various malignant cell lines in vitro. Anticancer Res 26(5a): 3561-3566.

Zhu, J. H., Kulich, S. M., Oury, T. D. and Chu, C. T., 2002. Cytoplasmic aggregates of phosphorylated extracellular signal-regulated protein kinases in Lewy body diseases. Am J Pathol 161(6): 2087-2098. DOI: 10.1016/s0002-9440(10)64487-2

Ziegler, D. R., Edwards, M. R., Ulrich-Lai, Y. M., Herman, J. P. and Cullinan, W. E., 2012. Brainstem origins of glutamatergic innervation of the rat hypothalamic paraventricular nucleus. J Comp Neurol 520(11): 2369-2394. DOI: 10.1002/cne.23043

Zola-Morgan, S., Squire, L. R. and Ramus, S. J., 1994. Severity of memory impairment in monkeys as a function of locus and extent of damage within the medial temporal lobe memory system. Hippocampus 4(4): 483-495. DOI: 10.1002/hipo.450040410

III Abbreviations

Table 6. Abbreviations

2DG	2-deoxyglucose
ADHD	attention deficit hyperactivity disorder
ADP	adenosine diphosphate
AgRP	agouti related protein
am	ante meridiem
AMP	adenosine monophosphate
AMPK	AMP activated protein kinase
Amy	amygdala
Arc	Arcuate nucleus
ASR	acoustic startle response
ATF	activating transcription factor
ATP	adenosine triphosphate
AUC	area under the curve
Bcl-2	B-cell lymphoma 2
BD	bipolar disorder
BDNF	brain-derived neurotrophic factor
BLA	basolateral amygdala
BSA	bovine serum albumin
BW	body weight
CA	cornu ammonis
Cat	catalogue
CNS	central nervous system
Ct	cycle threshold
D1R	dopamine 1 receptor
DARPP	dopamine regulated phosphoprotein
DAT	dopamine transporter
DG	dentate gyrus
DIO	diet induced obesity
DMEM	Dulbecco's modified eagle's serum
DMH	dorsomedial hypothalamus
DNA	deoxyribonucleic acid
dNTP	deoxyribonucleoside triphosphate
DSM	Diagnostic and Statistical Manual of Mental Disorders

i.e.	id est
i.p.	intraperitoneal
IC	IntelliCage
IL	interleucin
ITI	inter-trial interval
jnk	c-jun N-terminal kinase
KO	knockout
LH	lateral hypothalamus
LS	lateral septum
MAPK	mitogen-activated protein kinase
MAPKAPK	MAPK activated protein kinase
MAPKK	MAPK kinase
MKP	Dual-specificity MAPK phosphatase
MNK	MAPK-interacting kinase
MSH	melanocyte-stimulating hormone
MSK	mitogen- and stress-activated kinases
NAcc	nucleus accumbens
NAccSh	nucleus accumbens shell
Neo	neomycin
NGF	nerve growth factor
NGS	normal goat serum
NLK	nemo-like kinase
NMDA	N-Methyl-d-aspartate
NP	nose poke
NTS	nucleus of the solitary tract
OVX	ovariectomized
PAG	periaqueductal grey
PBS	phosphate buffered saline
PenStrep	penicillin-streptomycin
PFA	paraformaldehyde
PFC	prefrontal cortex
PLR	phosphatase of regenerating liver
pm	post meridiem

dusp	dual-specificity phosphatase
e.g.	exempli gratia
EC	entorhinal cortex
erk	extracellular-signal Regulated Kinase
ESC	embryonic stem cell
et al.	et alii/aliae
EUCOMM	European Mammalian Mutant Cell Repository
FBS	fetal bovine serum
Fig.	figure
GABA	gamma-Aminobutyric acid
GAPDH	glyceraldehyde 3-phosphate dehydrogenase
Gbr2	GABA receptor subdomain 2
GDP	guanine di phosphate
GE	glucose excited
GI	glucose inhibited
GLP	glucagon-like peptide
GLUT	glucose transporter
GPCR	G protein-coupled receptor
GTP	guanine tri phosphate
GTT	glucose tolerance test
GWAS	genome-wide association study
H&E	hematoxylin and eosin
HFD	high fat diet
HIER	heat induced epitope retrieval
Hippo	hippocampus
HPA	hypothalamus-pituitary-adrenal
HRP	horseradish peroxidase
Hypo	hypothalamus
i.c.v.	intracerebroventricular

PMSF	phenyl-methane-sulfonylfluoride
PPI	prepulse inhibition
PR	progressive ratio
PTEN	phosphatase and tensin homologue deleted on chr. 10
PTP	protein tyrosine phosphatases
PTSD	posttraumatic stress disorder
PVDF	poly-vinylidendifluoride
PVN	periventricular nucleus
RIPA	radioimmunoprecipitation assay buffer
RNA	ribonucleic acid
ROS	radical oxigen species
RSK	p90 ribsosomal S6 kinase
RT	room temperature
SAPK	stress activated protein kinase
SDS	sodium dodecyl sulfate
SGLT	sodium dependent glucose transporter
SN	substantia nigra
SNc	substantia nigra pars compacta
SNP	single nucleotide polymorphism
SOS	son of sevenless
TBS	tris buffered saline
TH	tyrosine hydroxylase
TNF	tumor necrosis factor
trkB	tropomyosin receptor kinase B
vHV-5	vaccinia virus H1 phosphatase gene clone 5
VMH	ventromedial hypothalamus
vs	versus
VTA	ventral tegmental area
WT	wild type

IV List of Figures

V List of Tables

VI Acknowledgment

First, I want to thank Prof. Matthias Tschöp for providing a great research environment at the Institute of Diabetes and Obesity at the Helmholtz Center Munich. Second, I thank Prof. Wolfgang Wurst for taking over the role of my second advisor and for the helpful discussion during the annual committee meeting.

I want to thank my first supervisor and mentor Prof. Paul Pfluger for giving me the opportunity to conduct this thesis in his laboratory: NeuroBiology of Diabetes. The exciting work of combining behavioral with metabolic aspects was an inspiring project. Special thanks goes to Dr. Sonja Schriever as deputy head of the research group. She always provided constructive input to the overlapping Dusp8 project and with practical work in the laboratory. Learning how to organize projects and mouse lists was really helpful during busy times. She also helped me with structuring the manuscript.

I also want to thank my colleagues of NBD: Dr. Katrin Pfuhlmann, Luke Harrison, and Raian Contreras, as well as Emily Baumgart. Working together with these friendly, fun, and supportive people added a lot of pleasure to the everyday lab work.

Moreover, I want to thank Dr. Sabine Hölter and Dr. Anni Zimprich for the collaboration of the assessment of cognition in mice. I learned a lot about murine behavior and its complex interpretation. I especially learned a lot of new phenotyping techniques. I also want to thank Jan Einicke and Bettina Sperling for their support carrying out parts of the behavior pipeline. Thanks to Annette Feuchtinger for the help with the histological stainings and the respective analysis. I also want to thank Dr. Daniela Vogt-Weisenhorn for providing advice and the function DAT antibody. Special thanks also to Emily Baumgart and Cassie Holleman for proofreading the manuscript.

I want to thank my friends and family, who supported and motivated me during rough times. I also want to thank all the people from the IDO and the entire HDC who became close friends during the last three and a half years. Sharing passionate experiences was always highly appreciated.